

9-89
MUJ

DRUG-NUCLEIC ACID INTERACTIONS

A THESIS

submitted to the University of Roorkee
for the award of the degree
of
DOCTOR OF PHILOSOPHY

By

ANWER MUJEEB

UNIVERSITY OF ROORKEE CENTRAL LIBRARY
Acc. No. 245429
Date 13-11-90
ROORKEE - INDIA



DEPARTMENT OF BIOSCIENCES AND BIOTECHNOLOGY
UNIVERSITY OF ROORKEE
ROORKEE-247 667 (INDIA)

AUGUST, 1989

Gratis



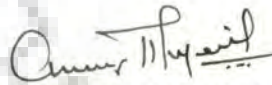


To Life, To Love and To Learning....

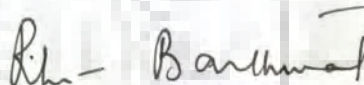
CANDIDATE'S DECLARATION

I hereby certify that the work which is being presented in this thesis entitled, 'Drug - Nucleic Acid Interactions' in fulfilment of the requirement for the award of the Degree of Doctor of Philosophy in Department of Biosciences & Biotechnology, University of Roorkee, Roorkee is an authentic record of my own work carried out during a period from September 1985 to August 1989, under the supervision of Dr. (Mrs) Ritu Barthwal.

The matter embodied in this thesis has not been submitted by me for the award of any other Degree.


(ANWER MUJEEB)

This is to certify that the above statement made by the candidate is correct to best of my knowledge.



Dated: 14.08.1989

Head
Department of Biosciences
and Biotechnology
University of Roorkee
ROORKEE-247 667

Dr.(Mrs.) RITU BARTH WAL
Reader & Head

Department of Biosciences & Biotechnology
University Of Roorkee
Roorkee 247 667, INDIA

The candidate has passed the Viva-Voce examination held on _____ at _____. The thesis is recommended for the award of Ph.D. degree.

Signature of Guide

Signature of External Examiner(s)

C O N T E N T S

	Page No.	
CANDIDATE'S DECLARATION		
ABSTRACT	.. i	
ACKNOWLEDGEMENTS	.. iv	
CHAPTER 1	GENERAL INTRODUCTION	.. 1
CHAPTER 2	LITERATURE REVIEW	
	..General Review	.. 12
	..Studies on daunomycin and its complexes	.. 18
	..Studies on actinomycin D and its complexes	.. 23
	..Theoretical Methods	.. 31
	..Scope of Thesis	.. 36
CHAPTER 3	MATERIALS AND METHODS	
	..Materials	.. 38
	..NMR sample preparation	.. 38
	..Nucleic Acid structure	.. 39
	..Phenomenon of Nuclear Magnetic Resonance	.. 47
	..NMR experimental parameters	.. 54
	..Strategies of complete assignment of nonexchangeable protons	.. 55
	..Theory of potential energy calculations	.. 58
CHAPTER 4	THE STRUCTURE OF DAUNOMYCIN	
	..Temperature Dependence	.. 63
	..Two Dimensional NMR Experiments	.. 68
CHAPTER 5	BINDING OF DAUNOMYCIN WITH DEOXYDINUCLEOTIDE d-CpG	
	..Temperature Dependence	.. 76
	..Two Dimensional NMR Experiments	.. 86
CHAPTER 6	THE STRUCTURE OF ACTINOMYCIN D	
	..Temperature Dependence	.. 95
	..Two Dimensional NMR Experiments	.. 99

CHAPTER 7

**POTENTIAL ENERGY CALCULATIONS
ON DAUNOMYCIN AND ACTINOMYCIN D
COMPLEXES WITH NUCLEIC ACID
BASES, BASE PAIRS AND MODEL
DINUCLEOTIDE SYSTEMS**

..Algorithmic Details	..	112
..Interactions with Bases	..	114
..Interactions with Base Pairs	..	120
..Interactions with Model Dinucleotide Systems	..	123
CONCLUSIONS	..	159
REFERENCES	..	161



ABSTRACT

As our knowledge of the action of antibiotics has increased, it has become clear that many of them attack on specific molecular target and there has been concentration on tracking down these molecules and investigating the nature of their interaction with drugs. A large number of antibiotics exert their effect primarily by interacting directly with the genetic material of cells i.e. with DNA. In doing so, these compounds impair the ability of DNA to act as a template for the processes of nucleic acid expression and synthesis.

Daunomycin is an anticancer antibiotic, isolated from *Streptomyces peucetius*; active mainly against acute lymphocytic leukemia. It inhibits *in vitro* growth of both normal and cancer cell lines and as a consequence nuclear damage is characteristically observed. Chromosomal and genetic abberation of several types are also produced by daunomycin.

Actinomycin D is an antibiotic metabolite containing two identical cyclic pentapeptide chains attached to a phenoxazone chromophore. It is very potent antitumor agent that inhibits DNA directed RNA synthesis and has found clinical applications in the treatment of chloriocarcinoma, but the extreme toxicity of the drug has percluded it from general use.

The present study has been undertaken to find a new insight of

the conformational features of these two drugs in solution by using One dimensional and Two dimensional NMR techniques. The structure of d-CpG.daunomycin complex in stoichiometric ratio 1:2 (D/N) has been deduced by means of 2D NMR techniques and variable temperature one dimensional NMR experiments. One dimensional NMR has been used to find chemical shifts due to stacking, change in T_m etc. while two dimensional NMR techniques; Correlation Spectroscopy (COSY) and nuclear Overhauser enhancement Spectroscopy (NOESY) serve as tools to assign all proton NMR signals unambiguously and determine conformational features such as sugar puckering, helix sense, glycosidic bond rotation and interproton distances in case of oligonucleotides.

Rigorous theoretical potential energy calculations on the complexes of these two drugs with various nucleic acid bases, base pairs and dinucleotide model systems have been carried out to investigate various forces and their magnitude involved in complex formation and with a view to find base/base sequence specificity at the site of interaction. Classical potential function has been used to estimate conformational energy. Total interaction energy calculated is a sum of electrostatic, dispersion, polarisation and repulsion terms. Minimum energy conformation of the complex has been worked out in each case. The charge distribution on each molecule under study, has been calculated by using orbital method of Complete Neglect Of Differential Overlap (CNDO).

Our NMR results are indicative of presence of specific conformations of daunomycin and actinomycin D at NMR concentrations. Presence of more than one conformers of daunomycin molecule has been observed in solution. Complex of d-CpG and daunomycin exhibits interesting results as change in helical sense of d-CpG after complex formation. A B-Z transition is expected in d-CpG from native to complexed state and base to sugar orientation has been found to be SYN and not ANTI/high ANTI as observed in d-CpG alone.

In case of actinomycin D it has been observed that peptide chains do not experience any change on increase in temperature. Resonances from the protons of two separate chains have been successfully assigned. Presence of an inverted dimer of actinomycin D in solution has been confirmed on the basis of NOEs seen in NOESY spectrum of the drug.

Energy calculations have shown that both drugs, daunomycin as well as actinomycin D, prefer C,G containing binding sites. However, the specific sequence of preferential sites is being found different for two drugs. Theoretical calculations for probes into helix unwinding capacity for both drugs suggest value of $\Delta\alpha$ -unwinding angle- as around 10° and 28° for daunomycin and actinomycin D, respectively. These observed values of unwinding angles are well in accordance with that calculated and reported by other workers using X-ray and other theoretical methods.

ACKNOWLEDGEMENTS

Too often we forget how much a spontaneous word of appreciation can mean and I am not an exception, but today I take this opportunity to express my gratitude in black and white, to all, who have contributed in making this tedious task, a success. Their efforts are reflected on almost every page of the thesis and I am grateful for their time, their patience and their willingness to help. It is physically impossible to list out every name but certain people deserve citation. To the remainder, willingly or unwillingly unsung, my apologies and my grateful thanks.

It is my distinct privilege to have had the meaning of research and education exemplified to me by my thesis advisor, Dr.(Mrs.) Ritu Barthwal, Head, Department Of Biosciences and Biotechnology, who through her teaching, research and writing, planted the seed that grew into this thesis. Her imaginative vision, perceptive guidance and generous encouragement deserve special recognition and thanks. It is but for her great judgement and consummate skill that this work has reached from initial speculations to a stage of reality. I express my inestimable reverence to her.

I venerate and thank Prof. C.B. Sharma (Ex. Head, Dept. of Biosc. & Biotech.) for his constant encouragement and providing me required inhome research facilities.

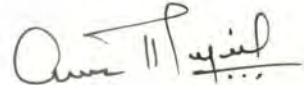
Financial assistance from Department of Science and Technology (DST) is fully acknowledged.

I have enjoyed working with my labmates- Shrikant and Anita, who cajoled and cudged to make my task simpler. I thank them for a friendly environment at work.

My belligerent but loving friends of BAD COMPANY kept my emotional and intellectual batteries charged in my most difficult times and never let me relax with a false feeling that 'I knew it all'. Though, it would take pages to pen down each and every name, deepfelt thanks are due to Navin, Hari, Veerkishan, Vipendra, Naren, Sorabh, Tariq, Kenneth and Sandeep Modi. Simultaneously, I remember all of my friends at TIFR, Bombay who made my stay there- a fiesta.

I don't find words to express my tender feelings of gratitude for Meenakshi, who has given generously of her time to help in more ways than I recount. Here, I put on records my admiration, sentiments for her assistance, emendation, incitement, inspiration, silence and support which, given in proper measure at the proper time, helped no end to bring this dissertation to fruition.

My family has contributed much to this thesis, both tangible and intangible, visible and (except to me) invisible ways. My mother has tolerated and provided much over the years including love and support. To all of them, goes my deepest sense of gratitude, love and thanks.


(ANWER MUJEEB)



CHAPTER 1

GENERAL INTRODUCTION

"To treat disease methodically and effectively, the nature and actions of the living tissues, in both the healthy and morbid conditions, must be correctly appreciated; the effects, which the articles of materia medica are capable of exerting under both these conditions, must be known from accurate observations, and not until then can the practitioner prescribe with any well founded prospect of success".

- ROBLEY DUNGLISON

October 15, 1839.

Crystal clear it is, that much of present day cancer chemotherapy relies heavily on inhibition of nucleic acid synthesis or interference with mitosis as a means of discriminating selectively against fast growing tumour cells. There is much pharmacological evidence from cytological, antimitotic and mutagenic effects, and the inactivation of viruses, indicating that DNA is the principal cell target for many antitumour agents. In this process, these agents impair the ability of DNA to act as a template for the processes of nucleic acid expression and synthesis - hence a diminution of cell growth is produced, with even cell death as an eventual outcome in some instances. Many of these have been the subject of intensive and increasing study over a period of time for two principal reasons; firstly, they have proved to be

powerful probes of nucleic acid structure and function and secondly, a number of them have clinically useful chemotherapeutic properties, of which anti-cancer activity is most prominent.

Anticancer agents, both naturally occurring and synthetic, which are employed clinically in treating cancer, fall into six broad categories (1) antibiotics (2) alkylating agents (3) antimetabolites (4) specific mitotic inhibitors (5) steroidal hormones and (6) are miscellaneous drugs such as cis-platinum complexes [121]. Out of these six classes (1) and (2) act primarily on DNA while members of (4) and (6) classes may do so. Alkylating agents were among the first clinical agents of recognised value and the study of their mechanism of action has clarified our view of cancer chemotherapy. It has led to increased understanding of DNA chemistry, structure and conformation and to the investigation of mechanism of repair of damaged DNA. Sulphur mustard, nitrogen mustard, chlorambucil, triazenes, azaridines and nitrosoureas are the examples of alkylating agents. The $-N(CH_2CH_2Cl)_2$ grouping of nitrogen mustard undergoes cyclisation in aqueous media to form aziridium ions - a representative of active forms of aziridine drugs as well, which attack electron rich centres in biological macromolecules. The property of Nitrosoureas of passing the blood barrier renders them to be especially useful in the treatment of central nervous system neoplasms, brain tumours and intracranial metastases.

The examples of antibiotics, which exert anticancer action, can be further classified in subclasses as (1) Quinone antibiotics (2) Streptonigrin (3) Saframycin A,C and (4) peptide and glycopeptide antibiotics and (5) Pyrrolo (1,4)-benzodiazepine antibiotics. Probably, the best known antibiotics used for the treatment of cancer are the anthracyclines, falling under subclass- quinone antibiotics, and comprising a large family including daunomycin, adriamycin, aclacinomycin and carminomycin. Mitomycin C, another quinone antibiotic, isolated from *Streptomyces caespitosus* is effective against a range of neoplasms including chlorioepithelioma, reticulum cell sarcoma and seminoma. Mytomycin C and its methylated homologue, porfiromycin are used clinically for treatment of malignancies of the breast, lung, colon and stomach. Streptonigrin, which is isolated from *Streptomyces flocculus* has received only limited use as an anticancer agent owing to its severe toxicity, but study of its mechanism of action on DNA has provided insight into the action of many other clinically important quinone antibiotics. Selective metal sequestration of streptonigrin provides a charged complex which binds to DNA. Streptonigrin was the first antitumour antibiotic for which it was shown by the ethidium binding assay that once bound to DNA, it is subject to an NADPH - mediated reductase action converting the quinone to a hydroquinone. The latter form of antibiotic is readily oxidised and causes single strand breaks in DNA. The saframycins, which are isolated

from *Streptomyces laevendulae*, comprise a family of five heterocyclic bis-quinone antibiotics. Two members of this group, saframycin A and S show promising anticancer activity against Ehrlich ascites tumour, murine L1210 and P388 leukemias and B16 melanoma. Saframycin A exhibits acid-catalysed equilibrium binding to DNA, reversible covalent binding to DNA in a base and groove-specific manner and also bio-reductive activation accompanied by DNA scission by a free radical pathway. Saframycins A and G reduced *in-situ* with NADPH cause oxygen dependent single strand breaks (but not double strand breaks) in supercoiled DNA.

The group of peptide and glycopeptide antibiotics includes bleomycin and tallysomycin as well as neo-carzinostatin, a polypeptide antibiotic, which binds to DNA and causes an oxygen-dependent single strand scission. Carrinophilin is another antitumour antibiotic produced by *Streptomyces sahachiroi* inhibits the growth of a wide spectrum of neoplasms in mammals and has been used clinically to treat human skin cancer, cancer of jejunum, reticulosarcoma and certain cases of chronic leukemia, produces interstrand cross-links in DNA and does not require enzymatic activation showing a preference for binding to G, C rich regions of DNA.

Pyrrolo (1,4) - benzodiazepine antibiotics - viz. anthramycin and tomamycin have been isolated from *Streptomyces refuincus* var. *thermotolerans* and *Streptomyces chromogenes* var. *tomamyceticus* respectively. Other members of this group are

sibiromycin and the neothramycins A and B. A structural feature common to all these antibiotics is the pyrrolo (1,4) - benzodiazepinone nucleus. The increasingly important role of anthramycin in chemotherapy has generated further interest in the molecular mechanism of action of these agents. They bind reversibly in the minor groove of DNA and preferentially at GC rich sites in an acid-promoted reaction.

An example of cytotoxic alkaloids exerting anticancer effect, is camptothecin. Camptothecin is isolated from the bark and stem wood of *Camptotheca acuminata*, a tree native to China. Camptothecin inhibits the growth of numerous experimental tumours and is used actively in the clinical treatment of cancer. Study of pharmacology of camptothecin reveals rapid inhibition of nucleic acid synthesis, fragmentation of DNA *in vivo* and lack of effect of camptothecin on proteins and replicating enzymes, strongly indicating that nucleic acids are the principal targets for the alkaloids.

DAUNOMYCIN

The antibiotic daunomycin - a subject to study here - and its 14 - hydroxy derivative adriamycin are highly cytotoxic compounds isolated from strains of *Streptomyces peucetius*. Whereas, the parent compound is restricted in its clinical usefulness to treatment of acute lymphocytic and myelogenous leukemia. Adriamycin is remarkable for its exceptionally wide spectrum of activity. It displays significant effects against

a variety of solid tumours, including several unresponsive to chemotherapy. These drugs are believed to exert the primary effect of inhibiting neoplastic cell growth by interacting directly with DNA. The *in vitro* growth of a number of normal and neoplastic cell lines is markedly inhibited by daunomycin. This inhibition is characterized ultrastructurally by cell damage, chiefly to the nucleus. Phase contrast and electron microscopy, and autoradiography have shown that chromosomal binding and damage, is the primary effect produced. Subcellular localization of daunomycin in cultured fibroblasts has shown exclusive uptake in nuclei and lysosomes, with a higher proportion of the former drug being localised in nucleus.

ACTINOMYCIN D

The actinomycins constitute a well known class of antibiotic metabolites isolated from several streptomyces. Actinomycin D-which is another drug subjected to investigations here - is produced by *Streptomyces parvulus*. It came into medical prominence as it proved to be extremely effective in certain kinds of cancer, viz. chloriocarcinoma. The extreme toxicity of actinomycin D has precluded its wider clinical use. Efforts have been made to understand its chemistry and biological action in order to reduce its toxicity while maintaining its biological activity. It has quite often been employed in molecular biology as a probe of nucleic acid functional processes. Actinomycin is believed to inhibit the

DNA directed RNA synthesis, specifically formation of mRNA. It also stops the production of RNA and ribosomal RNA. The mode of action is binding with DNA and thereby inhibiting the RNA polymerase enzyme from performing the building of RNA chains. However, role of two pentapeptide chains linked to phenoxazone chromophore in actinomycin, has been a matter of controversy since long.

ROLE OF NMR SPECTROSCOPY IN THE STUDY OF BIOLOGICAL SYSTEMS

Over a quarter century back, the nuclear magnetic resonance (NMR) experiments were described with biological macromolecules, and it was well anticipated that NMR method has the potentialities for studies of structure and dynamics of biopolymers such as proteins and nucleic acids and intermolecular interactions with these biopolymers. However, with a slow early progress, the technique has reached to its zenith where it has become possible to predict a three dimensional structure for a sufficiently large molecule or an adduct often a result of biomolecular interactions; entirely from NMR experiments. It relies on sequence-specific resonance assignments - for nucleic acids - of NMR signals and a knowledge of their chemical structure. The adaptation of two dimensional (2D) NMR techniques, soon after some initial reports (1,2), for the studies of bio-macromolecules has greatly enhanced the practicability of this approach. The great advantage of NMR technique lies in the truth that

molecular structures can be observed under actual biological conditions as being in solution form and even structural and biochemical changes in intact cells (*in vivo* NMR) can be monitored.

Characteristic resonance can be obtained from each magnetic nucleus in a biomolecule. The most commonly used resonances in NMR studies are ^1H , ^{13}C , ^{31}P , ^{15}N and also ^2H and ^{19}F in the molecules made labelled chemically or biosynthetically. Labelling here is subject to the fact that it should not disturb the biological properties of the molecule. ^1H -NMR gives rise to an envelope of overlapping lines in the region of 0-10 ppm. The spectral dispersion is greatly dependent of magnetic field strength. The advent of superconducting magnets has greatly promoted proton NMR by providing enhanced resolution. ^2H -NMR can be observed under proton decoupling by preparing deuterium labelled molecules by chemical or biosynthetic methods. The deuterium quadrupole moment causes hyperfine splitting due to residual interactions in partially ordered biological structures. A larger spectral dispersion of chemical shifts is observed in ^{13}C -NMR. However, the relative sensitivity - signal to noise ratio - remains poorer in ^{13}C -NMR as to ^1H -NMR. In ^{15}N -NMR chemical shifts are sensitive to primary structure as well as molecular conformation. Although nitrogen occurs in almost all biological molecules, yet due to low natural abundance (0.36%) of ^{15}N ($I=1/2$) and a low sensitivity has led to difficulties

in its detection and thus limiting applications of ^{15}N -NMR. ^{31}P NMR stands as an ideal probe for biological systems with spin $1/2$, 100% natural abundance, moderate relaxation times, a wide range of chemical shifts and non-interference from solvent peaks. Unlike ^1H and ^{13}C , phosphorus is present in a few biological molecules. This becomes obviously advantageous since one has to deal with fewer resonances and problems of assignments are almost non-existent. Adenosine di- and tri-phosphates (ADP and ATP) are the phosphorus - compounds which play a major role in energy storage and energy utilisation while phosphate metabolites are involved in glycolytic pathways. In ^{31}P -NMR chemical shifts are sensitive to the molecular conformation of the phosphate group, whereas, in partially ordered systems, the line widths reflect the orientation of the chemical shift tensor; thus ^{31}P NMR also becomes very informative in case of nucleic acid structure elucidation since backbone structure of RNA and DNA contains phosphorus nuclei.

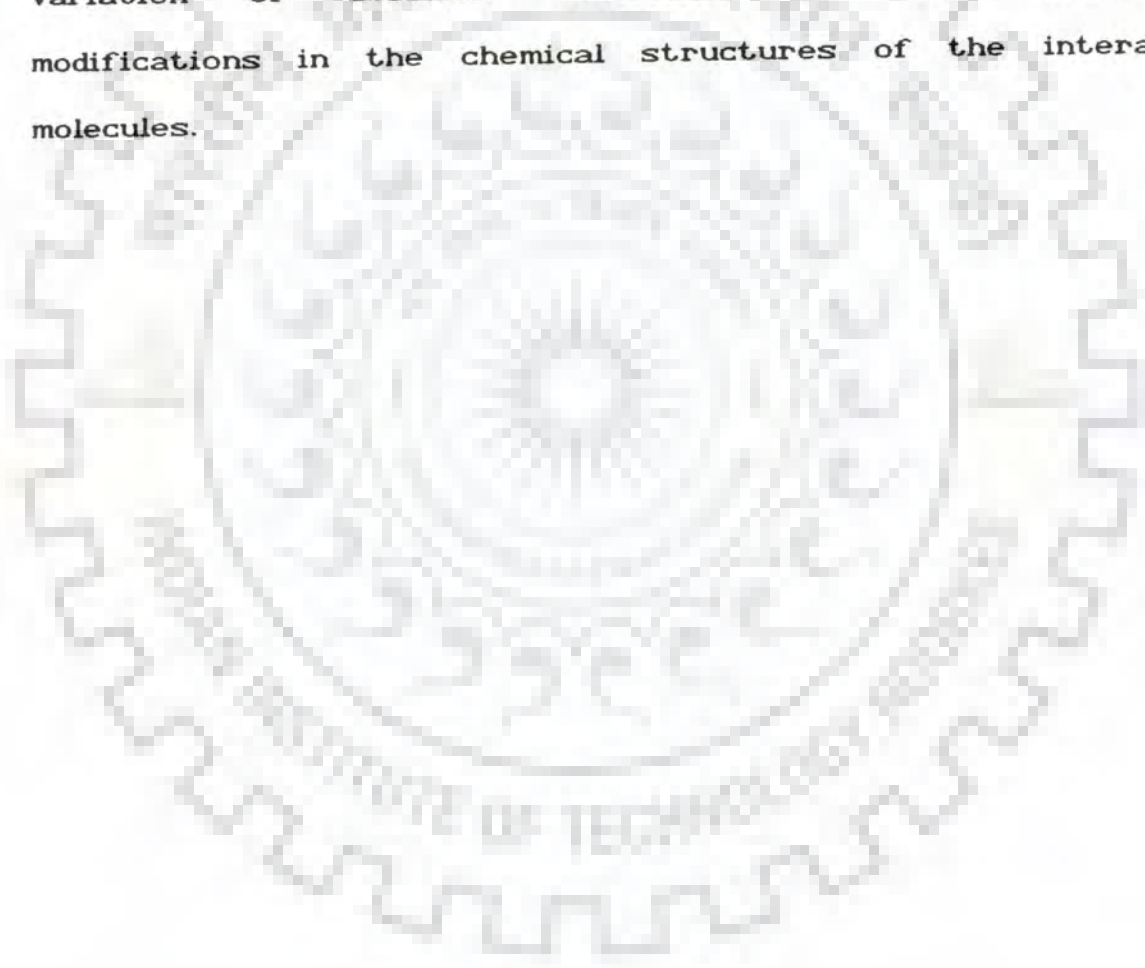
BIOMOLECULAR INTERACTIONS AND NMR

Among the early applications of NMR in biology, studies of intermolecular interactions has a prominent role. The range of potential applications is almost boundless including the prime interest in studies such as Drug - nucleic acid interactions in cancer chemotherapy and regulation of nucleic acid functions by specific interactions with proteins. Using modern NMR techniques, contribution can be made towards

detailed information on structural, thermodynamic and kinetic aspects of molecular interactions in such systems. In drug - DNA interaction studies, the structure and conformation of free drug molecule as well DNA fragments can be established by NMR and parallel studies on complexed form of both drug as well as macromolecule provide an insight of specific changes occurring in conformation and chemical behaviour of these molecules due to complexation. Sequence - specific ^1H -NMR assignments in the complex provide spectroscopic probes for distinguishing between different modes of drug binding. Qualitative analysis of intramolecular ^1H - ^1H NOE's can therefore provide direct evidence for distinguishing between intercalating drugs, which are sandwiched between neighbouring stacked base pairs, and drugs binding to outside of the DNA, lining either the major or minor groove. Independent evidence for distinguishing between intercalating drugs and outside binding drugs can be obtained from the imino proton chemical shifts : Intercalation causes upfield shifts, outside binding causes downfield shifts.

Since the interacting species may undergo reversible associations and the stability of the complexes may vary over a wide range, depending on solution conditions such as pH, ionic strength and temperature, NMR may be used to monitor the thermodynamic and kinetic stability of the complexes formed under different experimental conditions and to define optimised solution conditions.

Thus, it can be well justified that nuclear magnetic resonance (NMR) spectroscopy provides a powerful probe and outstanding potentialities for studies of intermolecular interactions with biopolymers. In particular with nucleic acids, these might turn out to be the biologically most relevant use of sequence-specific resonance assignments. It is further a big advantage of NMR that it allows extensive serial studies with variation of solution conditions or with symmetrical modifications in the chemical structures of the interacting molecules.



CHAPTER 2

LITERATURE REVIEW

General Review

The interaction of drugs with nucleic acid has been studied by a wide range of spectroscopic techniques and theoretical methods. The work has a special emphasis on the drugs which intercalate into DNA. The word 'intercalation' comes from Greek and literally means 'to insert between'. Thus an intercalating drug is one in which the planar portion of the drug molecule is inserted between the adjacent nucleic acid base pairs of a double stranded-region of DNA or RNA helix, although, the word intercalation is also used for situations in which an aromatic molecule is inserted between adjacent bases on a single-stranded nucleic acid. In 1971, Kreishman et al. [1] made a proton magnetic resonance study of the interaction of ethidium bromide with 3'-5' UpU and Polyuridylic acid and revealed that EthBr forms vertically stacked aggregates of the phenanthridium rings with uridine, 3'-uridine, 3'-uridine monophosphate and 5'-uridine mono-phosphate. Evidences for an intercalated complex with EthBr molecule sandwiched between adjacent uracil bases and oriented with the H(1) and H(10) protons of EthBr directed at the ribose-phosphate backbone of the dinucleotide UpU and Poly U, were produced. Binding of EthBr with C, G containing sequences were studied by Patel et al. in 1976 [2] by NMR for

different N/D ratios. Complex formation resulted in upfield shifts for the base protons at the terminal and internal base pairs of d-CGCG sequence and variable temperature NMR observations have shown an increase in transition midpoint for the duplex to strand conversion. Stronger binding of EthBr was observed to the self complementary d-CGCG (2 dC-dG intercalation sites) and d-CCGG (1 dC-dG site) duplexes compared to the d-GGCC with no dC-dG site. These studies suggested the sequence specificity of the drug to dC-dG. In 1977, same workers reported the sequence specific intercalated complex of proflavin with d-CCGG and d-GGCC [3]. They also proposed an approximate overlap geometry between the proflavin ring and nearest neighbour base pairs at the intercalation site from a comparison between experimental NMR chemical shift values and those calculated for various stacking orientations. In same year, Patel also observed the proflavin intercalation into Poly (dA-dT) by melting transition of the complex [4]. The NMR chemical shifts and line widths of nucleic acid base and sugar proton resonances and the proflavin ring protons were monitored at different Phosphate/Dye (P/D ratios - 24 and 8 in 2M salt solution.

Kallenbach et al. [5] in year 1978, deduced the structure of some mutagen-nucleic acid complexes. 9-aminoacridine complexed with d-GC, d-CG and d-ATGCAT, has shown upfield shifts in NMR chemical shift values, indicative of intercalative binding with a preference over GC site. Sugar pucker geometries at the intercalation site of propidium

di-oxide into miniature RNA and DNA duplexes in solution were probed [6] and found to be C3'-endo (3'-5') C2'-endo. In a series of X-ray studies of drug-nucleic acid interactions, Sobell et al. [7,8] reported the crystalline complex structures of 9-aminoacridine and proflavin with dinucleoside monophosphates, 5'-iodocytidyl(3'-5')guanosine. 9-amino group of acridine was found lying in the narrow groove of the intercalated base-paired nucleotide structure. Mixed sugar puckering patterns were observed in both cases with a twist angle between base pairs of about 10° and 36° in 9-amino acridine and proflavin complexes respectively.

Neidle et al. [11] determined the crystal structure of a 3:2 complex of the frame shift mutagen proflavin with the dinucleoside phosphate cytidyl-3'5'-guanosine. Complex was found having one drug molecule intercalated between Watson-Crick base pairs of the nucleotide duplex. Other two proflavin molecules were bound to the exterior of the miniature double helix.

The high-resolution crystal structure of the intercalation complex between proflavin and cytidyl-3'5'-guanosine (CpG) studied by Thermal motion analysis [12] reveals informations on the translational and vibrational motions of individual groups in the complex. The translational eigenvector T3 of the intercalated proflavin being directed toward the major groove of the CpG complex, suggests major groove approach of binding. In another effort, acridine-oligonucleotide

interactions, by NMR, were studied by Lancelot et al. [13], in year 1986. It was found that oligodeoxynucleotide d(TATC) was covalently attached to the 9-amino group of 2-methoxy-6-chloro-9-aminoacridine through its 3'-phosphate. Proton assignments were done by 2D NMR COSY and NOESY connectivities and it was derived from relative intensities of COSY and NOESY contour maps that duplex d(TATC) - d(GATA) adopts a B-type conformation and deoxyriboses preferentially adopt C2'-endo conformation. On way of study of DNA binding of non-intercalating drugs, Sasisekharan et al. [14] observed that interaction between a synthetic analogue of distamycin and DNA (Poly dA-dT and Poly dG-dC) cause red shift in UV spectrum and an induced CD band appears in 300-350nm region. It was suggested that interaction takes place through minor groove and partial loss in A-T base specificity might be existing due to replacement of N-methyl pyrrole of distamycin by benzene or due to increased curvature in backbone of ligand as a result of this replacement. Dhingra et al. [15] studied the interaction of puromycin and puromycin aminonucleoside with Poly A by proton NMR and found that certain resonances are shifted upfield in the complex while H8 of Poly A is shifted downfield. These observations were rationalised through an intercalative model for the complex in which the base of puromycin or puromycin aminonucleoside is sandwiched between the adjacent adenines on the poly A chain. An interaction of quercetin with DNA have shown an initial stabilising effect on its secondary structure but prolonged treatment was observed to lead to an extensive disruption of

the double helix, in the studies made by Alvi et al. [16]. Jones et al. [17] in 1987, investigated the site specificity of binding of antitumor antibiotics viz. Steffimycin B, adriamycin, echinomycin and ethidium bromide with DNA by CD first neighbour analysis. Ethidium bromide was found displaying non specific intercalation, while first three anti neoplastic antibiotics exhibited binding to sites comprised of guanine and cytosine. Efforts were made by Mendel et al. [18] to find evidence for Hoogsteen base pairing at echinomycin binding sites in DNA restriction fragments and it was found that sites were hyperreactive to diethyl pyrocarbonate which might have been due to an altered form of right handed DNA that is entirely Hoogsteen base paired.

Proton and ^{13}C NMR were used as investigative probe by Reid et al. [19] for studying neomycin B's interaction with phosphatidyl inositol 4,5-bisphosphate. A method of evaluation of parameters of complex formation and equilibrium association constants was suggested by Veselkov et al. [20] for proflavin and ribonucleotide monophosphate complex by NMR. Most favourable structures were determined for 1:1 and 1:2 dye-nucleotide complexes. Delepierre et al [21] investigated the intercalation of a 7H-pyridocarbazole monomer [(piperidyl)-2,1-ethane-yl-(10-methoxy-7H-pyrido[4,3-C] carbazolium)dimethane sulfonate] into d-(CpGpCpG)₂ minihelix, by 270 MHz and 400 MHz proton NMR. Strong upfield shifts observed on most aromatic resonances of both the drug and the nucleotide and nuclear Overhauser effects induced in some drug

resonances by irradiation of sugar protons confirms the intercalation of the 7H-pyrido carbazole monomer in base-paired minihelix d-CGCG. An important cancer chemotherapeutic agent, adriamycin, was found to interact with specific calcium binding proteins, in the plasma membrane of GH3/B6 pituitary tumor cells [23]. It was suggested that, the calcium binding site at the outer surface of the membrane is collisionally accessible to freely diffusing adriamycin and the toxin receptor site is located near the bound calcium ion. Binding of DNA restriction fragments (147 base pairs and longer) with ethidium bromide has been investigated recently by Slobodyansky et al. [24] by CD and Polyacrylamide Gel Electrophoresis (PAGE).

Proton resonance assignments in the NMR spectra of self complementary hexadeoxyribonucleoside pentaphosphate d(5'-3')-(GCATCG)₂ and its complex with the antibiotic nogalamycin, together with interproton distance constraints obtained from 2D-NOESY spectra have enabled Searle et al. [25] to characterize the three dimensional structure of these species in solution. Two drug molecules per duplex were found to be bound. Nogalamycin was found intercalated at the 5'-CA and 5'-TG steps with major axis of the anthracycline chromophore aligned approximately at right angles to the major axes of the base pairs.

Studies on Daunomycin & its Complexes

The investigations on structure of antitumor antibiotic - daunomycin and its interaction with nucleic acids cover a wide range of spectrum of techniques and approaches used so far. In 1964, Iwamoto et al. [26] elucidated the structure of daunomycin molecule from the results of 220 MHz NMR spectrum. They also proposed a stereochemical arrangement at the anomeric carbon atom of the sugar moiety daunosamine in daunomycin. This structure was reported in deuterated chloroform (CDCl_3) used as solvent. Crystal structure of daunomycin reported by Neidle et al. [27] in 1977, confirmed the structure suggested earlier with some substantial conformation differences. An intra molecular C(7)...O(9) hydrogen bond was invoked to account for a significantly stable molecular conformation. Different interatomic distances were also measured and reported. In a simultaneous study on 9-aminoacridine, quinacrine, proflavin and daunomycin, Bohner et al. [28] saw the effect of these intercalating compounds on DNA polymerase I and compared the results with the binding of these acridines with native DNA, which exhibited the inhibition of DNA polymerase. High resolution NMR studies on daunomycin - Poly (dA-dT) complex [29] suggested that either ring B and/or C of chromophore of daunomycin overlaps with adjacent nucleic acid base pairs. It was observed that a bulky halogen atom substitution at position 5 of the pyrimidine ring of synthetic DNAs does not perturb the intercalation of the antibiotic into poly (dA-dU). Contribution of electrostatic interaction

between amino sugar and phosphates of DNA backbone was also demonstrated by replacing NH_3^+ group at amino sugar of daunomycin molecule by dimethylglycine. X-ray investigations carried out by Quigley et al. [30] in 1980 on dCGTACG and its complexes with daunomycin revealed dramatic changes in sugar conformations of oligonucleotide and change in helix sense from B DNA to A DNA on complex formation. Mixed sugar puckering in complex was observed in which C1 sugar was C2' endo, G2 was C1' exo, T3 was O1' endo, as G2' endo, C5 as C2' endo and G6 was found to be C3' exo. Different glycosidic bond rotation values were also calculated and reported.

The helix-coil transition of the self complementary hexanucleotide d(pTpA)₃ has been studied by proton magnetic resonance spectroscopy [31]. It was seen that at 5°C, the effect of excessive fraying is evident since the central base pairs exhibit only 20% of the chemical shifts observed for poly (dA-dT). Poly (dA-dT) accompanying denaturation. Daunomycin interacted with hexanucleotide duplex at 5°C and stabilised it by 21°C at a drug/nucleotide ratio of 0.063. It was suggested that ring D of daunomycin does not overlap significantly with the central base pairs of the hexanucleotide and that it 'extends out' from helix. In another ¹H and ³¹P NMR study of daunomycin and Poly (dA-dT) complex [32] demonstrated that phenolic hydroxyl of anthracycline form intramolecular hydrogen bonds with quinone carbonyls and are shielded from solvent in the intercalation complex. A site specificity for alternating purine -

pyrimidine bases with neighbour exclusion was also reported. These observations were found in agreement with the structure of daunomycin dC-dG-dT-dA-dC-dG hexanucleotide crystalline complex, published by Quigley et al. [30]. Patcher et al. [33] used viscometric and fluorometric techniques to investigate deoxyribonucleic acid interactions with some anthracyclines like adriamycin, marecellomycin and aclacinomycin etc. Denaturation of calf thymus DNA and increasing ionic strength resulted in a marked decrease in DNA binding affinity to all the anthracyclines under investigation. It was observed that intercalative and electrostatic interactions are both important in the DNA binding. Viscometric studies indicated that under high ionic strength conditions which negated electrostatic effects, all drugs induced an unwinding - rewinding process of the closed superhelical PM-2 DNA. In an important report by Chaires et al. [34] the self association in daunomycin aqueous solution was reported. Self association was observed at concentrations greater than 10 μ M. The characterization of this aggregation was made on the basis of visible absorbance, sedimentation equilibrium and proton magnetic resonance (NMR) experiments. NMR data have shown that the aromatic protons of the anthracycline portion of the drug are most affected by self association, probably due to stacking of the anthracycline rings. Equilibrium dialysis and fluorescence titration were used to study daunomycin - DNA interaction by the same group of Chaires et al. [35]. Neighbour exclusion model, proposed gave an exclusion parameter of three to four base pairs.

Temperature monitored kinetics of the complex found the binding to be exothermic. Complete dialysis experiments have described that GC base pairs were preferred more as binding sites for the drug. Daunomycin binding to nucleosomes was also investigated [36] and was found to be extremely reduced, relative to the affinity for free DNA. Complex of daunomycin with H1-depleted 175 base pair nucleosome was studied and found that early melting transition of nucleosome is preferentially stabilised by daunomycin as well as ethidium bromide low levels, however, more pronouncely by EthBr. Dichroism and rotational relaxation time measurements indicated that daunomycin unfolds nucleosomes and nucleosome elongates along the DNA superhelical axis. Levels of daunomycin greater than about 0.15 per DNA base pair were found to promote nucleosome aggregation. It was proposed that daunomycin, because of its special intercalation geometry, strongly prefers free DNA regions over the bent helices found in nucleosomes and chromatin. This preference might be causing an increased local concentration of the drug in the genetically active regions of nuclear DNA, and presumably the abundance of such regions in tumor cells makes them sensitive to daunomycin. Daunomycin was also found to inhibit B-Z transition in poly d(G-C) by chairs et al. [37]. It was observed that both rate and extent of transition are decreased by the drug and under some conditions, daunomycin can convert Z form DNA back to B form. Slow and highly cooperative binding of daunomycin was consistent with a role for it as an allosteric effector on the B-Z equilibrium. Fluorescence and

absorbance analysis of interaction of daunomycin with calf thymus DNA was made by Chaires et al. [39]. The Von't Hoff analysis provided estimates for the enthalpy of the binding reaction over the NaCl range of 0.05-1.0 M. Daunomycin binding was exothermic and favourable binding free energy arose primarily from the large negative enthalpy. Observed thermodynamic parameters were considered as contributions of hydrogen bonding interactions at intercalation site. Transient electric dichroism study revealed that DNA binding drugs also effect the folding of chromatin from 10-30nm fiber [40]. It may be processed by drugs alone or in conjunction with multivalent cations. Daunomycin in accordance with actinomycin and distamycin inhibits compaction of chromatin beyond a critical point. In a rigorous $^1\text{H-NMR}$ study [41,42] conformation of daunomycin and its analogs was reinvestigated by Mondelli et al. recently. NMR studies were made, using different solvents, CDCl_3 , D_2O , DMSO, dioxane and pyridine etc., and using $^1\text{H-}^1\text{H}$ three bond and long-range coupling constants, the geometry of ring A of daunomycin chromophore, in each solvent was established. Intramolecular hydrogen bond 9-OH...O(7) and steric interactions between peri substituents on the A and B rings were recognized to be responsible for determining the conformation of ring A. Preferred conformation of sugar with respect to aglycone moiety were also determined for N-acetyldaunomycin, by transient nuclear Overhauser experiments.

It has also been reported recently that daunomycin inhibits on the late steps of RNA chain initiation during RNA-polymerase catalysed synthesis of RNA [43]. *In vitro* RNA synthesis from the A promoters of T7 bacteriophage by *Escherichia coli* RNA polymerase was found to be strongly inhibited by daunomycin. In another recent communication [44] polyelectrolyte effects on the intercalation equilibrium of interaction of daunomycin with synthetic alternating DNA sequences have been reported using fluorometric and UV-visible absorption method as investigation probes. Intercalation of drug reported here is anticooperative. Stoichiometry of binding was found to be one drug molecule for two base pairs. Binding affinity shown by the drug for different sites indicated a stabilising effect of the -CH₃ group on position 5 of the pyrimidines. The effect and influence of temperature and ionic strength on the free energy of complexation has also been examined.

Studies on Actinomycin D & its Complexes

Antitumor antibiotic actinomycin D, another pharmacologically important drug has been so far a subject of rigorous studies on its mode of binding to DNA and several reports on its behaviour have been found in the literature which are often found to be conflicting. In 1968, Miller et al. [45] studied the binding of actinomycin and its several analogs to DNA by equilibrium, kinetic and hydrodynamic methods and it was found that actinomycin binding can occur adjacent to any GC pair, but at a given site, binding produces a distortion of the

helix that greatly disfavours binding of another actinomycin molecule closer than six base pairs away. The source of this distortion was probably a pair of hydrogen bonds formed between the deoxyribose ring oxygens and the $-CONH_2$ groups attached to the chromophore. Probability of existence of several forms of the complex at equilibrium was proposed. A conformational change in peptide rings to adapt their structure to interact specifically with the DNA backbone was also not ruled out. Arison et al. [46] achieved complete assignment of nuclear magnetic resonance spectrum of actinomycin D in various organic solvents and in water at low temperature as well as at room temperature. Interactions of actinomycin D with 5'-deoxyguanylic acid was also reported and it was shown that complex formation occurs by base stacking and the pyrimidine ring is located above and below the phenoxazone chromophore of the drug. Proton NMR studies were extended by Angerman et al. in 1972 [47] to observe the aggregation of actinomycin in D_2O . At 220 MHz proton magnetic resonance results of concentration, pD , salt and temperature dependence of actinomycin in D_2O , unearthed that actinomycin D aggregates to form a dimer at concentration $4.6 \times 10^{-3} M$ and temperature and $18^\circ C$. It was further concluded that the actinoacyl groups further stack vertically in the dimer with one chromophore inverted with respect to the other. Sobell H.M., a pioneer worker in X-ray crystallography was successful to propose a three dimensional picture of actinomycin crystal (48). Different models for its binding with DNA were also proposed. Variable temperature 1H -NMR and

³¹P NMR were implied by Patel [49] to investigate the complex formation between actinomycin D and the deoxyhexanucleotides d-*ApTpGpCpApT* and d-*pGpCpGpCpGpC*. NMR spectra of complexes were also recorded in H₂O to observe ring-NH resonances. The stoichiometry of the complex was determined to be 1:2 Act D-hexanucleotide in solution. On the basis of large chemical shift difference, complexation site was suggested to be central GC base pairs. Patel extended his proton and phosphorus NMR studies of CG containing tetra and hexanucleotides for helix-coil transition complex formation with actinomycin D [50]. The loss of two fold symmetry of tetranucleotide duplex was observed on complex formation. An inhibition of synthesis of ribosomal proteins by actinomycin D was observed by Tsurugi et al.[51]. Actinomycin D treatment resulted in decrease of *in vitro* incorporation of labelled leucine into the newly synthesised ribosomal proteins on rat liver ribosomes. Stereochemical aspects of actinomycin DNA binding, were summarised by Sobell et al. [52] that used the intercalative and kinked type geometries in binding to DNA. Mixtures of nucleotides complexed with actinomycin were studied by proton NMR and presented as models for the binding of the drug to DNA by Krugh et al.[53]. A competitive binding of actinomycin with adenine and guanine nucleotides was reported in which guanine showed stronger binding than adenine nucleotides to the quinoid portion of the phenoxazone ring of drug. Krugh et al. in 1977 extended these studies and made some paramagnetic induced relaxation experiments on actinomycin D-nucleic acid complexes [54]. NMR and ESR

experiments have shown that Mn (II) used as paramagnetic probe-binds approximately two orders of magnitude to the 5'-phosphate group than to the 3'-5' phosphodiester linkage of deoxy-dinucleotides. It was noted that in actinomycin D complexes with nucleotides the addition of Mn (II) ion did not result in any observable change in chemical shifts, which suggests that the geometry of the complex, remains unperturbed on addition of Mn (II) ions. Reinhardt et al. [55] made ^{31}P NMR studies on some actinomycin-dinucleotide complexes. The internucleotide phosphorus resonances exhibit individual resonances in the slow exchange at -18°C and downfield of resonances from free nucleotide internucleotide phosphorus. This indicated the formation of a miniature intercalated complex. Inhibition of transcription catalysed by RNA polymerase was also observed due to actinomycin [56]. Binding studies of actinomycin D to DNA [57] in presence of spermine and polyamine have shown that spermine, having a binding constant of 104 to DNA, can interfere with actinomycin binding causing a steric impediment. Polyamines were found to induce a DNA conformation that binds actinomycin D less efficiently. Chiao et al. have studied 7-aminoactinomycin [58] and binding with DNA by fluorescence, CD, absorption and proton NMR methods. The presence of 7-amino group on actinomycin caused a large increase in the value of dimerisation constant as compared to actinomycin D and it was indicated that dimer formation takes place with chromophores stacked in an inverted manner. Results of these partition technique experiments to study the binding of actinomycin D to both calf thymus DNA and

poly (dG-dC), were reported by Wimble et al. [59]. These results exhibited humped Scatchard plots, which were indicative of cooperative binding and consistent for drug induced allosteric transitions in the DNA structure. Cooperativity was found to increase with a decrease in sodium chloride concentration. Significant inhibition of translation of DNA by *E. Coli* DNA polymerase-I was observed due to actinomycin D action [60]. Takusagava et al. in 1982 [61] undertook the crystallographic analysis of the 2:1 complex between deoxyguanylyl-3'-5'-deoxycytidine, d(GpC) and actinomycin D. The complex was found to form an unusual pseudo-intercalated structure and it was explained why actinomycin can not bind to RNA, replacing deoxyribose of the guanosine to a ribose sugar, the O2' hydroxyl group was found having unusually short contacts with the amino group N-2 of the phenoxazone ring. For an intercalated model distance between H2' and amino nitrogen N-2 would be short, so it was found clearly impossible to replace guanosine deoxyribose by ribose. A direct technique was reported by Van Dyke et al. [62] for determining the binding sites of small molecules on naturally occurring heterogenous DNA, using methidiumpropyl - EDTA. Fe(II) [MPE.Fe(II)] for cleavage of double helical DNA with low sequence specificity. They determined preferred binding sites on a *RsaI* - *EcoRI* restriction fragment from pBR322 for actinomycin and two minor groove binders, netropsin and distamycin. Actinomycin afforded a specific inhibition pattern of 14-16 base pair long with protected regions centered around one or more G-C base pairs. In a ³¹P

NMR study of interaction of actinomycin with DNA, a new downfield peak was observed due to slow dissociation kinetics of the compound [63]. Biosynthetic analogue of actinomycin D, substituted at one or both of the 3'-amino acids with azetidine -2-carboxylic acid, pipercolic acid or 4-ketoproline for one or both of the prolines have also been investigated for their conformational properties [64]. The α and β pentapeptide lactone rings were found experiencing different magnetic environments in all the analogs studied. Mirau and Shafer [65] elucidated the role of actinomycin pentapeptides in its binding with nucleic acids alongwith kinetics of all the actinomycin analogs studied for their property of DNA binding. A possibility of cis-trans isomerisation about one or two peptide bonds was expected, determining the slow DNA binding kinetics. Scope of proton NMR spectral editing techniques was hunted by Reid et al. [66] for selective observations of N-H protons in an actinomycin D complex with d-(AGCT). Same workers also used saturation transfer and nuclear Overhauser effect (nOe) NMR techniques to assign some non exchangeable protons in the above stated complex [67]. Intermolecular nOe's were observed between drug chromophore protons and nucleotide protons, suggesting existence of an intercalated complex between from G-C base pairs of the nucleotide double helix. In a dodecamer d-(C-G-C-G-A-A-T-T-C-G-C-G), binding of actinomycin was observed to destabilise kinetically the A-T base pairs in the central core [68]. Activation energies for exchange of imino protons indicated that the mechanism for exchange is the

opening of individual base pair. Binding of actinomycin D with left handed Z DNA helix was found possible by Gupta et al. [69]. However, this binding appeared to be less efficient than in the case of intercalated B DNA and it was conjectured that actinomycin D can cause Z to B transition at lower concentrations. DNase protection technique proved to be useful for determining the sequence specificity of equilibrium binding of actinomycin D to pBR322 DNA [70]. G,C rich sequence fragment have showed high affinity for actinomycin molecule. In another report of Takusagawa et al.[71], X-ray analysis of a complex of d(ATGCAT) and actinomycin D was made. A patterson map was calculated from preliminary diffractometer data and packing considerations of an intercalated model of the complex. A non-planar chromophoric system in actinomycin molecule was interpreted in acetone and chloroform solution by Juretschke et al. [72]. Essential role of 2-amino group in defining this characteristic was observed. First two dimensional NMR study of actinomycin D and d-ATGCAT complex was reported by Brown et al. [73] in 1984. They observed no significant change in conformation of pentapeptide lactones between bound and free drug. Gorenstein et al. [74] used ^{31}P and ^1H two dimensional NMR for assignment of proton and phosphorus signals in actinomycin d-AGCT complex, in which they used phosphoryl labelled d(Ap[^{17}O] Gp[^{18}O]Cp[^{16}O]T). It was confirmed that the drug intercalates between the GpC stacked base pairs, with a major change in C5'-O5' torsional angles. In an important study made by Flamee [75] in 1985, action of actinomycin D on transcription of T7 coliphage DNA

by *Escherichia coli* RNA polymerase was investigated. It was observed that drug molecule bound to DNA sometimes stops the synthesis of RNA. In contrast, it was also seen that antibiotic is released before RNA polymerase detaches from the template DNA and enzyme was able to resume the synthesis of RNA chain. On the same lines, Sobell reported that during DNA transcription, actinomycin binds to a premelted DNA conformation present within the transcriptional complex [76]. It results in immobilisation of the complex, interfering with the elongation of growing RNA chains. Modification was also proposed that actinomycin binds not to B-DNA but β -DNA which is composed of β structural units, possessing mixed sugar puckering pattern (3'endo (3'-5')2'endo). Kostura et al. [77] found actinomycin D inhibiting the initiation of protein synthesis in intact, nucleated mammalian cells. This inhibition was found to be independent of levels of mRNA, ribosomes or tRNA. In a comparative kinetic and equilibrium study of binding of actinomycin D with some d(TGCA) - containing dodecamers, Chen F.M. [78] found that d(TGCA) sequence is a stronger binding and a slower dissociation site than the d(CGCG) sequence and suggested that base pairs flanking the dG-dC intercalative site may modulate interactions of the pentapeptide rings of actinomycin with the minor groove. In a recently reported X-ray crystallographic study of actinomycin crystals, Ginell et al.[79] made a refinement in the crystal structure of the drug. Crystals were found having three actinomycin molecules per unit cell with similar geometrical features. The phenoxazone ring

systems deviated slightly from strict planarity. In another recent study, complex of actinomycin D and d-ATGCGCAT was subjected to 2D NMR investigations by Scott et al.[80], and a unique 2:1 adduct was observed. Two peptide chains were distinguished and assigned. All base pairs of octanucleotide were observed retaining Watson and Crick type H-bonding, however conformational changes in oligonucleotide on complex formation were evident. Peptide interactions in a close-pack region were considered to be responsible for unique 2:1 species and negative cooperativity in binding.

Theoretical Methods

Apart from all experimental techniques which have been implied to study various drug-nucleic acid interactions, theoretical methods as minimum potential energy calculations, molecular graphics and various other approaches have also been involved in these investigations. The first hand requirement in such studies comes from knowledge of coordinate systems of the particular complex and X-ray crystallographic studies provide such vital informations using which a theoretical approach could be made. Sobell et al. [81,82,101,102,103,104,112] have extensively worked to elucidate crystal structures of various drug-nucleic acid complexes. Berman et al. [83] used computer graphics to determine the conformation of a CpG molecule with ARNA conformation and its interaction with proflavin. They found that alternate sugar puckering is not prerequisite for intercalation and in complexes two torsion angles (ϕ and χ)

differ in value from those found in ARNA. A theoretical examination of sequence specificity of ethidium was made by Pack et al. [84] in 1977. On the basis of stacking energy values between ethidium cation and the base pairs, the preferred sequence was found to be pyrimidine (3'-5') purine as compared to purine(3'-5')pyrimidine.

Theoretical calculations on binding positions, conformations and relative minimum binding energies for thioxanthenones, lucanthone, and N-methylucanthone, were made by Miller et al. [9]. The specificity for base pair sequences in intercalation complexes was attributed primarily to the energy required to open B-DNA to an intercalation site and secondarily to the orientation of the terminal protonated nitrogen towards the carbonyl oxygen on cytosine.

Miller [85] was able to generate an algorithm (AGNAS) for determination of structure of nucleic acids and has applied the same to the BDNA structure and a counter clockwise helix. These studies were further extended [86,87,88,89,90] for generating all possible geometrical conformations of BDNA type tetramer duplex for combinations of different sugar puckers. Conformations with minimum energy were chosen as candidates for intercalation sites and to rationalize neighbour exclusion principle. Some prerequisites for binding to DNA via intercalation mechanism were also proposed. Ornstein et al. [91] made some theoretical observation of enthalpy ΔH for the intercalation of ethidium cation into DNA minihelices. It was

found that favourable contribution of the ethidium cation minihelix intermolecular interactions is responsible for the overall favourable nature of the intercalation process. Nuss et al.[92] calculated empirical energy functions for ethidium, 9 aminoacridine and proflavin cations complexes with GpC and CpG, rationalising the base sequencing. During transcription, biological activity of nucleoside analogs was studied theoretically by electrostatic energy calculations by Sanyal et al.[93]. Charge distribution on the molecules was calculated by CNDO/2 method. Same research group has also worked extensively on theoretical calculations for different drug and nucleic acid complexes over past few years [94,95,96,97,98], using formycin B, oxoformycin, ellipticine, showdomycin and pyrazolopyrimidine antibiotics. Quantum mechanical charge distribution and intermolecular interaction energies of these antibiotics with nucleic acid bases and base pairs were reported. Broyde et al.[99] explored the mechanism of deformation of DNA by polycyclic aromatic carcinogenic agents. The method involved the computation of classical potential energies as a function of conformation alteration. Various contributions of Vander Waals, electrostatic, torsional as deoxyribose strains were also computed using CpG and GpC and representative examples. The energy contour maps obtained in the χ, ϕ plane revealed the approximate size and shape of conformation space. A simple geometric and potential energy analysis of insertion small planar moieties in nucleic acid chains presented by Taylor et al.[100] reveals an unusual conformational flexibility in the intercalated forms of

nucleic acids. Relatively mobile nature of the sugar - phosphate backbone together with the fairly long stretches of chemical bonds linking adjacent bases produced a large number of theoretically feasible planar binding sites.

A detailed theoretical investigation of protein-nucleic acid interactions by second order perturbation theory was made by Govil et al.[105,106,107] in 1984. Aromatic amino acids tryptophan, tyrosine, phenylalanine and histidine were subjected to study hydrogen bonding and stacking energies of their interactions with nucleic acid bases and base pairs. Observations of the affinity of these aromatic residues for different base pairs showed that G.C base pair has highest preference for binding. Out of pyrimidine, bases cytosine was found to form most stable complexes with above stated aromatic amino acid residues. Sequence selectivity of daunomycin and some other anthracene and phenanthridine derivatives binding with double stranded polynucleotides investigated theoretically by Chen et al. [108,109,110] revealed stronger binding of the drug with poly (dA-dT).poly (dA-dT) and poly (dG-dC).poly (dG-dC). Adriamycin also exhibited stronger complexation with mixed hexanucleotide d(CGTACG)₂. Carcinogen-base stacking and base-base stacking in dCpdG modified by (+)and(-)7 β ,8-dihydroxy-9 α , 10 α -epoxy-7,8,9,10-tetrahydrobenzo(a)pyrene, were delineated by Hingerty et al.[111] using minimised semiempirical potential energy calculations. Conformers were found in low energy regions of enantiomers. In a combined experimental

and theoretical analysis of conformation of d-CpG modified by a carcinogen, 4-aminobiphenyl, Shapiro et al.[112] observed that because of twisted nature of biphenyl moiety, the carcinogen-base stacking inherently involves less overlap than that in the planar and rigid analogs. Molecular mechanics simulations by Rao et al.[113,114] for anthramycin complexes with six different deoxydecanucleotides containing C,G bases have shown the binding through minor groove with minimal distortions in DNA helix. These complexes were characterised by a net work of hydrogen bonds between drug and nucleotides with good packing interactions. A model for explaining induction of the -2 deletion mutation observed in 2-acetyl amino fluorine modified *Escherichia coli*, was proposed by Broyde et al.[115] using energy minimal method and model building by computer graphics. Recently, Parbhakan et al.[116] used computer simulation molecular dynamics to see the large scale flexibility of DNA and intercalation of actinomycin D. Stretching and unwinding of B and Z forms of DNA through a dynamic conformational pathway were to open an intercalation site. Unusually, the stretching and unwinding of a 5'(CG)3' step was found more favourable than for GC site in BDNA. Affirmation of neighbour exclusion for intercalation was found as forming of second intercalation site requires larger energy than formation of first site. O1'endo sugar puckering was found favourable at intercalation site.

Although, an extensive survey of the available reports on drug-nucleic acid interactions provides a panoramic view and

broad way to explain these molecular mechanisms, yet, there is a need of further refinement of the problem to understand the ongoing processes at molecular level in the light of recently developed advance techniques like 2D NMR and computer simulation etc. This surely should help to pave the way to understand the molecular basis of drug action.

Scope of Thesis

In the light of present day knowledge of drug-nucleic acid interactions, informations still seem to be rather limited. Daunomycin structure and its binding preference over a range of base sequences show different results, reported by several research groups [31,37,40,43,44]. However, there is a general consensus for the preference of daunomycin for alternating pyrimidine-purine sequences. We have explored the structure of daunomycin and actinomycin D and studied their binding with model dinucleotide-choosen to study preferential binding sites, by two dimensional NMR and theoretical methods. Theoretical method adopted here allows us to investigate, energetically allowed conformations of drug-nucleic acid complexes. Minimum energy conformation for a particular sequence suggests a peculiar mode of interaction. Helix unwinding capacity for both drugs has also been studied and compared with that of reported in literature.

At this moment, it is believed that our present study of model drug-nucleic acid system, may help to understand the

phenomenon of site specificity, structural aspects of these complexes and how specific sites relate to repair mechanisms, resistance and to anticancer efficacy of daunomycin and actinomycin. Chapter 3 carries the details of the materials used, NMR concentration ranges and the methods used in interpretation of NMR data as well as theoretical method's details. Chapter 4 discusses NMR studies on structure of daunomycin, while Chapter 5 is devoted to its interaction studies with deoxydinucleotide d-CpG by 2D NMR. Structure of actinomycin studied by 2D NMR is reported in Chapter 6. Chapter 7 contains the results and the discussion of theoretical calculations on drug-nucleic acid model complexes. Finally, the results of the present work have been concluded under the head Conclusions.



CHAPTER 3

MATERIALS AND METHODS

Materials

The deoxyoligonucleotide 5'-3' d-CpG was purchased from M/s Pharmacia Fine Chemicals Sweden. Storage was made at -20°C. Daunomycin was purchased from Sigma chemicals, USA and Actinomycin D was procured from SRL chemicals, India. Nucleotides and drugs were used as such in experimentation without further purification. Deuterium oxide (D₂O) with isotopic purity 99.96% was obtained from M/s Merck Sharp and Dohme Ltd., Canada and ICN Biochemicals INC. USA. DSS (Sodium 2, 2-dimethyl-2-silapentane-5-sulfonate), NMR reference standard was also purchased from Merck Sharp and Dohme Canada Ltd., Canada. All other chemicals used for buffer preparation etc. were of analytical grade.

NMR Sample Preparation

All NMR samples of drugs, oligonucleotide and their complex were prepared in D₂O and their concentrations were determined by absorbance measurements using Beckman DU-6 spectrophotometer. Values for extinction coefficients (ϵ) used for calculating concentrations, were as given below:

d-CpG ; $\epsilon = 9.02 \times 10^3 \text{ M}^{-1} \text{ cm}^{-1}$ at 260 nm.

Daunomycin ; $\epsilon = 9.80 \times 10^3 \text{ M}^{-1} \text{ cm}^{-1}$ at 480 nm

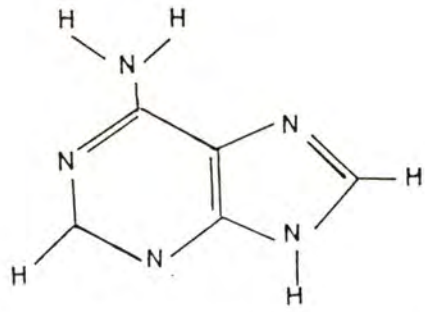
Stock solution of actinomycin was prepared by dissolving accurately weighed 5.0 mg of drug in 500 μ M of D₂O and required concentrations were achieved by rediluting the measured fractions of stock solutions. All sample were prepared in 10 mM deuterated phosphate buffer of pH 6.95, this way samples were controlled at neutral pH. Ethylene diamine tetra acetic acid (EDTA), 0.1mM, was added in each case to suppress paramagnetic impurities, which cause line broadening during NMR measurements. A very small quantity of DSS was added in all NMR samples as an internal reference standard. The various concentrations used for oligonucleotide/drug/mixture solutions are as given below:

Table 3.1: Concentrations of oligonucleotide and drugs used for NMR measurements

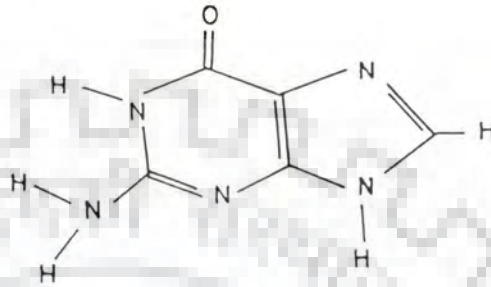
SAMPLE	CONCENTRATION	RATIO IN COMPLEX (D/N)
1. d-CpG	22.0 mM (duplex)	-
2. Daunomycin	4.95 mM	-
3. Actinomycin	5.5 mM	-
4. d-CpG + Daunomycin	11.0 mM+ 5.5 mM	1:2

Nucleic Acid structure

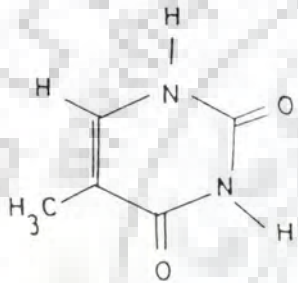
Ribonucleic acid (RNA) and deoxyribonucleic acid (DNA) are two major nucleic acids. Monomeric unit of RNA is ribonucleotide while for DNA it is deoxyribonucleotide. Primarily, there are three components for each nucleotide, (1) a nitrogenous, heterocyclic base (2) a pentose sugar (3) a phosphate moiety. Base is a derivative of either purine or pyrimidine. Adenine,



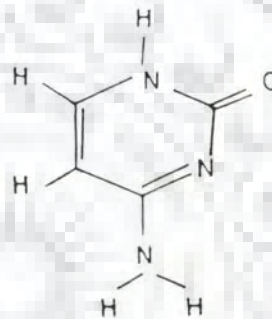
Adenine (A)



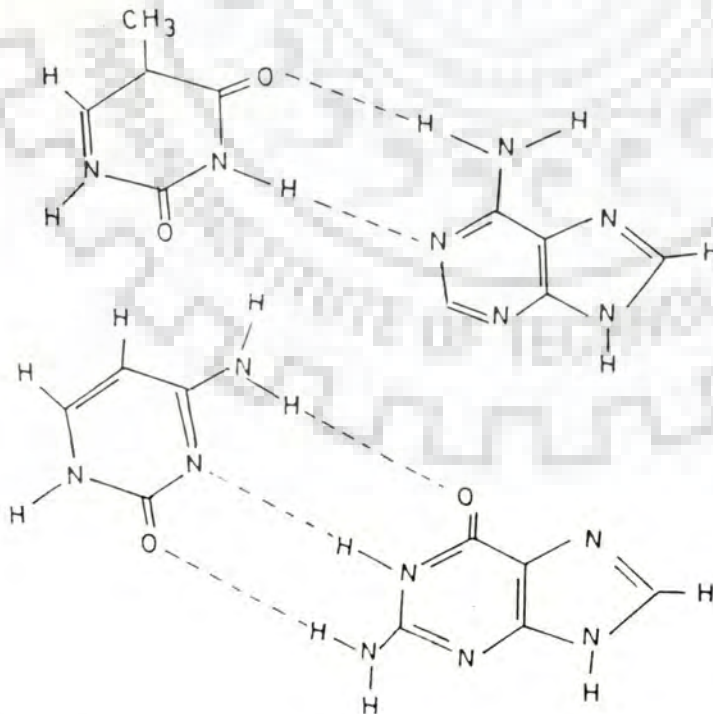
Guanine (G)



Thymine (T)



Cytosine (C)



A-T base pair

G-C base pair

Figure 3.1: Structure of Bases and Base pairs in nucleic acids

guanine are purine bases and thymine and cytosine are pyrimidines. Pentose sugar occurs in 'furanose' form in nucleic acids. Pentose sugar is linked through a -N-glycosyl bond to bases. Purines are covalently bonded to C1' of sugars through N9 atom and pyrimidines are linked through N1 atom. Further, nucleotide units are covalently linked through 'phosphodiester' bridges formed between 5'-hydroxyl units of one nucleotide and 3'-OH group of the next (n+1) unit. (Figure 3.2).

Each monomeric unit of polynucleotide chain has in addition to the glycosyl linkage, six single bonds along the phosphate backbone around which rotations are possible. At a microscopic level, various structures of nucleic acid can be defined in terms of a set of torsion angles shown in Figure 3.3. Angles α , β , γ , δ , ϵ and ζ constitute the backbone torsion angles while ν_0 , ν_1 , ν_2 , ν_3 and ν_4 decide the geometry of sugar ring. The different families of DNA structures are characterised by the values of these torsion angles. Table 3.2 summarises the available [127] values of the torsion angles for each of these models.

Glycosidic Bond Rotation

Orientation of Pyrimidine or Purine bases relative to sugar ring is defined by glycosidic bond angle (χ). Measurements of angle can be made either with respect to the position at C6 in pyrimidines and C8 in purines.

χ = O1' - C1' - N1 - C6 for pyrimidines

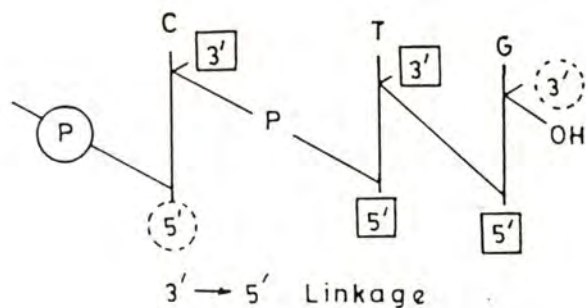


Figure 3.2: Schematic representation of 3'-5' linkage in nucleotides

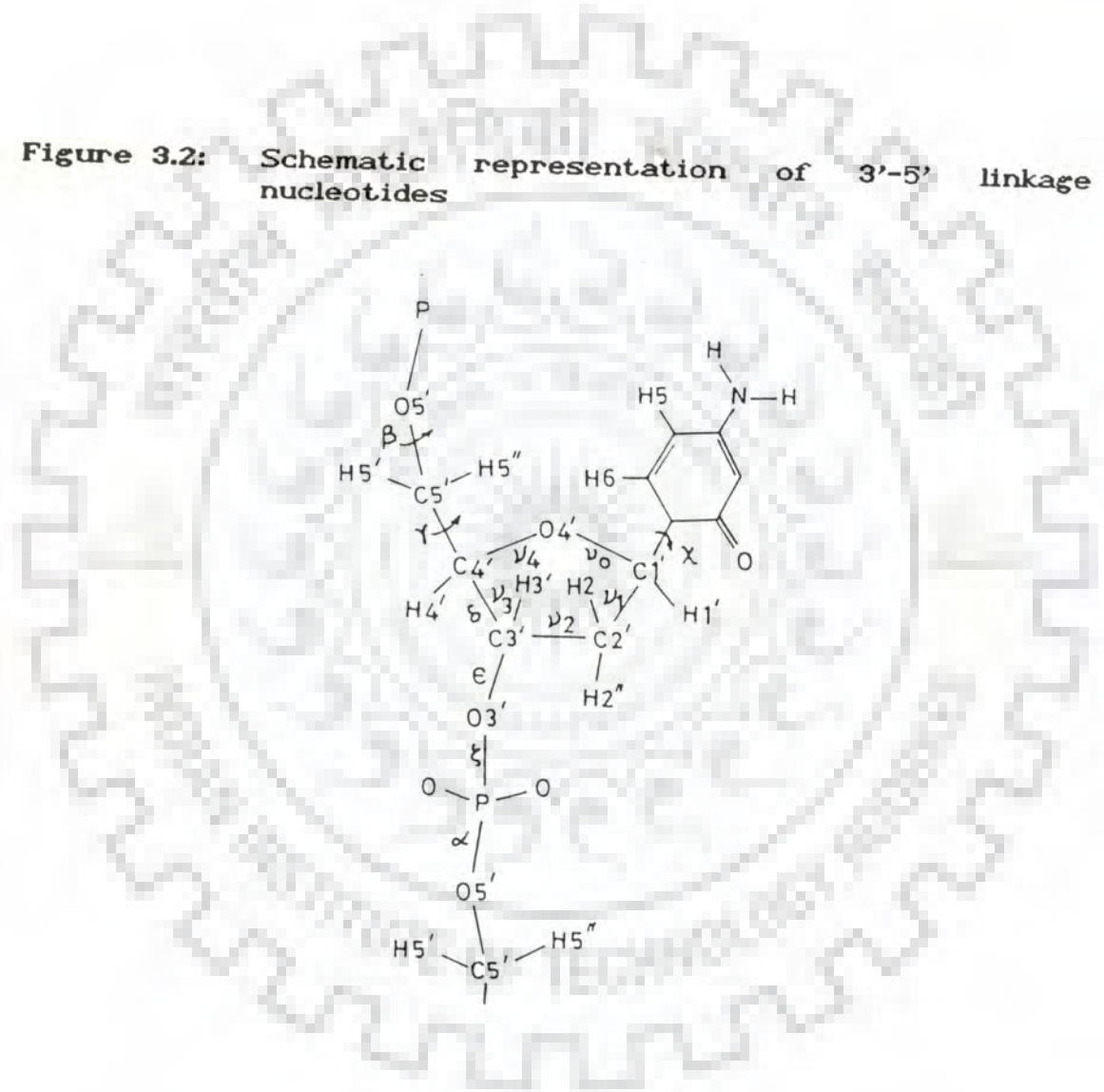


Figure 3.3: A mononucleotide unit, showing the nomenclature of the torsion angles

Table 3.2: Torsion angles for different DNA models

	A ^a	B ^a	G	C	G	C
α	-90	-41	47	-137	92	146
β	-149	136	179	-139	-167	164
γ	47	38	-165	56	157	66
δ	83	139	99	138	94	147
ϵ	-175	-133	-104	-94	-179	-100
ζ	-145	-157	-69	80	55	74
κ	-145	-102	68	-159	62	-148
Sugar	C3'-endo	C2'-endo	C3'-endo	C2'-endo	C3'-endo	C2'-endo

^a From Table 11.3 in reference 127

^b From Table 12.1 in reference 127

and

$$\chi = O1' - C1' - N9 - C8 \text{ for purines.}$$

Relative to the sugar moiety, the base can adopt two main orientations, called SYN and ANTI. They are described in Figure 3.4. In ANTI, the six membered ring in purines and O2 in pyrimidines is pointing away from the sugar, and in SYN, it is over or towards the sugar. A variant of ANTI, in which the bond C1' - C2' is nearly eclipsed with N1 - C6 in pyrimidine or N9 - C8 in purine nucleosides, is known as *high ANTI*, with glycosidic bond rotation angle as -90° . The term *high ANTI* actually denotes a torsion angle lower than ANTI.

Sugar Puckers

The centrally located five membered furanose ring is generally nonplanar. Out of five torsional angles $\nu_0 - \nu_5$, two are enough to explain the geometry of sugar ring. Atoms displaced from three or four atom planes and on the same side as C5' are called *endo*; those on the opposite side are called *exo* (Fig.3.5). According to Altona and Sundaralingam [123], the conformation of sugar ring is described by two parameters, pseudorotation phase angle P and δ . Sugar pucker torsion angles $\nu_0 - \nu_5$ can be related with these parameters as:

$$\nu_j = \nu_{\max} \cos [P + (j-2)\delta]$$

and

$$\tan P = \frac{(\nu_4 + \nu_1) - (\nu_3 + \nu_0)}{2 \nu_2 (\sin 36^\circ + \sin 72^\circ)}$$

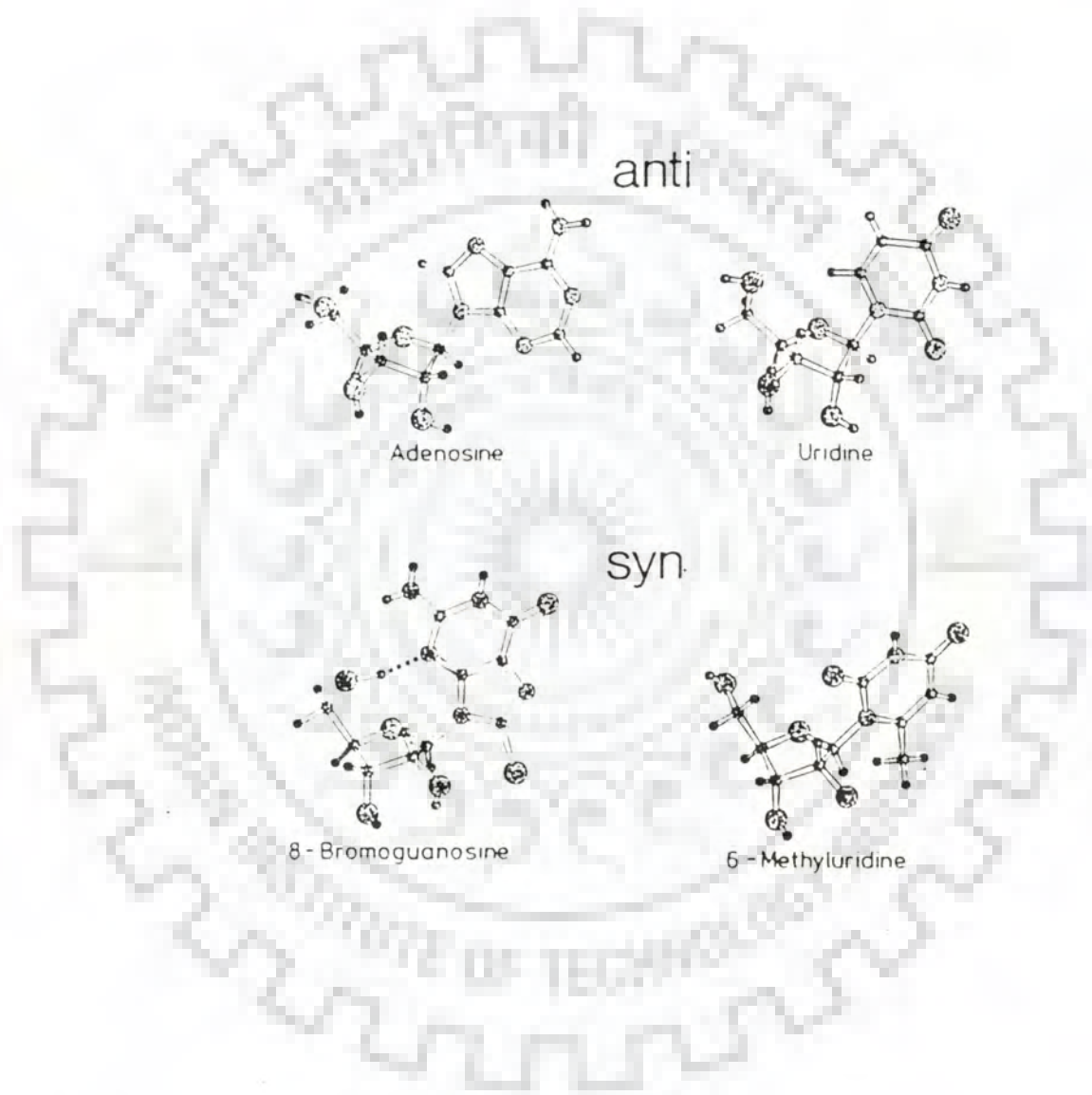


Figure 3.4: Illustration of overall geometry of nucleosides in SYN and ANTI orientations



Figure 3.5: Definition of sugar pucker modes

where ν_{\max} is maximum torsion angle.

Figure 3.6 shows pseudorotation cycle of the furanose ring in nucleotides, in which values of phase angles given in multiple of 36° . For each pseudorotation phase angle, conformation of sugar furanose ring is indicated.

Five conformational angles fix the geometry of sugar phosphate backbone. These angles, α , β , γ , δ , ϵ and ζ are related to the rotations along bond in atoms $P \rightarrow O5' \rightarrow C5' \rightarrow C4'$ and so on, sequentially. For example, α is defined as the rotation about $P - O5'$ bond. The definitions of each of these angles and their standard values for B DNA and other geometries are given Table 3.2.

Phenomenon of Nuclear Magnetic Resonance

We can observe the interaction between matter and electromagnetic forces by subjecting the sample simultaneously to two magnetic fields, one stationary and the other varying at some radiofrequency. At some particular combination, energy is absorbed by the sample and we can observe it as a change in signal, developed by an RF amplifier and detector.

Absorption of energy can be related to the magnetic dipole nature of spinning nuclei. Nuclei are characterised by spin quantum number I , which can have values 0,1,2,3... etc. For $I = 0$, nuclei do not spin and can not be considered here. Best resolution comes for the nuclei having I value $1/2$, for

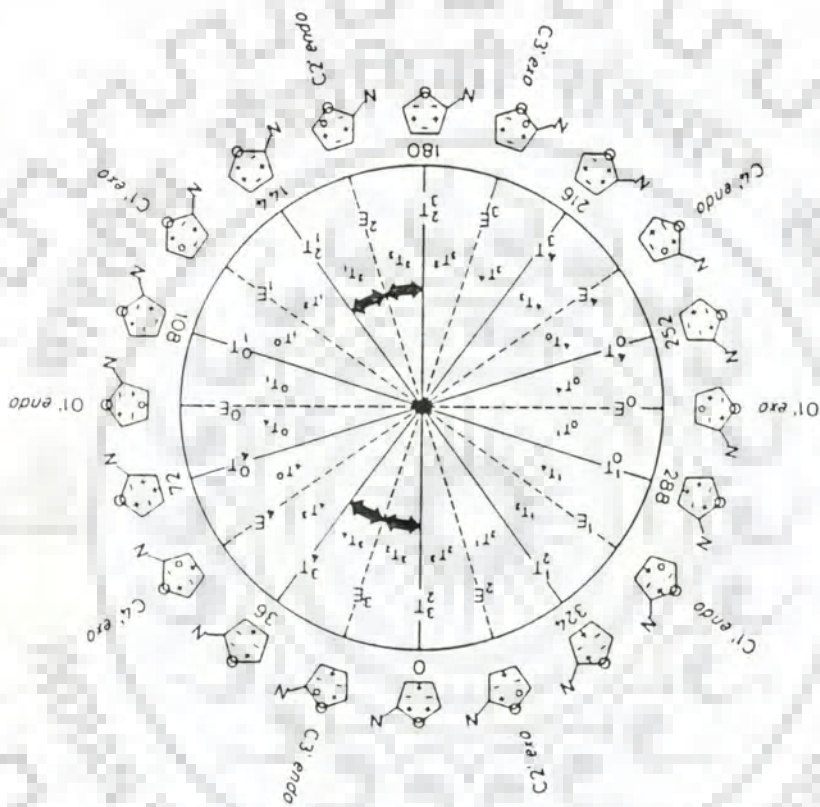


Figure 3.6: Pseudorotation cycle of the furanose ring in nucleosides. Values of phase angles are given in multiple of 36° .

example, ^1H , ^{19}F , ^{31}P , ^{13}C and ^{29}Si etc. Nuclei orient themselves in the presence of external magnetic field, H . $(2I + 1)$ are the possible orientations. For protons, difference between two energy levels is,

$$\Delta E = \frac{\mu H}{I}$$

where μ is gyromagnetic ratio. At a particular frequency of RF field, ν , the absorption takes place. This frequency is called 'Precession Frequency'.

$$\omega = 2 \pi \nu$$

where ω is angular frequency of precession and

$$\frac{\omega}{H} = \frac{2 \pi \mu}{\hbar I} = \frac{\mu}{\hbar I} = \nu$$

Each of nucleus is surrounded by moving electrons. Under the influence of external magnetic field, these electrons circulate in such way as to oppose the field. It results in lowering the magnitude of external field experienced by nucleus. Therefore, the frequency will have to change slightly as to bring surrounded nuclei into resonance. The chemical shift, δ , defines the location of a NMR signal along radio frequency axis and reflects the electronic environment around each nucleus and is generally given relative to that of a reference as:

$$\delta \text{ (ppm)} = \frac{\nu_{\text{ref}} - \nu_{\text{sample}}}{\nu_{\text{ref}}} \times 10^6$$

The magnitude of δ is determined by the diamagnetic effects of

circulating electron currents, paramagnetic effects from neighbouring atoms and interatomic currents. Effect of neighbouring nuclei on the field experienced by nucleus of interest causes spin-spin splitting of NMR signals. The interaction is mediated by bonding electrons and depends on the distance between nuclei, the type of chemical bond, bond angle and nuclear spin. The three bond spin-spin coupling constant 3J (H - C - C - H) is a function of dihedral angle and therefore, used in finding conformation of various molecules and changes in conformation due to interactions.

The concept of Two Dimensional NMR was first suggested by Jeener in 1971 and later on Ernst and his coworkers analysed it experimentally [122] in 1976, thus initiating a fertile field. Here, the spectral information is spread into a plane by using two time and frequency axes. Using multiple excitation, it is possible to obtain relationship between nuclear spins which interact either through J (so called COSY spectra) or through dipolar interaction (i.e. NOESY spectra). Besides assignments of proton signals, these coupling parameters then become the building blocks for obtaining three dimensional structure of biological molecules.

The two dimensional spectrum has two frequency axes (ω_1 , ω_2) and the intensities are represented along the third axis. Thus, each peak in a 2D spectrum occupies volume as against an area in the 1D spectrum. Two frequencies in a 2D spectrum are generated by fourier transformation of a time domain data

matrix of two independent time variables t_1 and t_2 .

$$S(t_1, t_2) \rightarrow S(\omega_1, \omega_2)$$

The two time variables are generated by segmentation of the conventional time axis of the FT-NMR experiments. The period t_1 is called evolution period, t_2 is termed as detection period and it is only during the latter that the data (FID) is collected (Fig. 3.7a). COSY (correlation spectroscopy) is the most fundamental of all the 2D NMR techniques, and produces spectrum illustrated in Fig.3.8 for 2 spin system. Cross peaks appear between two protons which are J-coupled. Both diagonal and cross peaks have multiple structure, but whereas the cross peaks have antiphase components (+ -) along the frequency axes, the diagonal peaks have inphase components (+ +). Separation between components is a measure of coupling constant J. The number of components depends upon the values of flip angle, ϕ , of the second pulse. For $\phi = \pi/2$, the number of components is at maximum, but $\phi = \pi/4$ often helps a great deal in simplifying the cross peaks.

The NOESY experiment provides a completely different type of information. The cross peaks arise from dipolar coupling correlations (distance correlation) between protons. In such experiment the mixing time τ_m is an important time parameter which determines the number and intensities of cross peaks. During this time period, the protons in close spatial proximity exchange magnetisation through a process called, "cross relaxation". Measurement of peak intensities as a

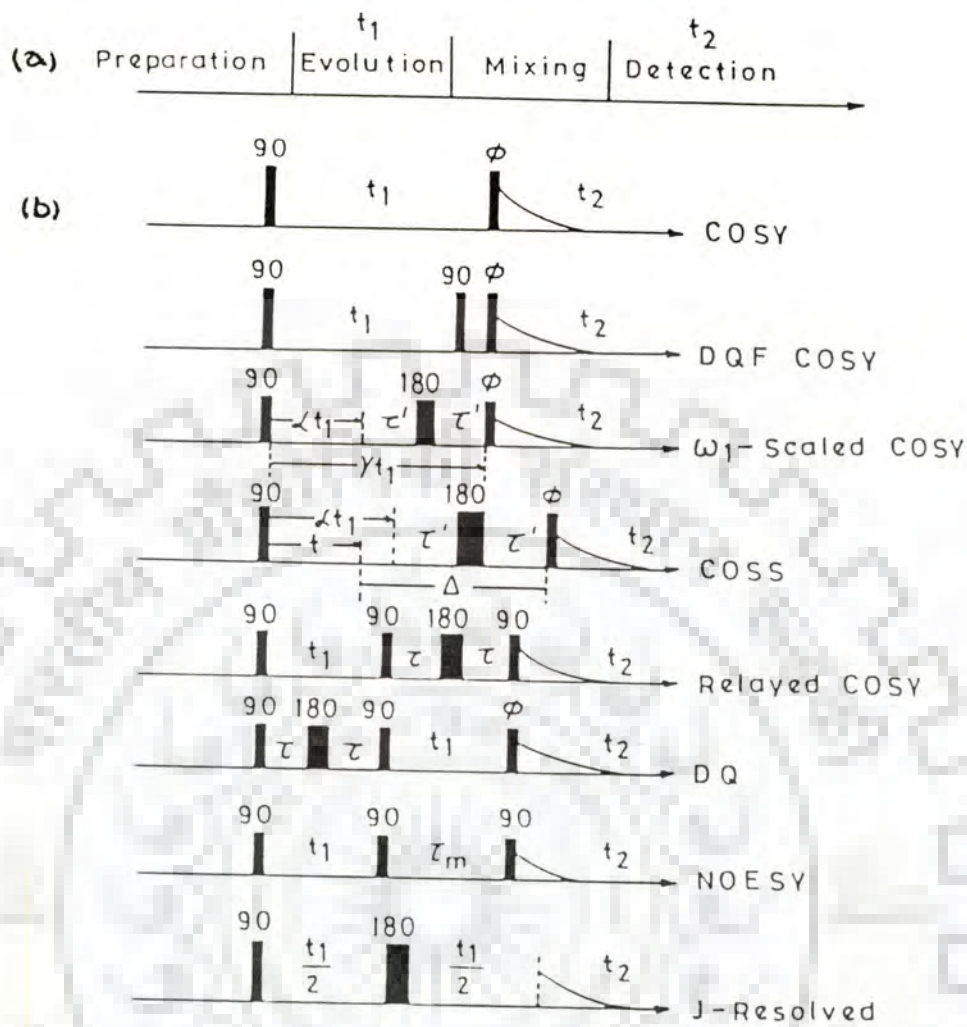


Figure 3.7:(a) Segmentation of the axis in a generalised experimental scheme of 2D NMR spectroscopy and (b) Pulse sequences for a selected sets of 2D NMR experiments

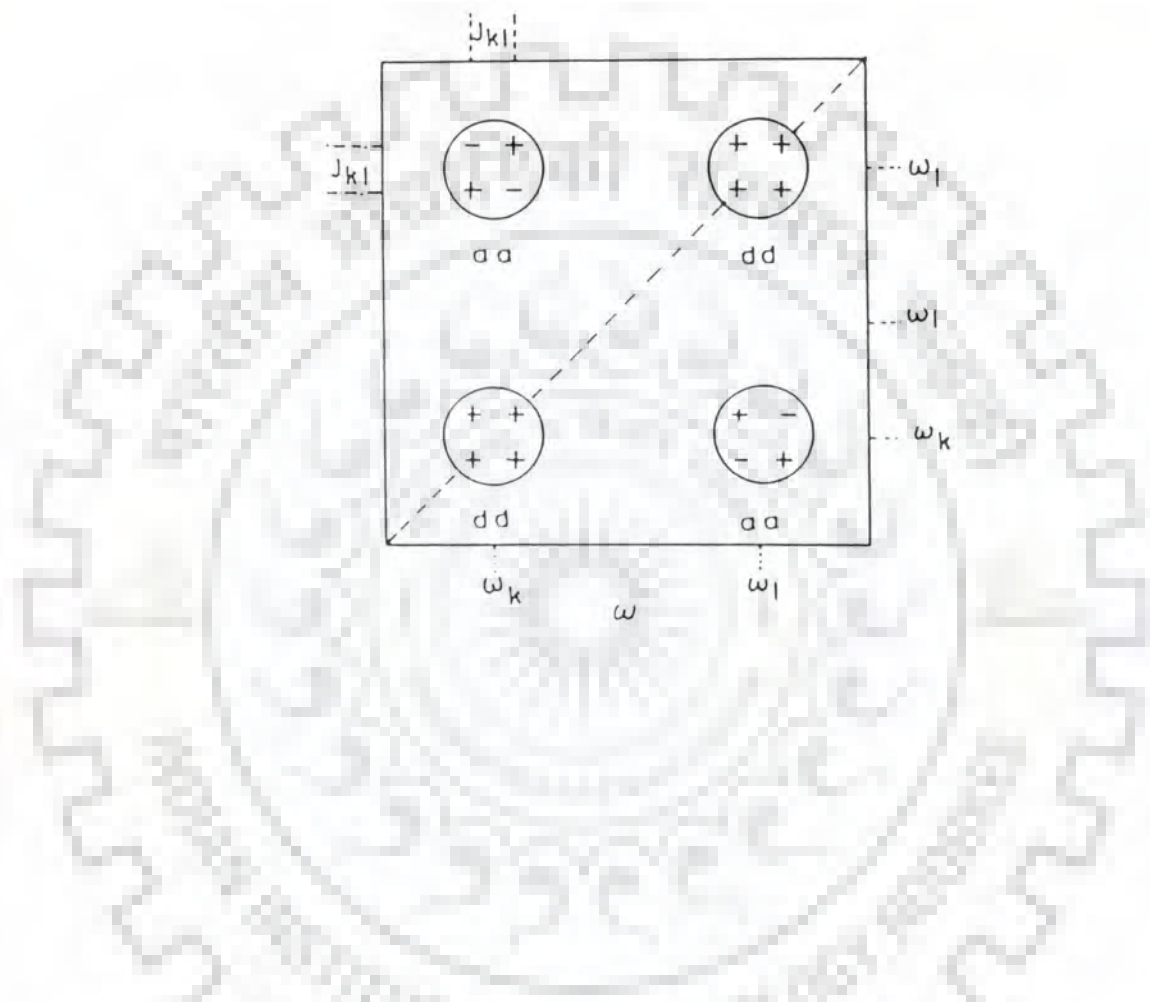


Figure 3.8: Schematic COSY spectrum of a two spin system. ω_k and ω_l are the resonance frequencies of spins k and l . J_{kl} is the coupling constant. The cross peaks have anti-phase character and absorptive character (aa) along both frequency axes. The diagonal peaks have in phase components and dispersive character (dd) along both axes.

function of mixing time allows the estimation of inter-proton distances. NOESY cross peaks of sizable intensity occur only for inter-proton distances of less than 4.0 \AA .

NMR Experimental Parameters

Proton NMR experiments, reported in this thesis, were carried out on 500 MHz high resolution Bruker AM 500 FT-NMR spectrometer equipped with Aspect 3000 computer, available at DST sponsored National FT-NMR facility, located at Tata Institute of Fundamental Research, Bombay. Typical NMR parameters for one dimensional NMR experiments were, pulse width $12.5 \mu\text{sec}$ (60° pulse). Number of data points (SI) 8-16K. Spectral width 5000 Hz, no. of scans 64-400, digital resolution of 0.15-1.22 Hz/point. RG (Receiver Gain) value was optimised in each case to obtain best possible signal to noise ratio. In temperature variable experiments, temperature range was 277-340 K. All 2D NMR COSY and NOESY experiments were carried out at room temperature, value 297 K. 1024-2048 data points (SI) were taken along t_2 axes, while 256 - 512 data points (TD) were taken along t_1 axis; 60 - 400 scans contributed to each experiment. PW was 12.5-15.0 μsec with SW 5000Hz. A resolution of approximately 4.0 Hz/point was achieved. Relaxation delay was given for a period of 1.0 sec and in NOESY experiments mixing time (τ_m) of 600 - 800 msec was used. On fourier transformation, data were zero filled in t_2 dimension to enhance resolution.

Strategies of Complete Assignment of Non Exchangeable Protons

The assignment of proton resonances, determination of sugar conformation, helix sense, and glycosidic bond rotation etc. are made with the help of 2D NMR experiments and carried out in three steps. To begin with, a well resolved 1D spectrum is obtained and it is attempted to identify and resolve all the base proton resonances of nucleotide. In second step, sugar proton resonances within the same nucleotide unit are interconnected by 2D COSY and spin system network is worked out, for each sugar residue, in the third step. Interconnectivities between base protons and sugar protons of the same nucleotide unit and adjacent nucleotide unit are established by 2D NOESY experiment. In NOESY, cross peak is generated because of dipole-dipole interaction in which magnetisation is transferred through space from one proton to another. The efficiency of cross saturation is proportional to the inverse of the sixth power of the distance and becomes undetectable for protons that are farther than 4\AA [123]. On the basis of presence and absence of various cross peaks in sugar spin network, in COSY spectrum, sugar moiety conformation can be established. Strategy is shown in Fig.3.9.

Complete sequential assignment is made by using 2D-NOESY spectrum [124,125,126]. Quantification of DNA structure from NMR data has also been reported by Chary et al. [135]. For right handed structures with sugars in C3'endo/C2'endo/O1'endo

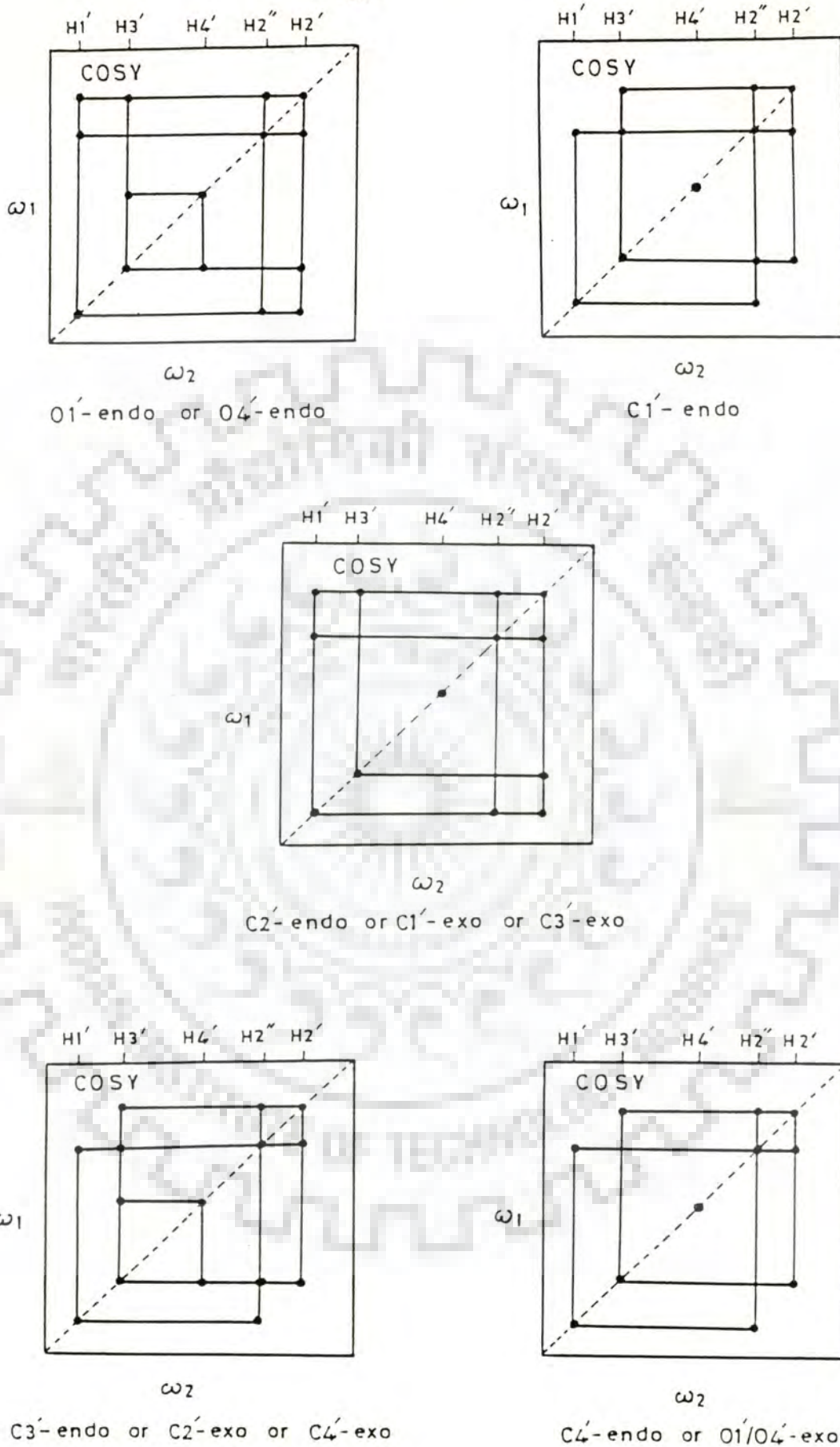


Figure 3.9: Schematic representation of spin net work of various sugar conformations, in COSY spectrum

conformations, a convenient strategy is as follows:

$(GH8/CH6)_n \dots (CH2', H2'', H1')_n$ intra residue nOe's

$(GH8/CH6)_n \dots (CH2'', H1')_{n-1}$ inter residue nOe's

However, for left handed structures, expected set of intra and inter nOe's are different and are as follows:

$GH8 \dots H1'$

$CH6 \dots H5'', H2'$ intra residue nOe's

$GH8 \dots (H5'')_{n-1}$

$CH6, CH5 \dots (CH2')_{n-1}$

$CH1' \dots (H5'')_{n+1}$

Glycosidic bond rotation nature viz. SYN, ANTI, *high* ANTI is also established by the observations of certain nOe's:

SYN

$GH8/CH6 \dots H1'$ strong

$GH8/CH6 \dots H2', H2''$ weak

high ANTI

$GH8/CH6 \dots H2'', (CH2'')_{n+1}$ strong

ANTI

$GH8/CH6 \dots H2'$ strong

GH8/CH6.....H2", (H2") n+1

weak

Use of above stated strategies has been made in present studies. The possibilities of observed n0e's were also checked and studied by dreiding stereo model building, thus inferring the possible conformation in each case.

Theory of Potential Energy Calculations

We have estimated the conformational energy using classical potential function (CPF). Such an approach has widely been used in the study of protein structure [137, 138], nucleic acid geometry [139, 140, 141] and drug nucleic acid interactions [142, 92]. In this approximation the total potential energy, V , is assumed to be

$$V = V_a + V_r + V_{el} + V_{\theta}$$

where,

V_a = Van der waal's attraction energy,

V_r = repulsion energy,

V_{el} = electrostatic energy, and

V_{θ} = torsional energy

The interactions due to stretching and bending of covalent bonds are neglected as the vibrational constants are considerably higher than the torsional barriers.

Van der waal's attractive energy also known as London's dispersion energy arises from the interaction between fluctuating, transient dipoles on the two atoms concerned and is of the form $\sum_{i < j} - A/R_{ij}^6$ where i and j are non bonded atoms and A_{ij} depends on the polarisabilities of atoms i and j . An expression for A_{ij} has been derived as:

$$A_{ij} = \frac{3/2 \text{ eh}^2 / \sqrt{M} \cdot \alpha_i \cdot \alpha_j}{\sqrt{\alpha_i / N_i} + \sqrt{\alpha_j / N_j}}$$

where α_i, α_j are the polarisabilities on atoms i and j and N_i, N_j are the effective number of polarisable electrons on atoms i and j [143]

The repulsion energy expression

$$V_r = \sum_{i < j} \frac{B_{ij}}{R_{ij}^n}$$

is an empirical one where B_{ij} is calculated by imposing a condition that the minimum in total potential energy occurs when the separation between pairs of atom is equal to the sum of Van der waal's radii R_0 for a given pair of atoms i and j .

The electrostatic energy expression

$$V_{el} = \sum_{i < j} \frac{q_i q_j}{\epsilon R_{ij}}$$

where q 's are the partial charges on atoms arising due to the differences in electronegativity of atoms participating in

covalent bonds and calculated by standard quantum mechanical approaches. The effective dielectric constant ϵ is taken as 4.0.

The torsional potential is characterised by the bond about which the rotation is considered and arises from the exchange interactions between the orbitals of the bonded atoms. It is taken as

$$V(\theta) = V_1 (1 + \cos 3(\theta)) + V_2 (1 + \cos 2(\theta))$$

where V_1 , V_2 are the barrier heights and have been taken as 1.5.

The interaction energy between two molecules has been determined by treating the interaction as a perturbation to the isolated system and partitioned into physically meaningful energy terms. The details of method are reviewed by Claverie [144] and used by Govil and coworkers [145, 105, 106, 107]. The interaction energy is sum of electrostatic (E_{el}), polarisation (E_{pol}), dispersion (E_{disp}) and repulsion energies (E_{rep})

$$E_{int} = E_{el} + E_{pol} + E_{disp} + E_{rep}$$

The molecular charge distribution has been expressed as a set of atomic charges, q , and atomic dipoles, μ , obtained by the CNDO (Complete Neglect of Differential Overlap) method. For electrostatic interaction

$$E_{el} = E_{qq} + E_{q\mu} + E_{\mu\mu}$$

where

E_{qq} is monopole-monopole interaction

$E_{q\mu}$ is monopole-dipole interaction

$E_{\mu\mu}$ is dipole-dipole interaction

The explicit expression for these are

$$E_{qq} = \sum_i^{(1)} \sum_j^{(2)} \frac{q_i q_j}{r_{ij}}$$

$$E_{q\mu} = \sum_i q_i \langle \bar{\mu}_j \cdot R_{ij} \rangle \cdot |R_{ij}|^{-3}$$

$$E_{\mu\mu} = \sum_i \sum_j \langle \bar{\mu}_i, \bar{\mu}_j \rangle \left[|R_{ij}|^{-3} - 3 \langle \bar{\mu}_i \cdot R_{ij} \rangle \langle \bar{\mu}_j \cdot R_{ij} \rangle |R_{ij}|^{-5} \right]$$

The polarisation energy of a binary complex is given as

$$E_{pol} = E_{pol} (2 \rightarrow 1) + E_{pol} (1 \rightarrow 2)$$

Where $E_{pol} (1 \rightarrow 2)$ stands for energy due to polarisation of molecule 2 by 1. Further

$$E_{pol} (2 \rightarrow 1) = -\frac{1}{2} \sum_u^{(1)} \epsilon \cdot A_u \cdot \epsilon^{(2)}$$

where $\epsilon^{(2)}$ is electric field induced by molecule 2 at midpoint of bond u of molecule 1 and A_u is the polarisability tensor of bond u of molecule 1.

The dispersion and repulsion terms considered together in Kitaigorskii type formulae are

$$E_{disp} + E_{rep} = \sum_i^{(1)} \sum_j^{(2)} E(i, j)$$

where,

$$E(i, j) = K_i K_j \left[\frac{-A}{Z_{ij}^6} + B e^{-\gamma Z_{ij}} \right]$$

$$Z_{ij} = \frac{r_{ij}}{R_{ij}^0}$$

$$R_{ij}^0 = \left[(2R_i^\omega) \cdot (2R_j^\omega) \right]^{-1/2}$$

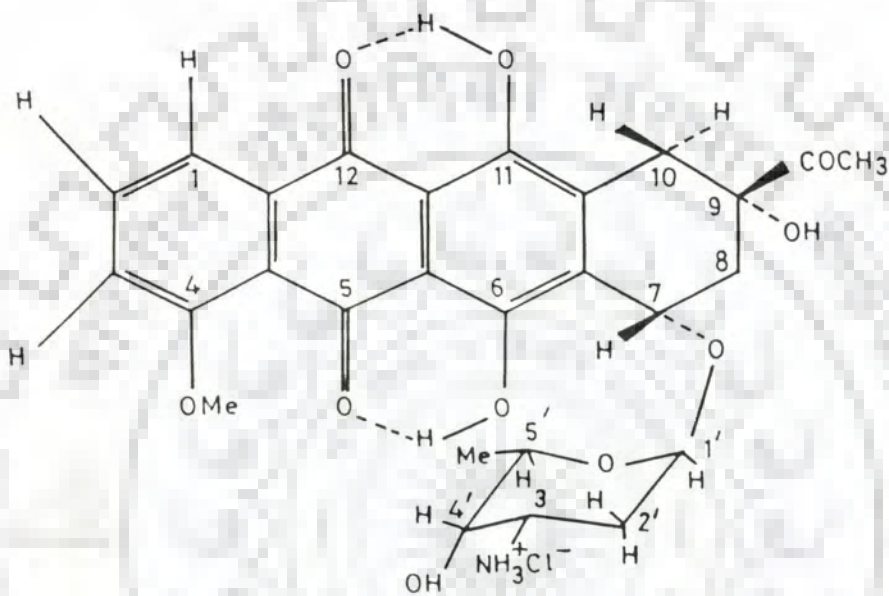
where R_i^ω and R_j^ω are Vander waal's radii of atoms i and j ; A , B , γ are constants i.e. $A = 0.214$, $B = 47000$ and $\gamma = 12.35$; parameters K_i , K_j are taken from Caillet and Claverie [146]. The calculated interaction energies have been used to give insight into forces stabilising nucleic acid-drug associations.

CHAPTER 4

THE STRUCTURE OF DAUNOMYCIN

The conformational properties of daunomycin have been investigated by one dimensional and two dimensional proton NMR; at 500 MHz. In one dimensional variable temperature proton NMR experiments, resonances of non-exchangeable drug protons were monitored as a function of temperature in the range 277-350 K. Two dimensional homonuclear correlation spectroscopy (COSY) and nuclear Overhauser enhancement spectroscopy (NOESY) experiments were carried out and spectra were analysed to deduce the structural aspects of drug - daunomycin.

Figure 4.1 shows proton NMR spectra of daunomycin in D₂O as a function of temperature. Resonance positions of different nonexchangeable drug protons on NMR scale were assigned as reported in literature [41] and later on unambiguously confirmed with the help of COSY and NOESY experiments. The observed chemical shifts have been plotted versus temperature in Figure 4.2 and values have been tabulated in Table 4.1. Aromatic ring protons 1H, 2H and 3H show large downfield shifts being about 0.20, 0.15 and 0.16 ppm, respectively. These shifts suggest a probable presence of aggregates at experimental concentration (4.95 mM) at which aromatic moieties may stack over each other and destack on increase in



Structure of Daunomycin



Figure 4.1: The 500 MHz proton NMR spectra of daunomycin (4.95mM) at different indicated temperatures in D₂O (pH 6.95). Ref. DSS.

Daunomycin alone (4.95 mM)

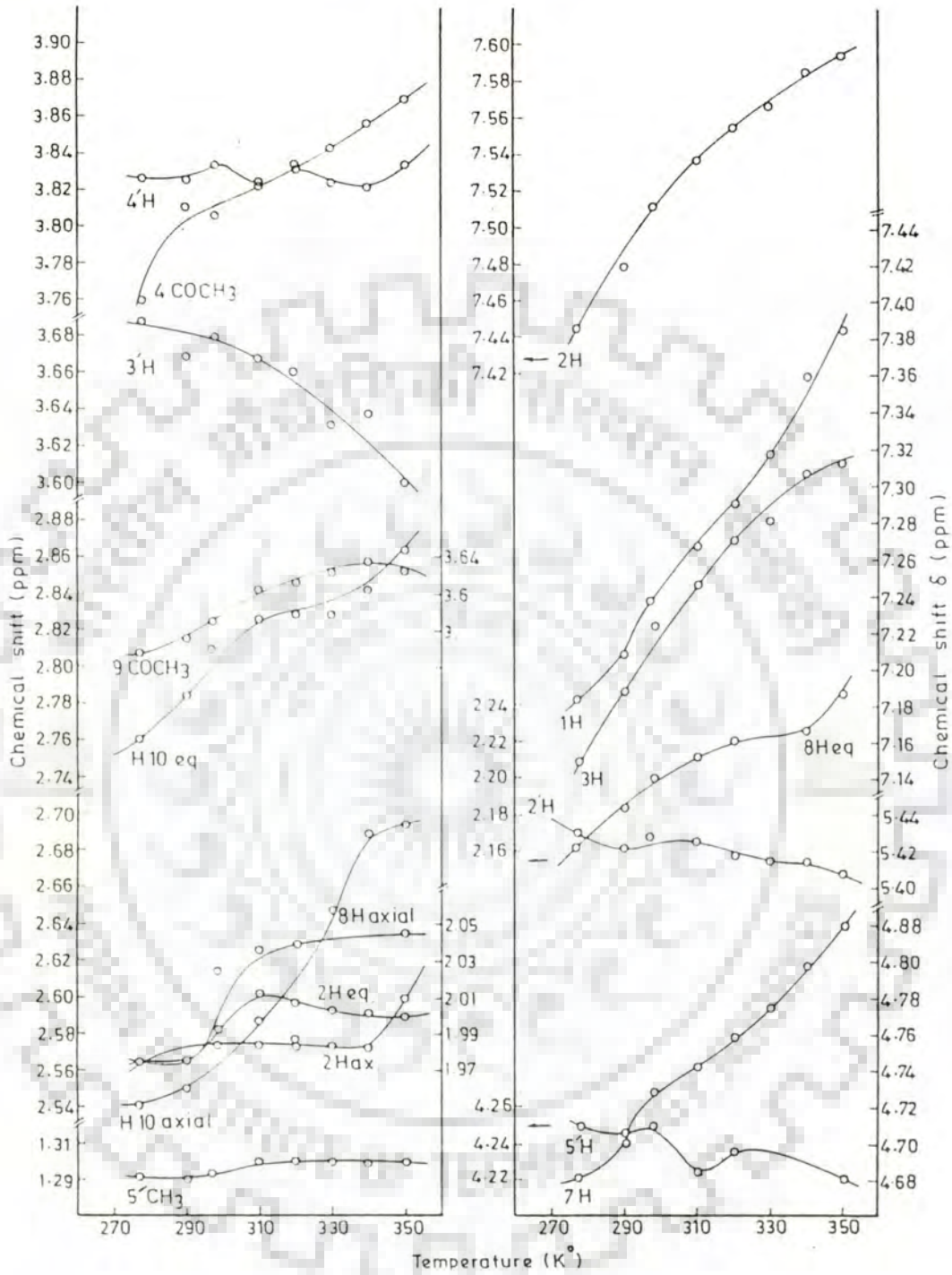


Figure 4.2: Chemical shifts of non-exchangeable protons of daunomycin as a function of temperature.

Table 4.1: Chemical shift values (in ppm) of various protons at 500 MHz of Daunomycin in D₂O (pH 6.95) in temperature range 277 - 350K

Temp. (K)	2H	1H	3H	1'H	7H	5'H	5'CH ₃
277	7.445	7.184	7.149	5.430	4.680	4.254	1.292
290	7.479	7.208	7.180	5.423	4.703	4.246	1.296
297	7.514	7.239	7.226	5.429	4.728	4.250	1.302
310	7.528	7.269	7.253	5.425	4.744	4.224	1.303
320	7.554	7.290	7.272	5.419	4.760	4.237	1.302
330	7.568	7.319	7.282	5.415	4.775	-	1.302
340	7.587	7.360	7.308	5.412	4.798	-	1.302
350	7.595	7.385	7.315	5.409	4.820	4.222	1.300

Temp. (K)	4'H	4COCH ₃	3'H	10Heq	10Hax	9COCH ₃	8Heq
277	3.827	3.761	3.688	2.761	2.541	3.599	2.164
290	3.827	3.872	3.670	2.786	2.554	3.606	2.185
297	3.836	3.805	3.682	2.811	2.507	3.615	2.200
310	3.823	3.823	3.668	2.827	2.588	3.623	2.214
320	3.834	3.834	3.663	2.744	2.577	3.627	2.223
330	3.826	3.845	3.633	2.830	2.648	3.633	1.988
340	3.822	3.858	3.639	2.844	2.691	3.640	2.225
350	3.818	3.871	3.608	2.864	2.695	3.634	2.225

Temp. (K)	2Heq	2Hax	8Hax
277	1.975	1.975	1.975
290	1.975	1.975	1.975
297	1.995	1.987	1.996
310	2.013	1.988	2.013
320	2.010	1.986	2.010
330	1.987	1.987	1.988
340	1.983	1.983	1.983
350	1.980	2.010	1.980

temperature. A simultaneously observed change in chemical shift values of H10_{ax}, H8_{ax} and H_{eq} protons indicate a change in conformation of ring A of daunomycin. Sugar protons do not show any pronounced change with increase in temperature.

Efforts were also made to calculate spin-spin coupling constant, 'J' values using 1D NMR signal splittings and that from Karplus-altona equation using theoretically calculated dihedral angles from Dreiding models. 'J' values from different signals have been categorised in Table 4.2. These coupling constant values have been found in agreement with that already reported in literature [41]. The coupling constant value ${}^3J_{1'-2'}$ is found to be zero in our case; while reported values are 1.3 Hz and 3.9 Hz for ${}^3J_{1'-2'}$ and ${}^3J_{1'-2''}$, respectively. NMR spectral resolution in above experiments was 1.221 Hz/point, which gives an idea that these coupling constant values must be less than 2.4 Hz or ± 1.221 Hz as the coupling is not visible at this resolution. The torsion angle C5' - O - C1' - H1' was calculated as 55° and 90° for two optimised distance values of 1.8Å and 3.6Å from Dreiding model. This angle suggest specific orientation of sugar moiety with respect to ring A. COSY spectrum of daunomycin is depicted in Figure 4.3. Complete spin system net work has been worked out and assignments of different drug protons have been unambiguously made. A strong cross peak observed in aromatic region of spectrum shows correlation between 2H and 3H & 1H proton signals. At room temperature 3H and 1H are overlapped, so only one cross peak is observed.

Table 4.2: ^1H - ^1H Coupling-constant values (Hz) for Daunomycin in D_2O (4.95mM).

Coupling	J(Hz)
1H-2H	7.87
2H-3H	7.81
10Hax-10Heq	18.00
8Heq-8Hax	14.50
H3'-H2'	7.16
H3'-H4'	9.58
H5'-5'CH ₃	6.59
H2'-H2''	13.99
1H'-H2'	1.30
1H'-H2''	3.90

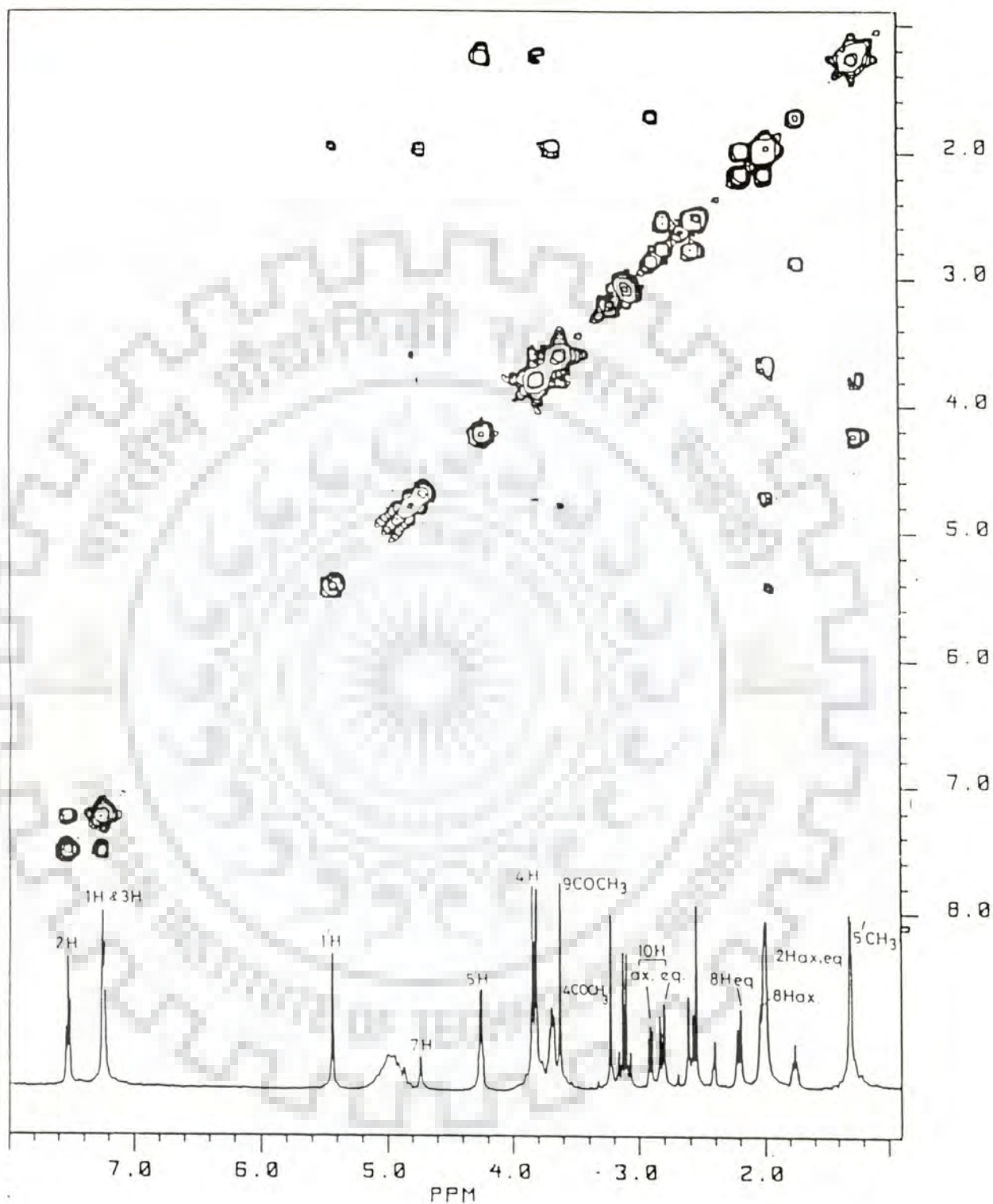


Figure 4.3: 500 MHz COSY spectrum of daunomycin in D₂O at 297K. Ref DSS - symmetrised spectrum

Coupling is detected between 4'H - 5'CH₃, but 4'H and 5'H do not show any cross peak. Strong couplings are observable between 3'H - 4'H, 10Heq - 10Hax., 8Heq - 8Hax and 7H - 8Heq & ax protons. NOESY spectrum of daunomycin (Figure 4.4.) exhibits some interesting results. An account of relative intensities of nOe's, seen in NOESY spectrum is as follows:

2H.....1H and 3H	strong
2H.....4COCH ₃	strong
1'H.....2'H _{ax}	strong
1'H.....2'H _{eq}	strong
1'H.....7'H	weak
3'H.....5'H	strong
3H.....4COCH ₃	strong
5'H.....4'H	strong
5'H.....8Heq	weak
5'CH ₃ ...5'H	strong
5'H.....8Hax	weak
4'H.....5'CH ₃	strong

Observed strong nOe's between 2H, 3H and 4COCH₃ signals suggest a spatial vicinity for these protons. However, this is found to be at maximum when these protons 2H, 3H and 4COCH₃

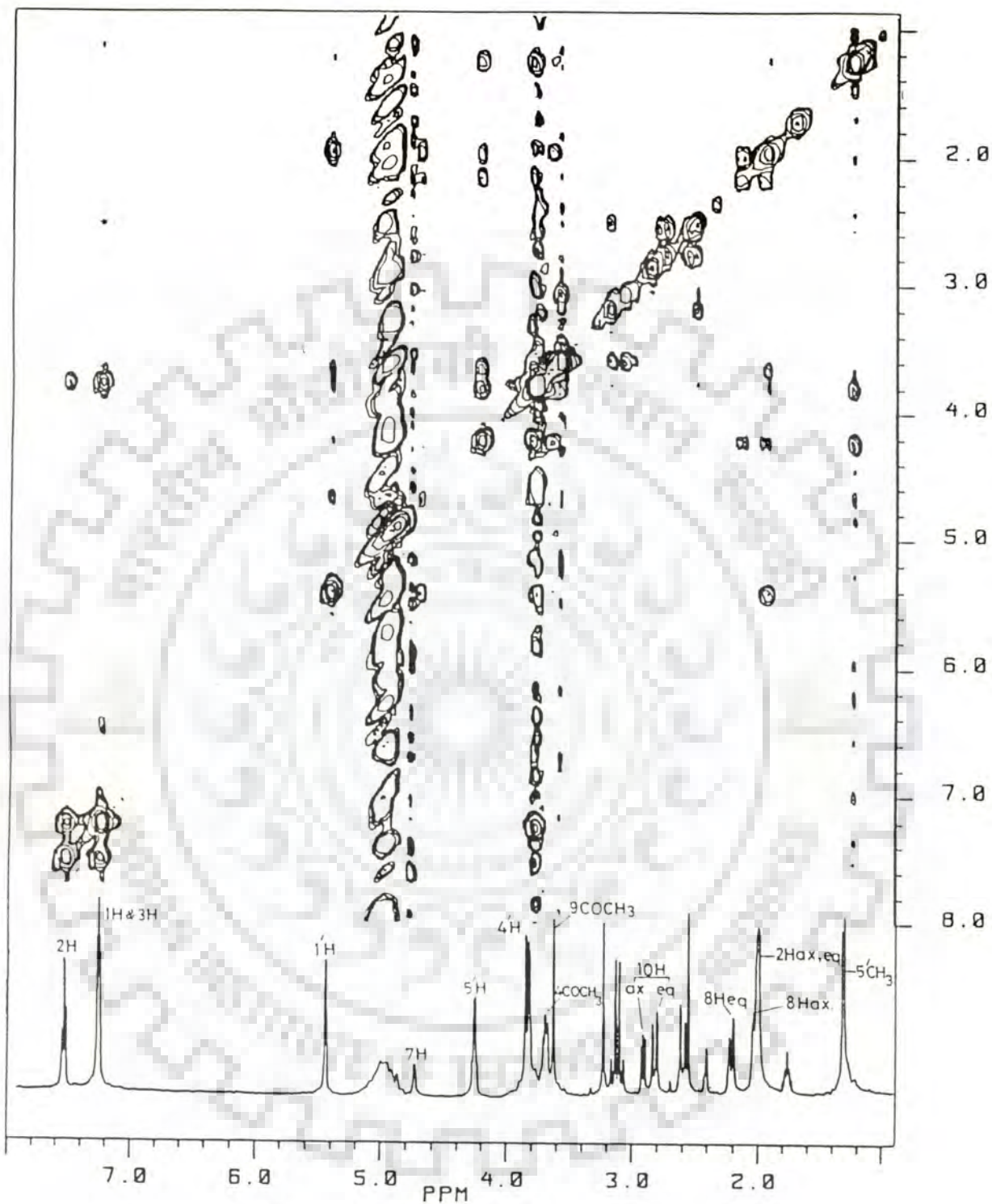


Figure 4.4: 500 MHz NOESY spectrum of daunomycin (4.95mM) in D₂O at 297 K. Ref. DSS - unsymmetrised spectrum

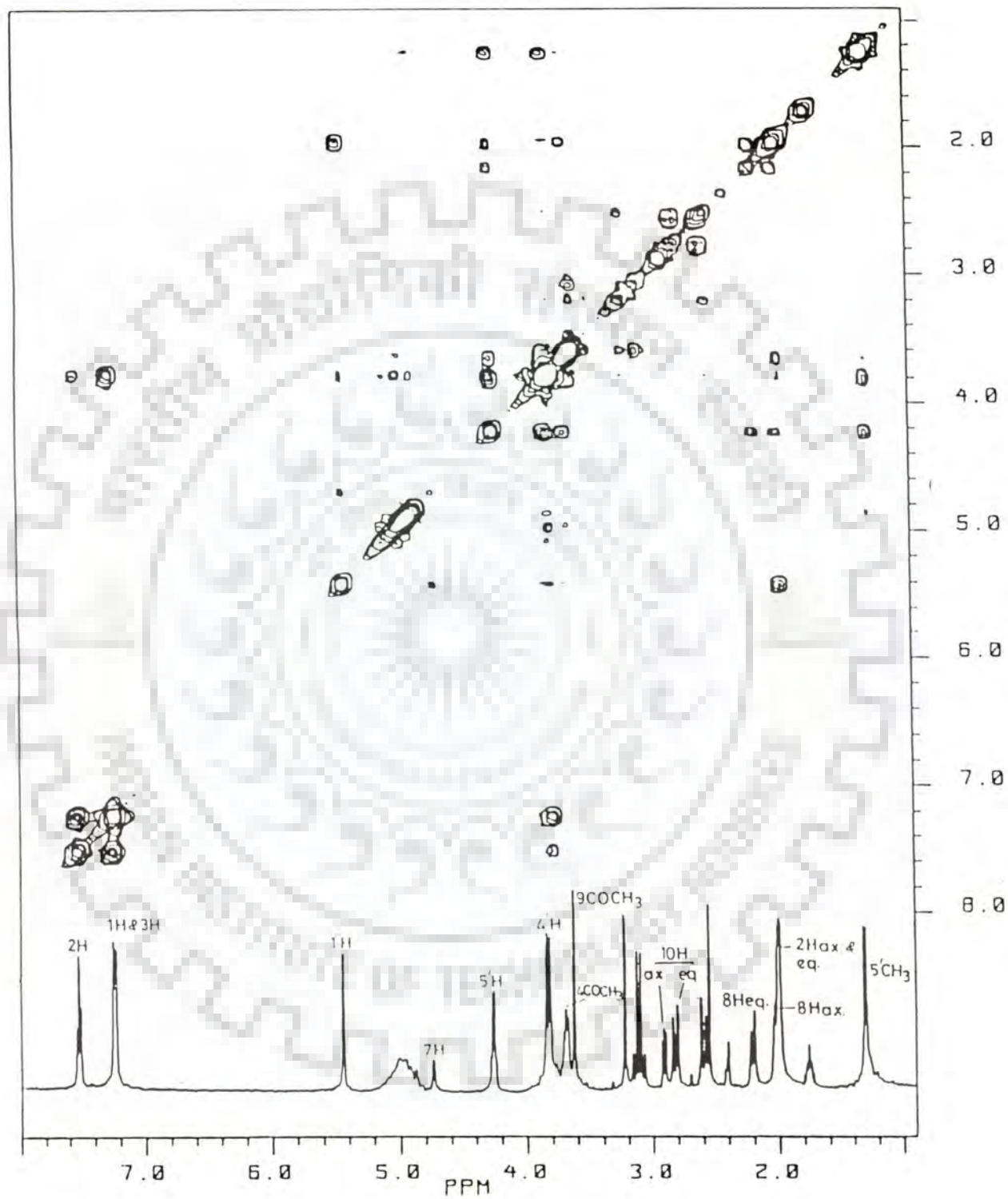


Figure 4.4: ...Continued...symmetrised spectrum

are collinear. The distances for 2H and 4COCH₃ and 3H - 4COCH₃ were calculated to be around 3.7Å and 1.7Å, respectively. Since, the distance in such an arrangement is less for 3H-4COCH₃ than 2H thus justifying the stronger nOe of 4COCH₃ with 3H than 2H. Dihedral angle (3C-4C-O-4'C) is found to be 90° in such condition. NOESY cross peak between 1'H and 7H, suggests the orientation of sugar ring with respect to planar ring system. The torsional angle C5'-O-C1'-H1' for closest distance of 1.8Å comes out to be 55°. But distance between 7H and 1'H also depends on the torsion angle 7C-O-C1'-H1'. nOe seen for 5'H - 3'H suggests that both of these protons are SYN to each other, it is possible when 5'H is axial thus showing nOe with 3'H. Interproton distance between these two protons in above conformation is 3.6Å. Measured closest distance in Dreiding models for 5'H - 4'H was found to be 2.2Å, thus showing strong nOe. Absence of a COSY cross peak for 5'H - 4'H could be justified as the torsional angle H5'-C5'-C4'-H4' is such that coupling constant $^3J_{4'H-5'H}$ is ≈ 0.0 , this angle value was calculated to be 85°.

The idea of presence of more than one conformer in solution at experimental concentration can not be ruled out and gets strength due to the simultaneous appearance of two nOe's; 4COCH₃...2H and 4COCH₃...5'H. Methoxy group at position 4 can not be in close contact simultaneously with 2H ring proton as well as 5'H at sugar moiety. So it can be well suggested that more than one conformers or aggregates are present in

aqueous deuterated solution of daunomycin. Chemical shifts observed for different proton signals in present work, are in general agreement with that reported by other workers. H₂ resonance shows a chemical shift value of 7.51 ppm at room temperature while for the same resonance, a value of 7.68 ppm has been reported by Patel [134]. Self association of daunomycin has been studied by Chaires et al.[34] and it is well expected that daunomycin shows self-association in NMR concentration range [134], as its self association is reported at concentrations higher than 10 μ M. Kollman et al.[41] suggested half-chair conformation for ring A as they observed splitting in H₇ and H₈ resonance, which could have been due to H-7 and H-8 coupling. Our NMR results do not show any splitting in H-7 proton signal, which contradicts these reported results.

As it has also been reported [41], that the conformation of ring A in the solid state is a slightly flattened half chair ^oH₈, on the basis of observed rotational angle values obtained from X-ray atomic coordinates. It was explained on the basis of packing of molecules in crystals. However, in daunomycin complex with hexanucleotide d(CpGpTpApCpG) (Quigley et al.[30]), ring A seems to be a less distorted half-chair and probably similar to the conformation observed in solution.

CHAPTER 5

BINDING OF DAUNOMYCIN WITH DEOXYDINUCLEOTIDE d-CpG

The complex of daunomycin with deoxydinucleotide d-CpG has been studied by proton NMR at 500 MHz, in stoichiometric D/N ratio 1:2. Two dimensional NMR experiments, COSY and NOESY, were carried out to fully assign the spectrum and were analysed for structural informations of the complex.

Temperature Dependence

Variable temperature one dimensional NMR experiments were carried out in temperature range 277 - 320 K. Results have been shown in Figure 5.2. Figure 5.3 shows the plots of chemical shifts of various protons of drug as well as d-CpG, as a function of temperature. On increasing temperature, sharpening of all the nucleotide proton resonances is observed, accompanying the resonances of daunomycin. Large changes in chemical shifts, $\Delta\delta$, due to increase in temperature are observed for CH1' and CH2' protons of nucleotide, being about 0.28 ppm and 0.12 ppm, respectively (Table 5.1). These changes are quite pronounced even for cytosine base ring proton i.e. CH5 and CH6. Contrary to it, sugar protons associated with guanine base and GH8 resonance of base ring proton show little change with increase in temperature. Mid point transition, T_m value, calculated from curves of GH8, CH5 and CH6 protons ranges from 299-301 K. Thus, it can be assumed

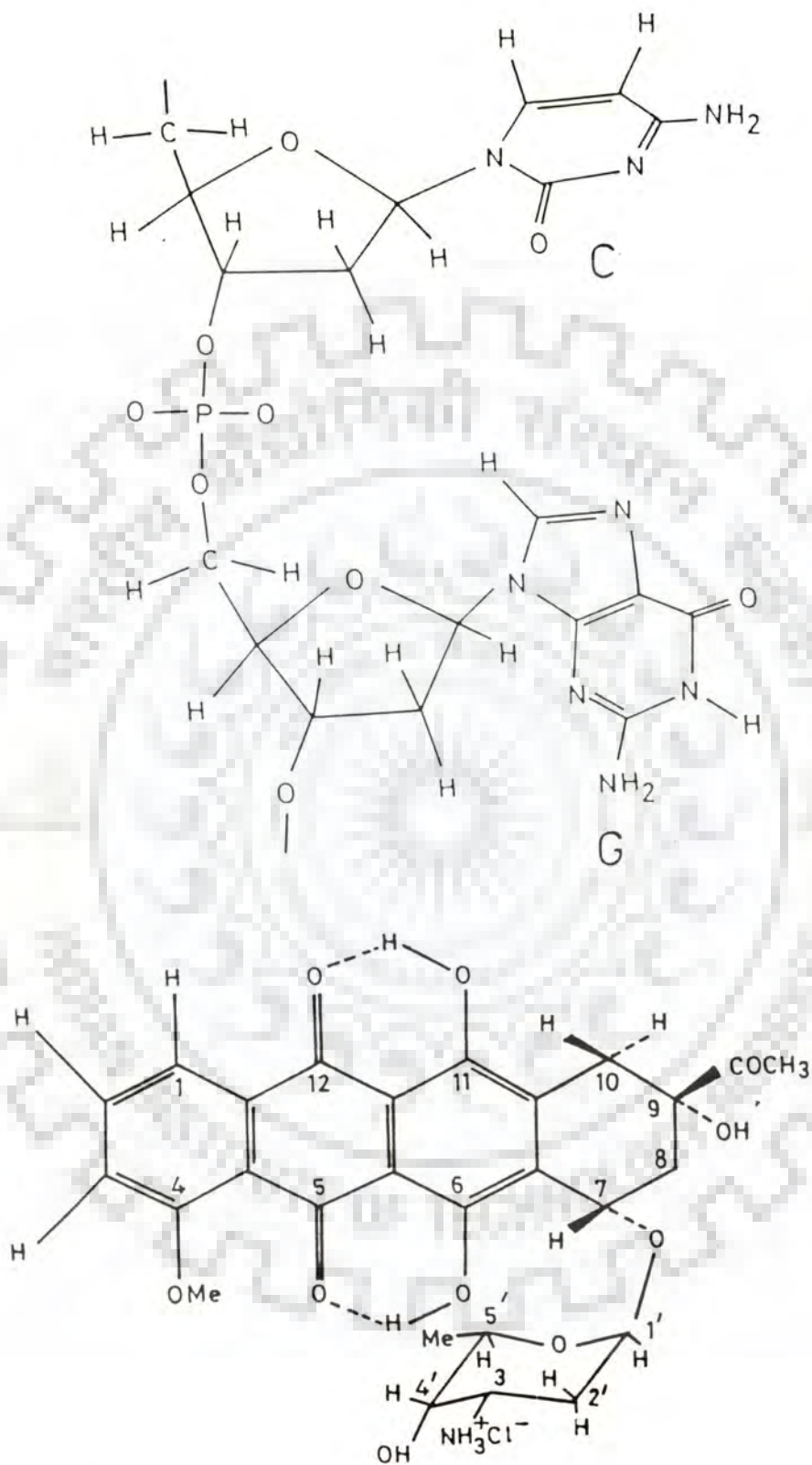


Figure 5.1: Structure of (a) deoxydinucleotide d-CpG and (b) Daunomycin

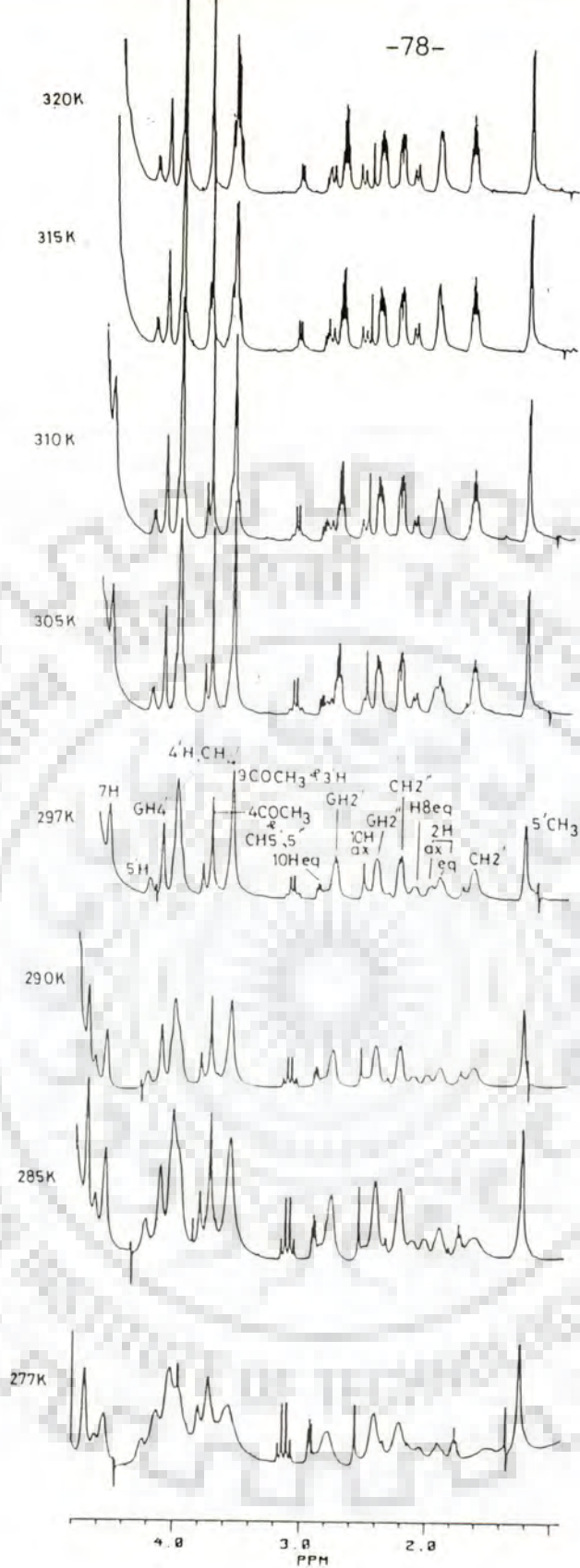


Figure 5.2: (a)

500 MHz proton NMR spectra of 1:2 complex of 5.5mM daunomycin and 11.0 mM (duplex) d-CpG at indicated temperatures, in D₂O (pH 6.95). Ref.DSS, in range 1.0 - 4.8 ppm

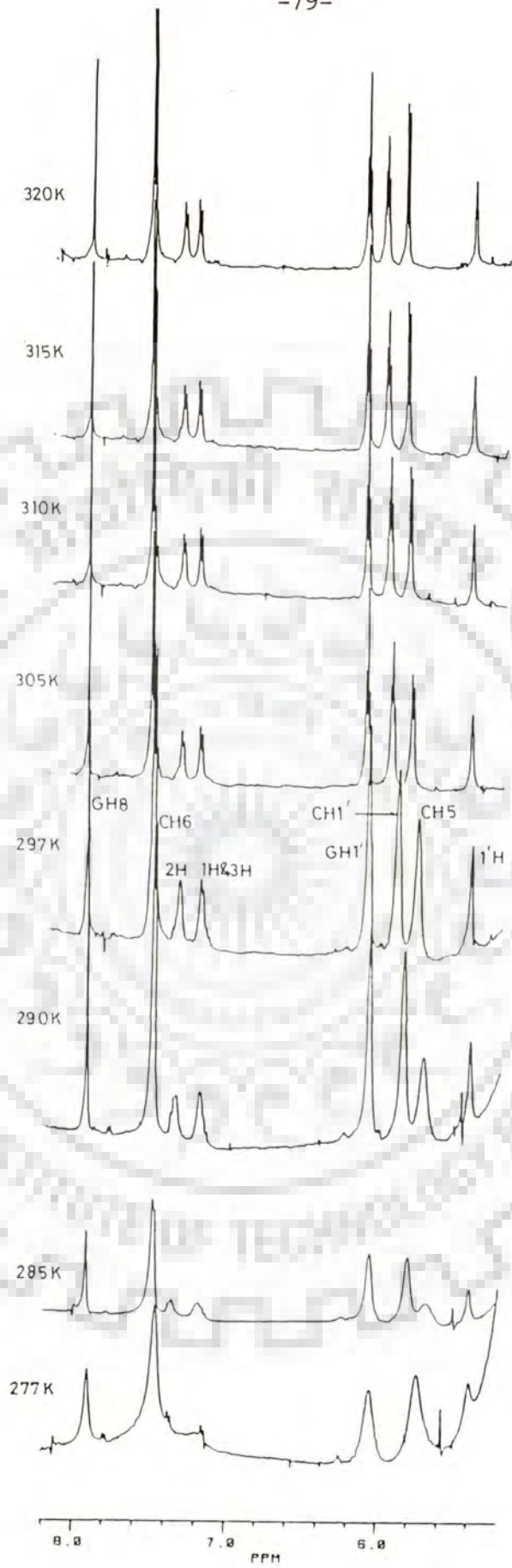


Figure 5.2: (b)

500 MHz proton NMR spectra of 1:2 complex of 5.5 mM daunomycin and 11.0 mM (duplex) d-CpG at indicated temperatures, in D₂O (pH 6.95). Ref. DSS, in range 5.2 - 8.2 ppm

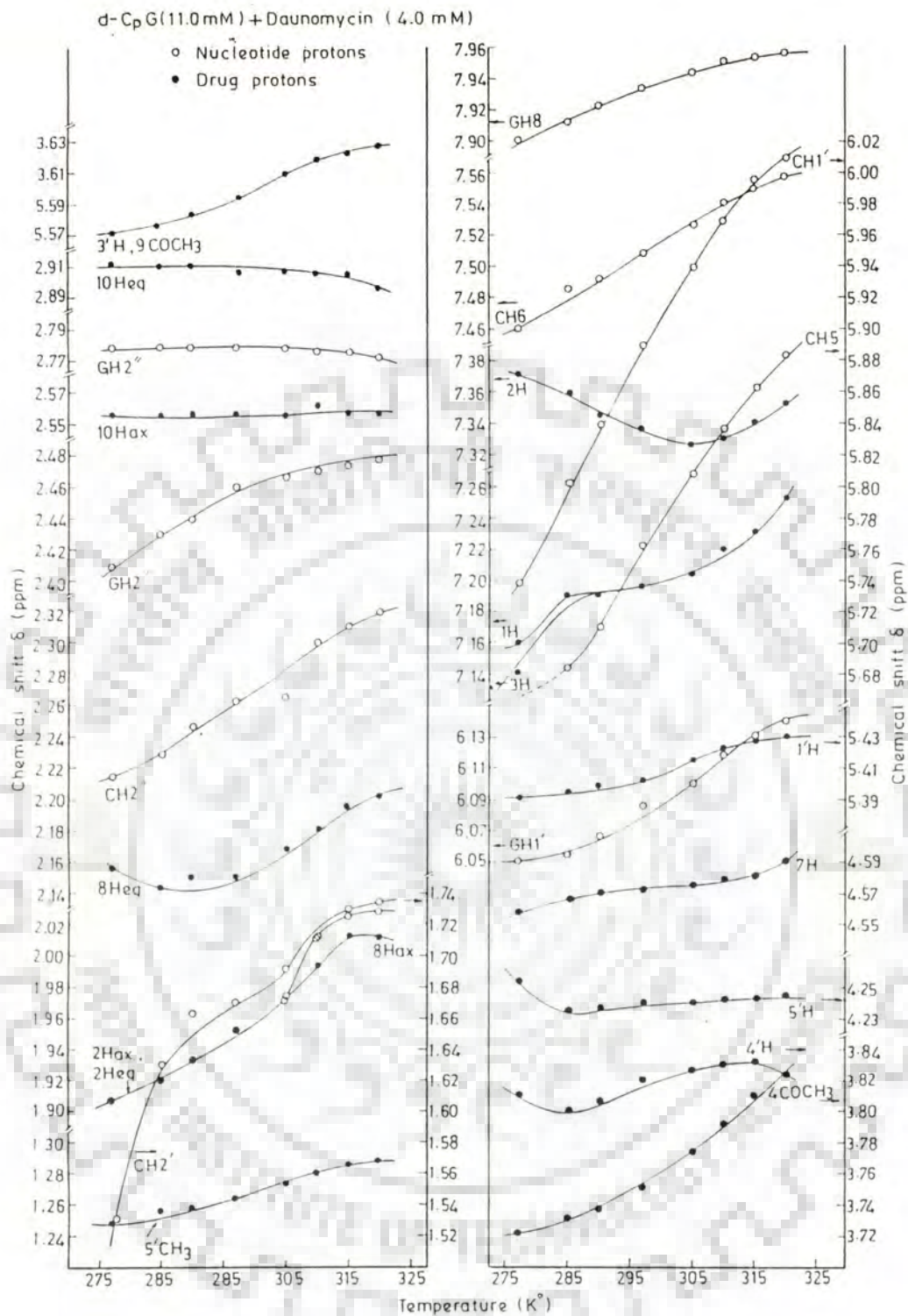


Figure 5.3: Chemical shifts of nucleotide and drug protons in daunomycin d-CpG complex, as a function of temperature

Table 5.1: Chemical shift values (in ppm) of daunomycin and d-CpG protons in 1:2 complex, at indicated temperatures

Temp. (K)	GH8	CH6	CH5	CH1'	GH1'	CH2'	CH2''
277	7.900	7.461	-	5.740	6.050	1.530	2.216
285	7.916	7.486	5.864	5.803	6.055	1.629	2.229
290	7.924	7.492	5.711	5.840	6.067	1.664	2.247
297	7.934	7.508	5.763	5.890	6.087	1.670	2.263
305	7.944	7.520	5.810	5.941	6.108	1.693	2.266
310	7.950	7.539	5.840	5.971	6.122	1.711	2.301
315	7.953	7.550	5.865	5.997	6.133	1.729	2.311
320	7.954	7.558	5.884	6.019	6.141	1.730	2.321

Temp. (K)	GH2'	GH2''	2H	1H	3H	1'H	7H
277	2.779	2.409	7.370	7.160	7.140	5.390	4.560
285	2.777	2.431	7.360	7.190	7.190	5.394	4.567
290	2.780	2.441	7.344	7.190	7.190	5.399	4.570
297	2.780	2.461	7.336	7.196	7.196	5.402	4.572
305	2.779	2.466	7.327	7.205	7.205	5.414	4.575
310	2.778	2.470	7.331	7.221	7.221	5.421	4.579
315	2.777	2.475	7.340	7.240	7.239	5.427	4.581
320	2.773	2.475	7.349	7.256	7.256	5.431	4.593

Table 5.1:.....Continued.....

Temp. (K)	5'H	5'CH ₃	4'H	4COCH ₃	3'H	10Heq	10Hax
277	4.253	1.249	3.810	3.722	3.572	2.911	2.555
285	4.235	1.257	3.803	3.730	3.577	2.911	2.555
290	4.235	1.259	3.803	3.737	3.584	2.910	2.555
297	4.237	1.264	3.820	3.751	3.594	2.908	2.553
305	4.240	1.274	3.827	3.774	3.610	2.907	2.565
310	4.243	1.281	3.830	3.792	3.617	2.907	2.556
315	4.246	1.286	3.832	3.810	3.623	2.906	2.556
320	4.245	1.289	3.825	3.825	3.625	2.895	2.554

Temp. (K)	9COCH ₃	8Heq	2Heq	2Hax	8Hax
277	2.572	2.156	1.907	1.907	1.907
285	2.578	2.143	1.921	1.921	1.921
290	-	2.152	1.934	1.934	1.934
297	3.594	2.150	2.017	2.017	1.952
305	3.610	2.169	1.975	1.975	1.954
310	3.619	2.184	2.011	2.011	1.996
315	3.623	2.197	2.027	2.027	2.013
320	3.625	2.207	2.025	2.025	2.011

that a rich population of d-CpG remains double helical at room temperature. However, the change in mid point transition temperature is not very different from that of observed in d-CpG alone studies (295-297K). A little change of 2 K in T_m value of d-CpG has been observed after complex formation. Many of the daunomycin protons behave independent of temperature and the state of the nucleotide. On melting of helix, aromatic proton resonance (from 1H&3H) shifts downfield by 0.12 ppm. Small changes in chemical shifts for 5'CH₃, 4COCH₃, 8H_{eq}, and 3'H&9COCH₃ signals, are also observed. The shifts in aromatic proton signals are similar to those seen for daunomycin - d(pTpA)₃ complex (31). But H1' chemical shift change is smaller than that reported by Phillips et al.[31]. In fact, the daunomycin chemical shifts observed here represent an average of the chemical shifts of the free drug and the bound drug. Aromatic protons of the drug as well as nucleotide base protons exhibit an upfield shift in chemical shift values on complex formation (Table 5.2). It indicates that drug intercalates between base pairs and shift arises due to ring-current shielding. At the same time, ring protons other than 1H, 2H and 3H on D ring of daunomycin (see Figure 5.1) do not show any major change in chemical shift. It may be suggested in the light of above fact that it might be due to partial overlapping of planar ring system of daunomycin with nucleotide base pairs. It is consistent with reports of Patel et al.[29].

Table 5.2: Changes in chemical shift ($\Delta\delta$ in ppm) of Daunomycin and d-CpG protons at indicated temperatures

SYSTEM	TEMP.	GH8	CH6	CH5	CH1'	GH1'	CH2'	GH2'
d-CpG alone	277	8.008	7.562	5.903	6.015	6.185	1.598	2.843
	297	8.032	7.578	5.944	6.080	6.216	1.664	2.821
	320	8.020	7.597	5.963	6.108	6.235	1.774	2.797
d-CpG + DNM	277	7.900	7.461	-	5.740	6.050	1.530	2.779
	297	7.934	7.508	5.763	5.890	6.087	1.670	2.780
	320	7.954	7.558	5.884	6.019	6.141	1.730	2.773
$\Delta\delta$ (in ppm)	277	0.108	0.101	-	0.275	0.135	0.068	0.064
	297	0.098	0.070	0.023	0.190	0.129	0.006	0.041
	320	0.066	0.039	0.079	0.089	0.090	0.044	0.024

SYSTEM	TEMP.	2H	1H	3H	1'H	7H	5'H	5'CH ₃
DNM alone	277	7.445	7.184	7.149	5.430	4.680	4.254	1.292
	297	7.514	7.239	7.226	5.429	4.728	4.250	1.302
	320	7.554	7.290	7.272	5.419	4.760	4.237	1.303
d-CpG + DNM	277	7.370	7.160	7.140	5.390	4.560	4.253	1.249
	297	7.336	7.196	7.196	5.402	4.572	4.237	1.264
	320	7.349	7.256	7.256	5.431	4.593	4.245	1.289
$\Delta\delta$ (in ppm)	277	0.075	0.024	0.009	0.040	0.120	0.001	0.043
	297	0.178	0.043	0.030	0.027	0.156	0.013	0.038
	320	0.205	0.034	0.016	-0.012	0.167	-0.008	0.013

Table 5.2:Continued....

SYSTEM	TEMP.	4'H	4COCH ₃	3'H	10Heq	10Hax	9COCH ₃	8Heq
DNM alone	277	3.827	3.761	3.688	2.761	2.541	3.599	2.164
	297	3.836	3.805	3.682	2.811	2.507	3.615	2.200
	320	3.834	3.834	3.663	2.744	2.577	3.627	2.223
d-CpG +	277	3.810	3.772	3.572	2.911	2.555	-	2.156
	297	3.820	3.751	3.594	2.908	2.553	3.594	2.150
	DNM	320	3.825	3.825	3.625	2.895	2.554	3.625
$\Delta\delta$ (in ppm)	277	0.017	-0.011	0.116	-0.150	-0.014	-	0.008
	297	0.016	0.054	0.088	-0.097	-0.046	0.021	0.050
	320	0.009	0.009	0.032	-0.151	-0.023	0.002	0.016

SYSTEM	TEMP.	2Heq	2Hax	8Hax
DNM alone	277	1.975	1.975	1.975
	297	1.995	1.916	1.996
	320	2.010	2.010	2.010
d-CpG +	277	1.907	1.907	1.907
	297	2.017	2.017	1.952
	DNM	320	2.025	2.025
$\Delta\delta$ (in ppm)	277	0.068	0.068	-0.068
	297	-0.022	-0.021	0.044
	320	-0.015	-0.015	-0.001

Two Dimensional NMR Experiments

Figures 5.4 and 5.5 are the results of COSY and NOESY experiments on the complex of 11.0 mM d-CpG and 5.5 mM daunomycin at 297 K. Assignments of various NMR signals to specific protons of nucleotide and daunomycin were made using uncomplexed state spectra of d-CpG and drug as a reference and later on assignments were checked by NOESY spectrum analysis. Following cross peaks are seen in COSY spectrum:

Drug protons:

2H	1H&3H
5'H	5'CH ₃
8 H _{eq}	8 H _{ax}
2'H _{ax}	2'H _{eq}
10H _{ax}	10H _{eq}
9COCH ₃	8H _{ax}
3'H	4'H
4COCH ₃	4'H
7H	8H _{ax}

Dinucleotide protons:

CH6	CH5
GH1'	GH2'
GH1'	GH2''
GH2'	GH2''
GH3'	GH4'
CH1'	CH2''

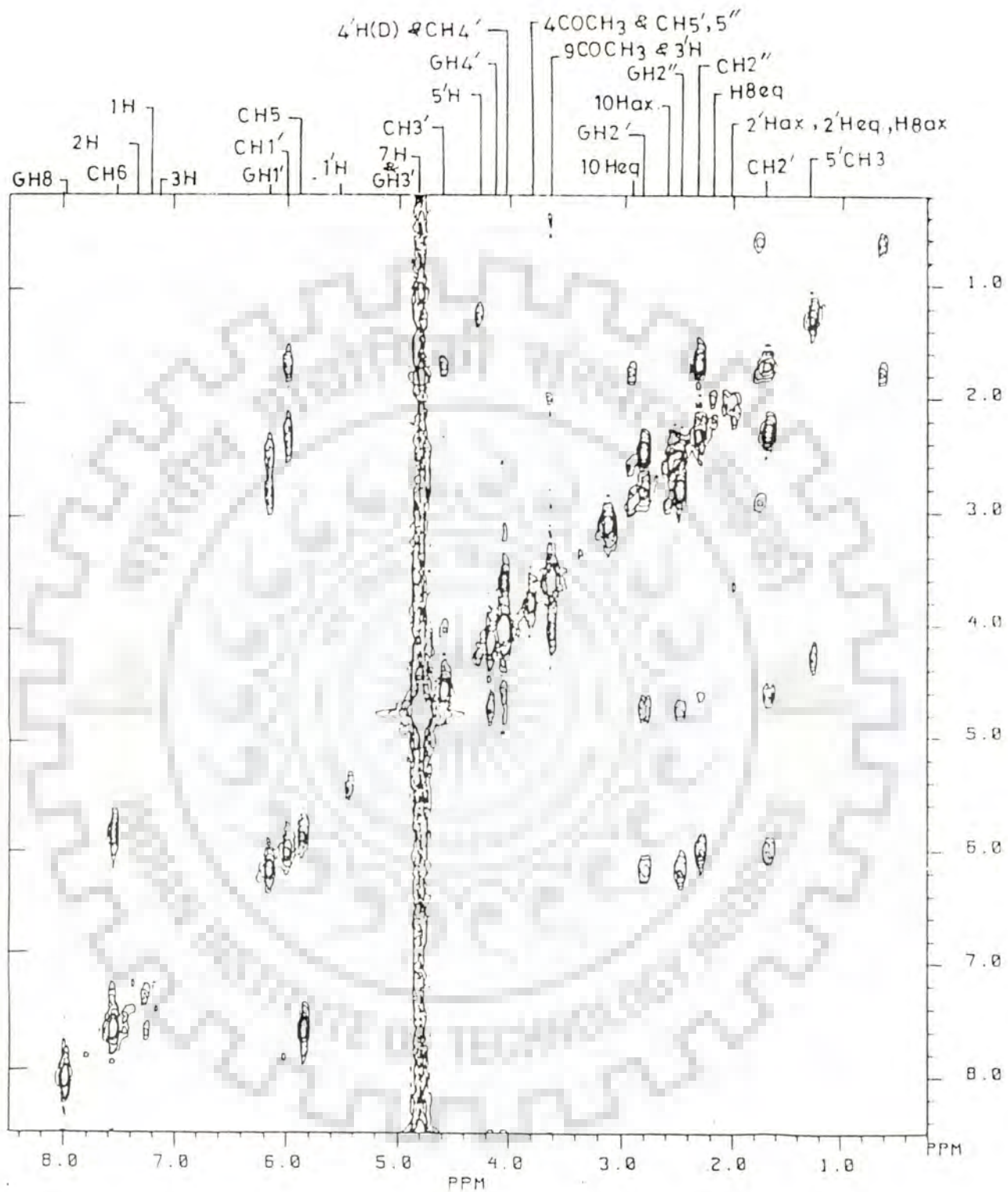


Figure 5.4: 500 MHz COSY spectrum of daunomycin - d-CpG complex in D₂O (pH 6.95) at 297 K. Ref. DSS - unsymmetrised spectrum

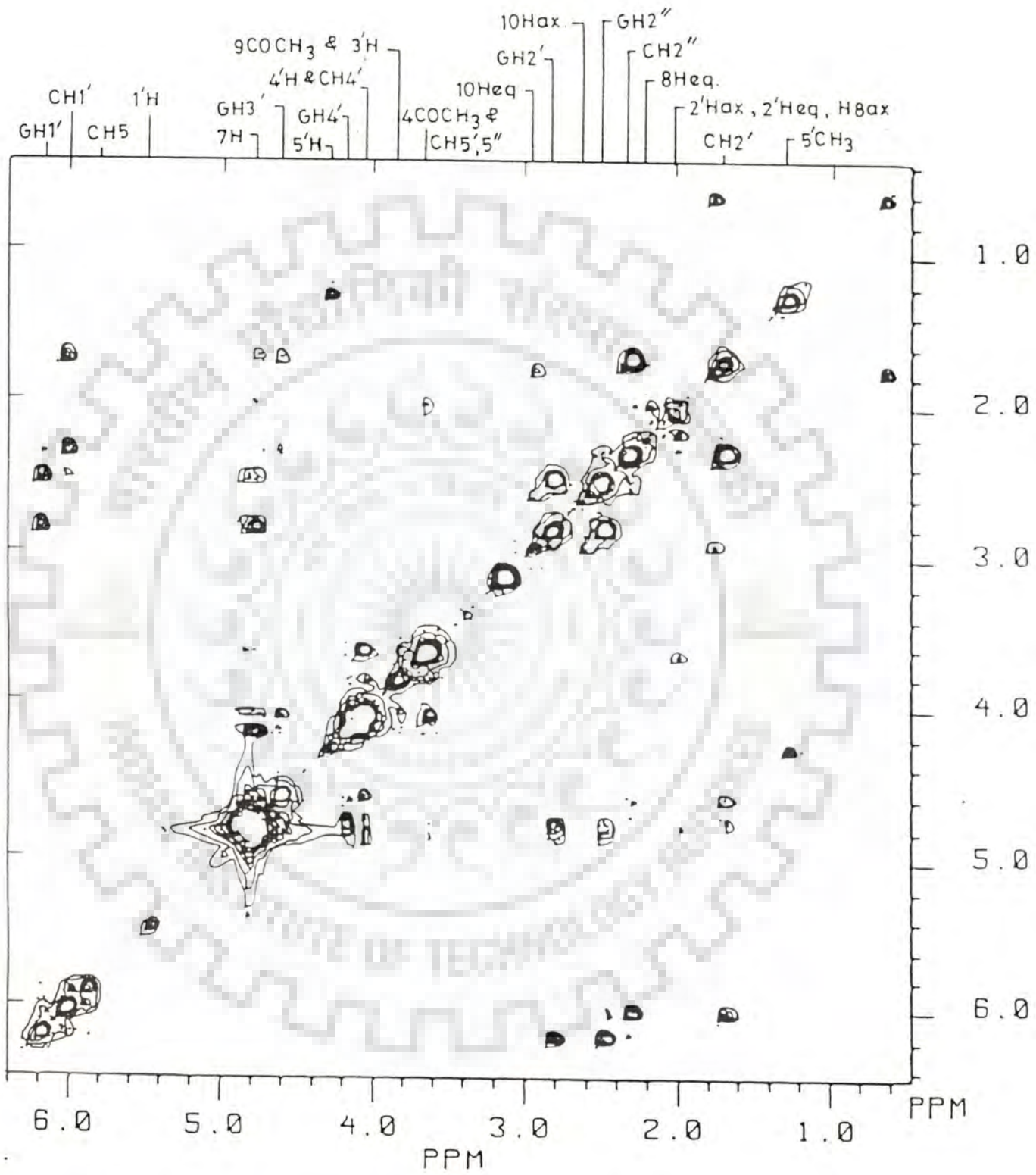


Figure 5.4: ...Continued...symmetrised spectrum

CH1' CH2'
 CH2' CH3'
 CH2' CH2''
 CH3' CH4'

COSY spectrum easily makes distinguished- two sugar spin networks associated with C and G of d-CpG. GH1' and CH1' both show strong couplings with their H2' and H2'' protons. In both cases, H2' shows a sure connectivity with H3' proton resonance. However, GH3' lies embedded in HDO signal tail and hence such cross peak could not be found for G base sugar. Its position is established from GH4' resonance which shows a clear cross peak with GH3'. Since both sugar show H3'-H4' connectivities as well as presence of H2'-H3' is established, it may be inferred that both sugar possess O1'-endo sugar conformation. This inference is made on the basis of strategy discussed in Chapter-2. This way, it may be observed that on complex formation d-CpG do not show any change in sugar conformations and they remain O1'-endo as explored in uncomplexed state of d-CpG.

Figure 5.5 exhibits a number of cross peaks in NOESY spectrum. The results of relative intensities in NOESY spectrum are as follows:

GH8.....GH1'	strong
GH8.....GH4'	weak
GH8.....GH2'	strong
* GH8.....10Heq	strong
GH8.....GH2''	strong
GH8.....CH2'	weak

* GH8.....5'CH ₃	weak
* CH6.....3H & 1H	strong
* CH6.....2H	strong
CH5.....CH5	strong
CH6.....CH1'	strong
CH6.....CH3'	weak
* CH6.....4'H & CH4'	weak
CH6.....CH5' & 5"	strong
CH6.....CH2"	strong
CH6.....CH2'	strong
* 2H.....CH5' & 5"	weak
2H.....3H & 1H	weak
4COCH ₃3H & 1H	strong
GH1'.....GH4'	strong
GH1'.....GH2'	strong
GH1'.....GH2"	strong
CH1'.....CH3'	weak
* CH1'.....CH4' & 4'H	weak
CH1'.....CH2"	strong
CH1'.....CH2'	strong
CH5.....CH5' & 5"	weak
1'H.....4COCH ₃	weak
1'H.....3'H	weak
1'H.....2'H _{ax} & eq	weak
1'H.....5'CH ₃	weak
CH3'.....CH4'	strong
* CH3'.....9COCH ₃ & 3'H	strong
CH3'.....CH2"	strong

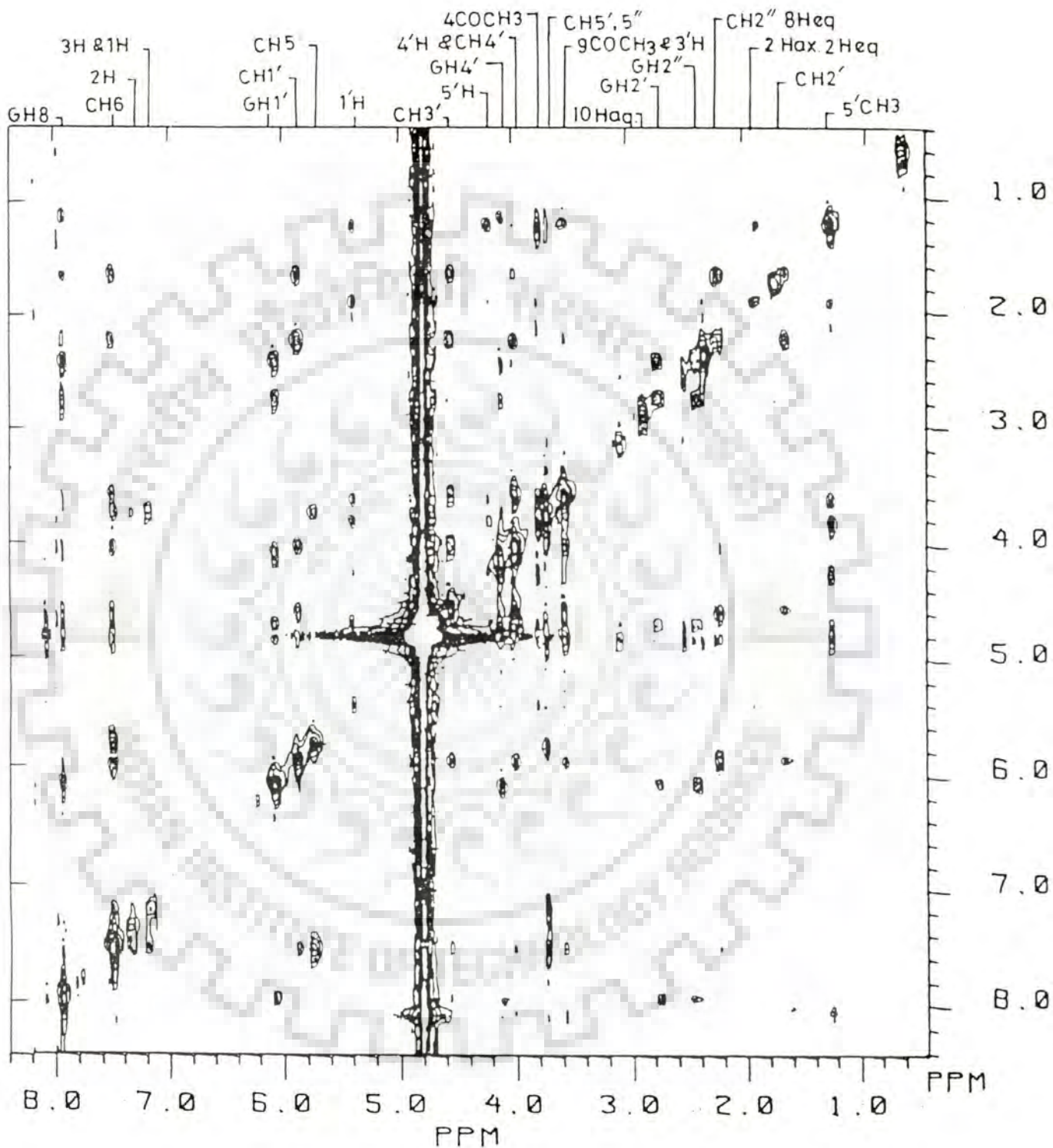


Figure 5.5: 500 MHz NOESY spectrum of daunomycin d-CpG complex in D₂O (pH 6.95) at 297 K. Ref. DSS unsymmetrised spectrum

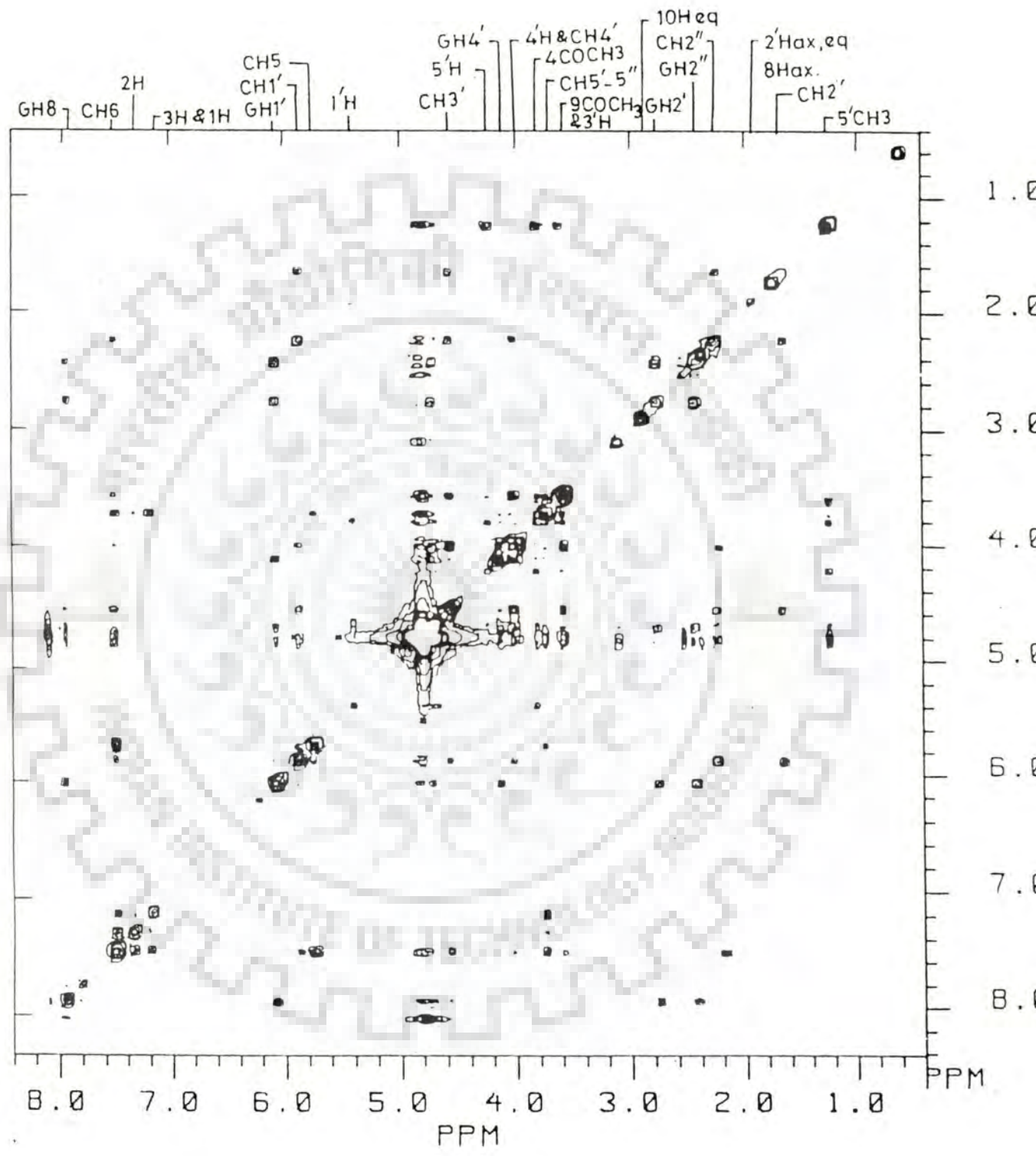


Figure 5.5: ...Continued...symmetrised spectrum

CH3'.....CH2'	strong
* 5'H.....CH5' & 5''	weak
5'H.....3'H	weak
5'H.....5'CH ₃	strong
* GH4'.....5'CH ₃	weak
4'H.....4COCH ₃	weak
4'H.....3'H	strong
* 4'H.....CH2''	strong
4COCH ₃3'H	strong
4COCH ₃5'CH ₃	strong
* CH5' & 5''.....9COCH ₃ & 3'H	strong
5'CH ₃9COCH ₃ & 3'H	strong
GH2'.....GH2''	strong
CH2'.....CH2''	strong
2'H _{ax} & _{eq}5'CH ₃	weak
* ...Inter molecular nOe's are marked with an asterik	

A change in helix sense of d-CpG is observed on complex formation. Presence of strong NOESY cross peaks of base protons GH8 and CH6 with their H1' protons and CH6 with CH5' and 5'' suggest a left-handed DNA structure of d-CpG in complex. Inter-residue nOe GH8-CH2' also strengthens above idea. Also, the change in glycosidic bond rotation (χ) values from ANTI to SYN can not be ruled out on the basis of base to H1' nOe's. Adoption of left handedness by native d-CpG in crystal has been reported by Wiswamitra et al.[136]. Crystal structure analysis revealed that alternating d(CpG) sequences have the ability to adopt left handed Z-DNA structure even at

the dimer level. Deoxy-CpG complexed with mitroxantrone, another anticancer drug, has shown that drug interacted with d(CpG) Z-DNA dimer helical fragments. Shapiro et al.[112] has observed SYN orientation of guanine base in d-CpG complexed with 4-aminobiphenyl. We have also observed identical behaviour in present studies, bases with SYN orientations, in dCpG complexed with daunomycin.

Additional NOESY cross peaks observed between drug and d-CpG protons suggest specific orientation of drug molecule in the complex. Dreiding model building studies suggest that drug chromophore ring D protrudes into helical groove; such that methoxy group is not in vicinity of any nucleotide proton. Removal of the methoxy group has been reported associating with effectiveness of daunomycin [30]. Protons on ring A of the chromophore (10 H_{eq}) show intermolecular nOe with GH8. GH8 also shows weak nOe with 5'CH₃ proton of daunomycinon sugar. COCH₃ group at position 9 on ring A of daunomycin chromophore shows strong nOe with H3' proton of furanose sugar associated with cytosine. On the basis of all these observed intermolecular nOe's, specific structure of the complex is thus being inferred.

CHAPTER 6

THE STRUCTURE OF ACTINOMYCIN

Solution conformation of Actinomycin D has been studied by two dimensional NMR, at 500 MHz. 5.5 mM solution of Actinomycin was prepared in 0.1 mM phosphate buffered D₂O. Sample was repeatedly lyophilised and finally redissolved in 99.9% D₂O. Because the solubility of Actinomycin D in water is low at room temperature, binary solvent system of 1/100 part dimethylformamide (deuterated) and D₂O was used in NMR sample. pH value was monitored at 6.95. Temperature variable one dimensional NMR experiments were carried out in temperature range 277-320 K. Two dimensional COSY and NOESY experiments were carried out at room temperature, 297K.

Temperature Dependence

Figure 6.1 shows one dimensional NMR spectrum of actinomycin D recorded at different temperatures in temperature range 277 - 320 K, in range 0.0 to 4.8 ppm. No major change is observed in nonexchangeable protons of actinomycin as temperature increases. Chemical shift values of various drug protons at different temperatures have been tabulated in Table 6.1 and $\delta(\text{ppm})$ Vs temperature curves for drug protons have been shown in Figure 6.2. Assignments of different proton signals have further been confirmed by 2D NMR analysis. Proton on

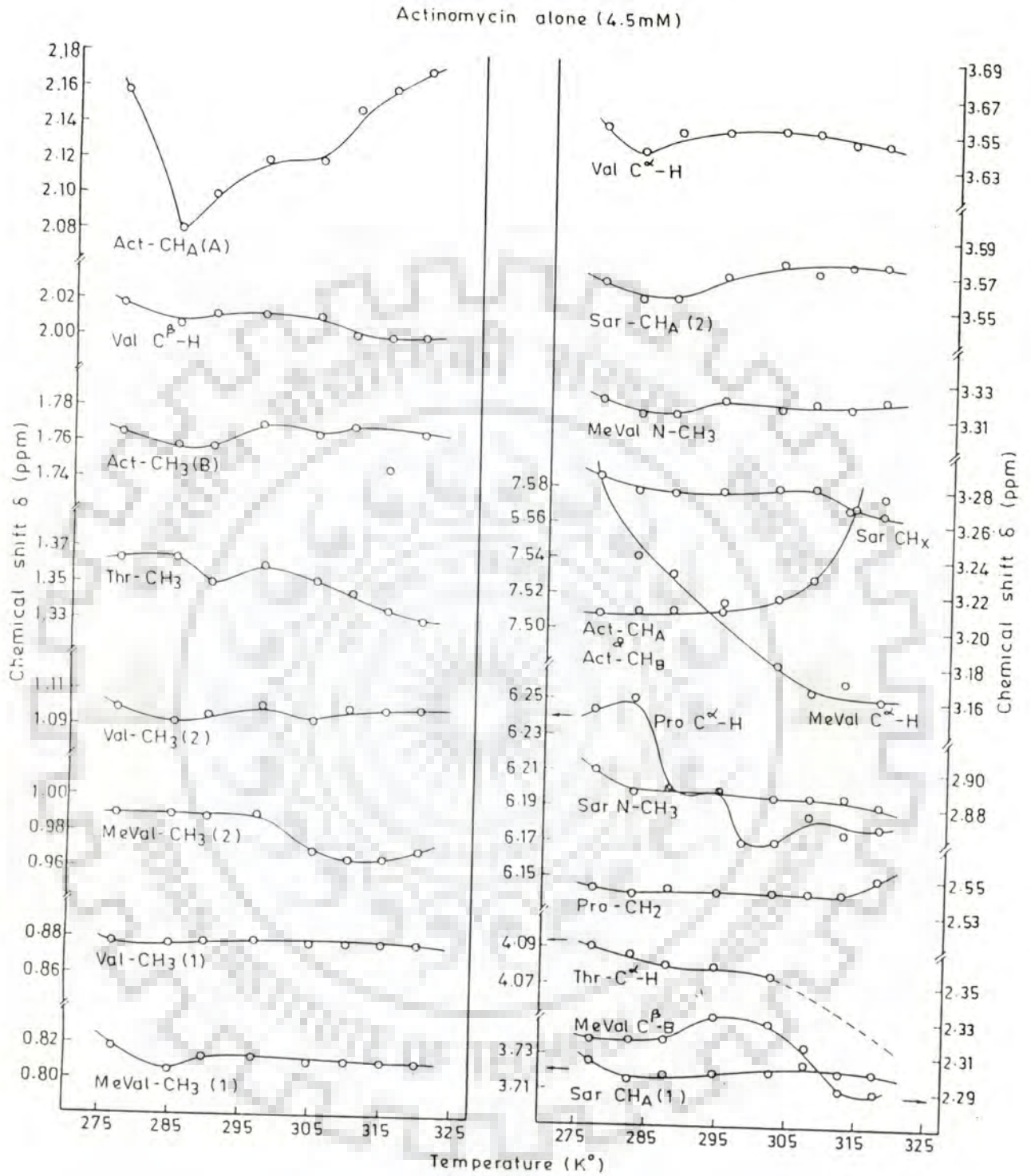


Figure 6.2: Chemical shifts of nonexchangeable protons of actinomycin, as a function of temperature

Table 6.1: Chemical shift values (in ppm) of various protons at 500 MHz of Actinomycin in D₂O (pH 6.95) in temperature range 277 - 320K

Temp. (K)	Act CH _A & Act CH _B	Pro C ^α -H	Thr C ^α -H	Sar CH _A (1)	Val C ^α -H	Sar CH _A (2)	MeVal N-CH ₃
277	7.509	6.244	4.093	3.727	3.565	3.653	3.320
285	7.511	6.215	4.086	3.716	3.552	3.639	3.313
290	7.511	6.200	4.079	3.719	3.552	3.652	3.313
297	7.517	6.191	4.079	3.719	3.571	3.652	3.323
305	7.519	6.191	4.075	3.720	3.577	3.652	3.315
310	7.531	6.175	-	3.725	3.572	3.652	3.318
315	7.572	6.175	-	3.720	3.575	3.645	3.315
320	7.575	6.150	-	3.715	3.575	3.645	3.320

Temp. (K)	Sar CH _x	MeVal C ^α -H	Sar N-CH ₃	Pro CH ₂	MeVal C ^β -H	Act- CH ₃ (A)	Val C ^β -H
277	3.286	3.286	2.900	2.546	2.320	2.160	2.019
285	3.278	3.239	2.887	2.539	2.320	2.081	2.006
290	3.277	3.232	2.893	2.545	2.320	2.100	2.013
297	3.280	3.213	2.893	2.542	2.333	2.119	2.013
305	3.275	3.180	2.889	2.544	2.327	2.121	2.011
310	3.280	3.165	2.885	2.545	2.314	2.147	2.005
315	3.267	3.170	2.885	2.545	2.290	2.160	2.007
320	3.265	3.160	2.880	2.550	2.290	2.175	2.005

Temp. (K)	Act CH ₃ (B)	Thr CH ₃	Val CH ₃ (2)	MeVal CH ₃ (2)	Val CH ₃ (1)	MeVal CH ₃ (1)
277	1.765	1.365	1.106	0.993	0.878	0.819
285	1.758	1.365	1.093	0.993	0.867	0.806
290	1.758	1.350	1.097	0.987	0.878	0.813
297	1.765	1.362	1.103	0.993	0.878	0.813
305	1.771	1.352	1.094	0.970	0.871	0.811
310	1.747	1.345	1.100	0.965	0.870	0.810
315	-	1.335	1.100	0.965	0.870	0.810
320	1.765	1.335	1.097	0.970	0.867	0.810

chromophoric rings of actinomycin, Act-CH₃(A) shows a little larger downfield shift with increase in temperature. With respect to this, change observed in δ (ppm) value of Act - CH₃(B) is rather low. Two peptide chains have also been identified and were marked as 1 and 2. Protons at different peptide residues of these chains were successfully distinguished and assigned. For some of the protons viz. C ^{β} -H, C ^{α} -H of Valine, MeVal N-CH₃, C ^{α} -H of Proline etc. signals were found overlapped for two peptide chains. Temperature dependent behaviour of pentapeptide chain proton signals suggests that no major change in conformation occurs as temperature increases. The presence of only one conformation of the peptide rings has been suggested as it might be due to interannular Val-NH to Val-CO hydrogen bonds, which serve to lock the pentapeptide in a single structure [65]. Interaction with DNA may then result in loss of those hydrogen bonds, permitting the pentapeptide to take on an alternate and timely suitable conformation.

Two Dimensional NMR Experiments

COSY spectrum of 5.5 mM actinomycin solution has been shown in Figure 6.2. Previous work [47] had established many proton assignments for actinomycin in aqueous solution by binary solvent titrations from deuteriobenzene through deuterio methanol to D₂O. These assignments were confirmed and further extended by COSY and NOESY spectra. On the basis of cross peaks seen and spin system correlation, the assignments of

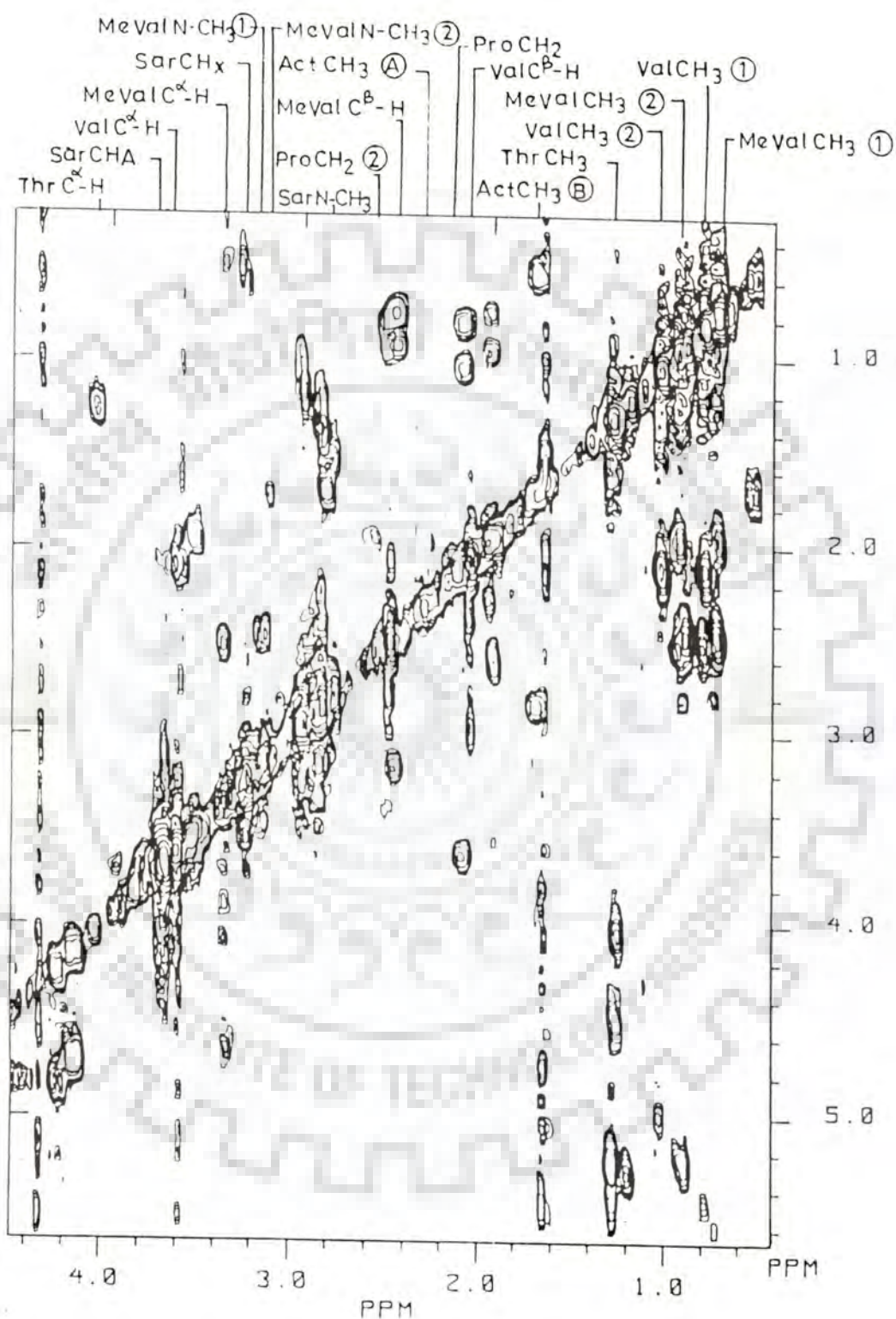


Figure 6.3: 500 MHz COSY spectrum of actinomycin (5.5mM) in D₂O at 297 K. Ref. DSS - unsymmetrised spectrum

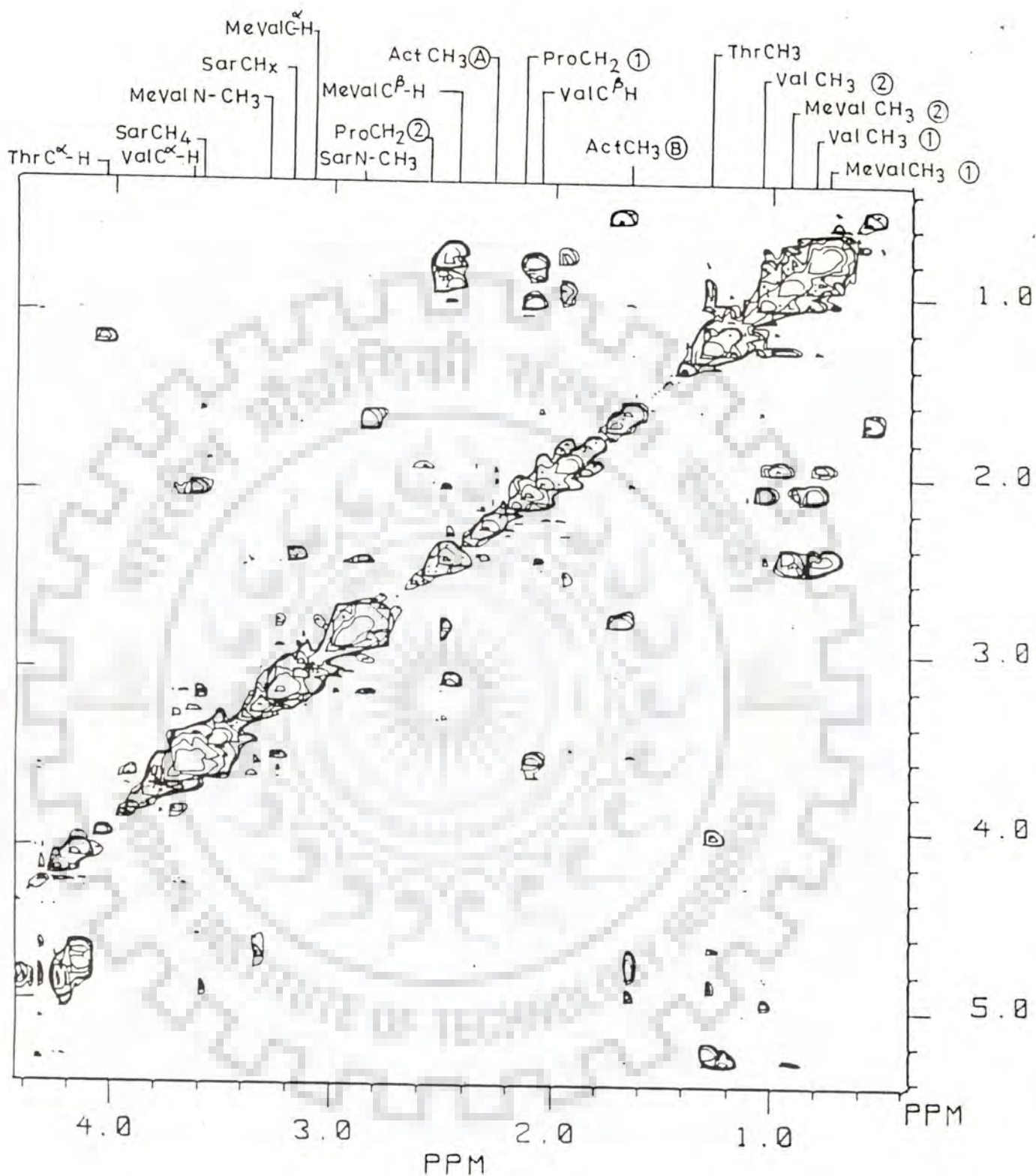


Figure 6.3: ...Continued... symmetrised spectrum

Angerman et al. were confirmed except for Thr C^α-H (4.08 ppm), Thr C^β-H (6.1 ppm). Positions of other resonances have been found nearly in agreement. Two sets of COSY connectivities could be identified for Val-CH₃, MeVal-CH₃, Pro-CH₂ and Pro C^α-H protons from two pentapeptide chains. Various COSY connectivities which are seen in COSY spectrum are listed below :

Val CH₃(1).....ValC^β-H

Val CH₃(2).....Val C^β-H

MeVal CH₃(2).....MeVal C^β-H

Thr CH₃.....Thr C^α-H

Thr C^α-H.....Thr C^β-H

Pro CH₂(1).....Pro C^α-H(1)

ProCH₂(2).....Pro C^α-H(2)

Sar N-CH₃.....Sar CH_x

Sar CH_x.....Sar CH_A

Val C^β-H.....ValC^α-H

MeVal C^α-H.....MeVal C^β-H

MeVal C^α-H.....MeVal N-CH₃

Analysis of NOESY spectrum of actinomycin D shown in Figure 6.4, provides fresh insight into the more detailed aspects of its conformation. A list of NOESY connectivities seen is as given below:

Thr C ^α -H.....Thr-CH ₃	weak
*Thr C ^α -H.....Act-CH ₃ (2)	strong
Val C ^α -H.....Val-CH ₃ (2)	strong
Sar CHx.....MeValCH ₃ (2)	weak
MeVal C ^α -H.....MeVal N-CH ₃	strong
Sar CHx.....Sar N-CH ₃	weak
MeVal C ^α -H.....MeVal CH ₃ (2)	strong
Sar N-CH ₃MeVal CH ₃ (1)	weak
Sar N-CH ₃MeVal CH ₃ (2)	strong
MeVal C ^β -H.....MeVal CH ₃ (1)	strong
MeVal C ^β -H.....MeVal CH ₃ (2)	strong
Act-CH ₃ (1).....ActCH ₃ (2)	weak
Val C ^β -H.....Val-CH ₃ (1)	weak
Val C ^β -H.....Val-CH ₃ (2)	weak
*Val C ^β -H.....Act-CH ₃ (2)	strong

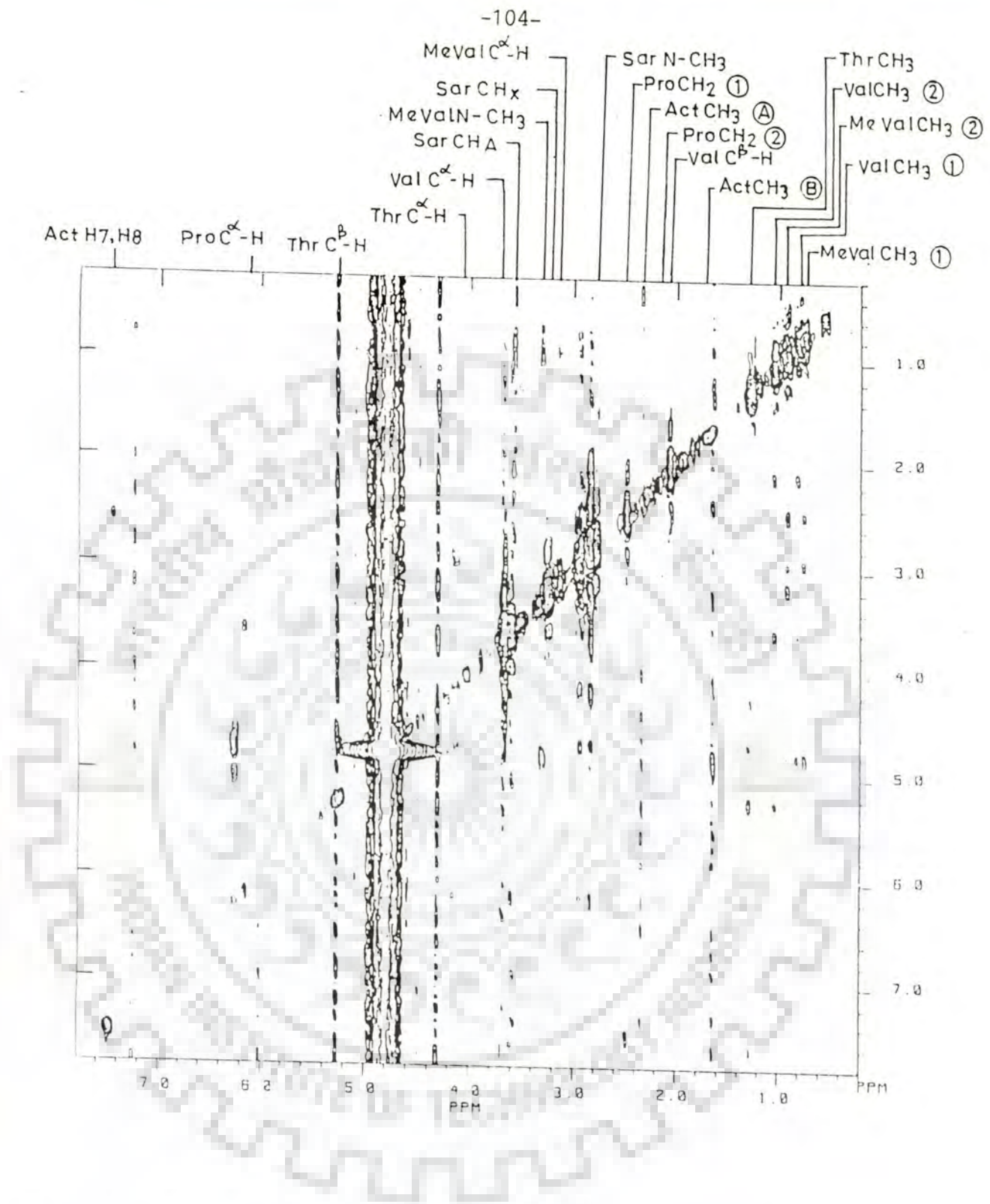


Figure 6.4: 500 MHz NOESY spectrum of actinomycin (5.5mM) in D₂O at 297 K. Ref. DSS - unsymmetrised spectrum

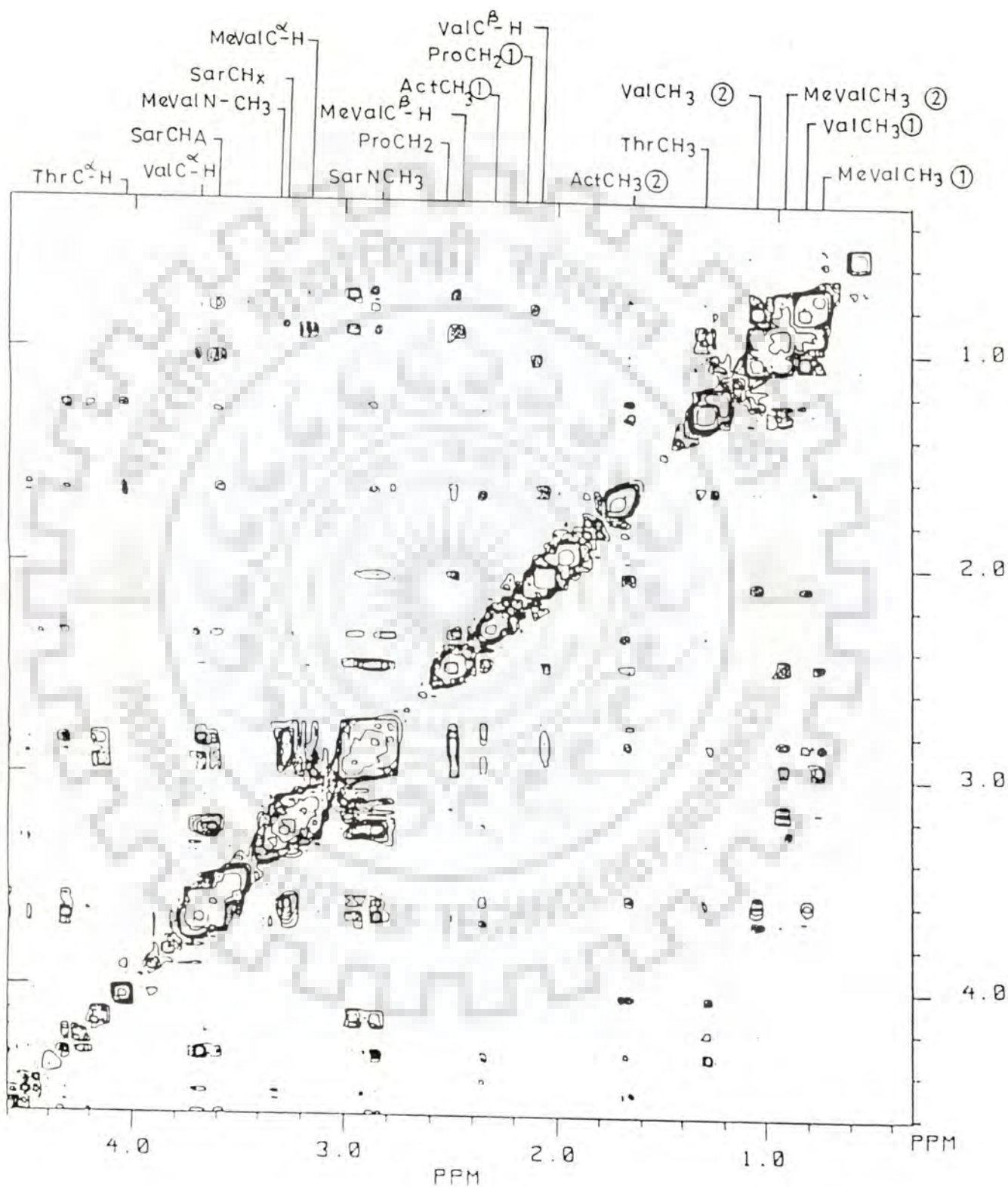


Figure 6.4: ...Continued... symmetrised spectrum

*Act-CH ₃Thr-CH ₃	strong
Val CH ₃ (1).....Val-CH ₃ (2)	strong
MeVal-CH ₃ (1).....MeVal-CH ₃ (2)	strong
Val C ^α -H.....Pro C ^α -H(2)	strong
Sar-CH ₃Pro C ^α -H(1)	strong
Thr-CH ₃Thr C ^β -H	strong
Val-CH ₃Thr C ^β -H	strong
* shows intermolecular nOe's	

Intra residue nOe's of peptide chains suggest orientations of side chain protons and substituted groups. Measurement of inter proton distances (Table 6.2) from Dreiding stereo model of actinomycin agrees with intensities of nOe's seen for different protons. A weak nOe between Sar-CH_x and Sar N-CH₃ protons is justified as measured distance between these two protons is 4.0Å. Some unusual and conformationally forbidden nOe's are also seen in NOESY spectrum of actinomycin. Thr C^α-H shows nOe's with Act-CH₃(2) with a strong magnitude. This NOESY connectivity is only possible if it is intermolecular; as in accordance, nOe of Act CH₃(1) with Act-CH₃(2) and further NOESY cross peaks of Val C^β-H with Act-CH₃(2) and Act-CH₃(1) showing nOe with Thr-CH₃ with equally strong magnitude, are also expected to be intermolecular. This idea is further confirmed from Dreiding model building. Above results indicate the presence of a

Table 6.2: Values of various interproton distances measured from dreiding model of actinomycin D. Values were optimised on the basis of nOe's observed in NOESY spectrum

		nOe	Distance in Å ^o
1.		Thr C ^α -H.....Thr CH ₃	2.4
2.	*	Thr C ^α -H.....Act CH ₃ (2)	-
3.		Val C ^α -H.....Val-CH ₃	3.3
4.		Sar CHx.....MeVal CH ₃ (2)	2.2
5.		MeVal C ^α -H.....MeVal N-CH ₃	1.9
6.		Sar CHx.....Sar N-CH ₃	4.0
7.		MeVal C ^α -H.....MeVal CH ₃	2.1
8.		Sar N-CH ₃MeVal CH ₃	1.6
9.		Sar N-CH ₃MeVal CH ₃	4.2
10.		MeVal C ^β -H.....MeVal CH ₃	2.4
11.		MeVal C ^β -H.....MeVal CH ₃	2.3
12.	*	Act-CH ₃Act CH ₃	3.3
13.		Val C ^β -H.....Val-CH ₃	2.3
14.		Val C ^β -H.....Val-CH ₃	2.4
15.	*	Val C ^β -H.....Act CH ₃	-
16.	*	Act CH ₃Thr CH ₃	-
17.		Val CH ₃Val CH ₃	2.0
18.		MeVal CH ₃MeVal CH ₃	2.0
19.		Val C ^β -H.....Pro C ^α -H	4.5
20.		Sar CHA.....Pro C ^α -H	1.9
21.		Thr CH ₃Thr C ^β -H	2.4
22.		Val CH ₃Thr C ^β -H	2.3

* nOe's marked with asterik are intermolecular

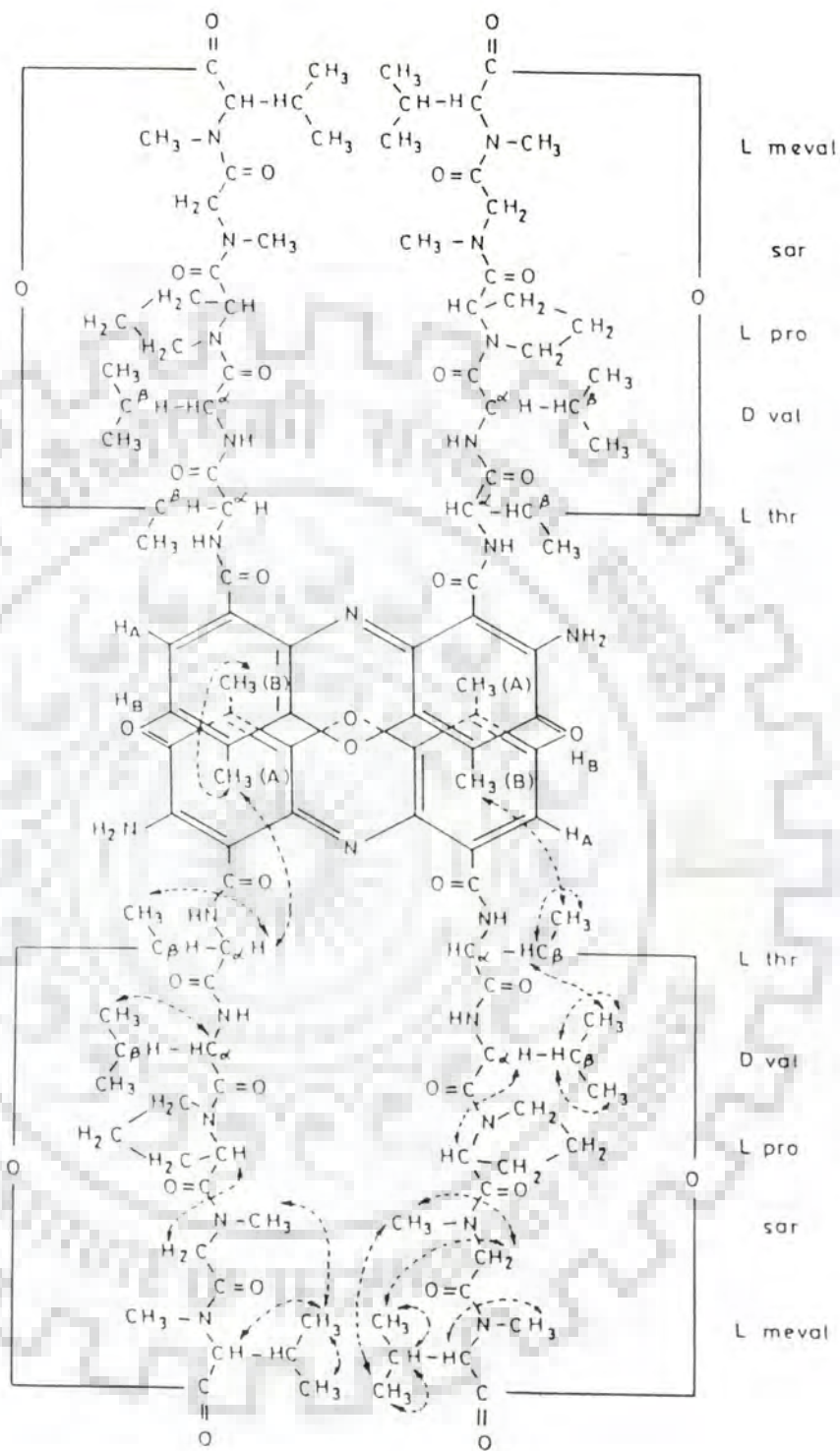


Figure 6.5: Structure of inverted dimer of actinomycin. nOe's seen in NOESY spectrum are shown by arrows

dimer structure of actinomycin in solution. The dimer probably exists in an inverted stacked form [Figure 6.5] as this configuration satisfies the presence of above listed nOe's, which are expected to be intermolecular. These results are in agreement with that reported by Danyluk et al.[47]. It was reported that dimer is formed by an interaction between the actinocyl group protons and these groups stack vertically in the dimer with one chromophore inverted with respect to the other.

Further, it can be accounted, that on increasing temperature, monomer:dimer ratio does not seem to be changing as practically no proton on peptide chains shows any remarkable change with temperature. However, little changes observed for actinocyl protons can be attributed to difference in dimer structure at different temperatures. At higher temperatures, aggregation of actinomycin molecule may also cause same effect on chemical shift values. Infact, the increased thermal motion at higher temperatures would cause a slight reduction in π electron overlap and a consequent loosening (lateral and vertical displacement) of the actinocyl groups, which leads to an increased shielding of CH₃(A) in agreement with its observed behaviour.

CHAPTER 7

POTENTIAL ENERGY CALCULATIONS ON DAUNOMYCIN AND ACTINOMYCIN D COMPLEXES WITH NUCLEIC ACID BASES, BASE PAIRS AND MODEL DINUCLEOTIDE SYSTEMS

The interaction between planar drugs and nucleotides is the best characterised prototypal, 'drug-receptor' interaction. There is sufficiently digged well of physico-chemical informations on these interactions, supporting an intercalated structure of the complexes. The phenomenon of intercalation refers to the insertion of planar aromatic rings between base pairs of nucleic acid, since Larman in 1961 proposed the intercalation hypothesis.

The primary mode of interaction of actinomycin D and daunomycin has also been found to be by intercalation. It is widely accepted that the planar portions of these drugs insert themselves between the adjacent base pairs of nucleotides (c.f. Chapter-2).

The act of intercalation here, brings up 'stacking' of these planar ring systems, which refers literally, the overlapping arrangements of parallel planar molecules (viz. base pairs and drug chromophores) separated by a Vander Waal's distance ($3.0 - 3.5\text{\AA}$). The stacking interaction is driven or stabilised by induced dipole interactions between the π electron clouds of

aromatic rings and most favoured in aqueous solvents.

In present work, energy involved in these stacking interactions has been estimated by second order perturbation method. The total interaction energy is a sum of electrostatic, polarisation, dispersion and repulsion energy terms (c.f. Chapter-3 for details). The electrostatic term of energy is computed by considering the terms upto second order i.e. consisting monopole-monopole, monopole-dipole and dipole-dipole components. For the calculations of dispersion and repulsion energy terms, Kitaigorodskii type formula has been used [133].

Molecular charge distribution on the molecules under study were calculated by Complete Neglect of Differential Overlap (CNDO/2) method. In case of drugs, daunomycin and actinomycin D, only the planar portion of drug was taken for CNDO calculations. In daunomycin, amino-sugar part attached to chromophore was ignored and was replaced by hydrogen. For actinomycin D, two peptide chains have been excluded and only planar chromophore was subjected to CNDO calculations. The molecular charge distribution on the nucleic acid bases and base pairs has also been calculated by the same method. Geometries used, were the results of single crystal X-ray diffraction studies by Voet and Rich [117]. Structure of daunomycin and actinomycin D have been adopted from X-ray studies reported in literature [120, 52].

ALGORITHMIC DETAILS

Algorithm used in searching the configurations with minimum stacking energy allows the entire configurational space to be scanned. The various steps of the procedure are as described below:

The nucleic acid bases/base pairs are taken in X-Y plane and the Z axis passes through an arbitrary point close to the centre of the molecule. The dyad axis is chosen as X-axis taking its origin at the helix centre. Drug chromophore is oriented parallel to the X-Y plane with an initial separation of 3.2\AA approximately, along Z axis (Fig.7.1). For calculating energy, while sandwiching chromophore between two self-complementary base pairs, distance between these two base pairs is doubled as to generate an intercalation site and drug chromophore is held exactly in the middle. For scanning configurational space, base pairs system is held rigid while chromophore is rotated along Z-axis at an interval of 10° , and for each configuration, translating the chromophore along the X and Y axes in a step of 0.5\AA .

This procedure gives the optimised orientation of the drug chromophore relative to base pair system/model dinucleotide system. With this orientation, the interaction energy is calculated as a function of separation between two molecules along Z-axis. These values are further refined by repeating the steps at finer intervals of 1° for rotation and 0.1\AA for translations. Corresponding interaction energy is finally

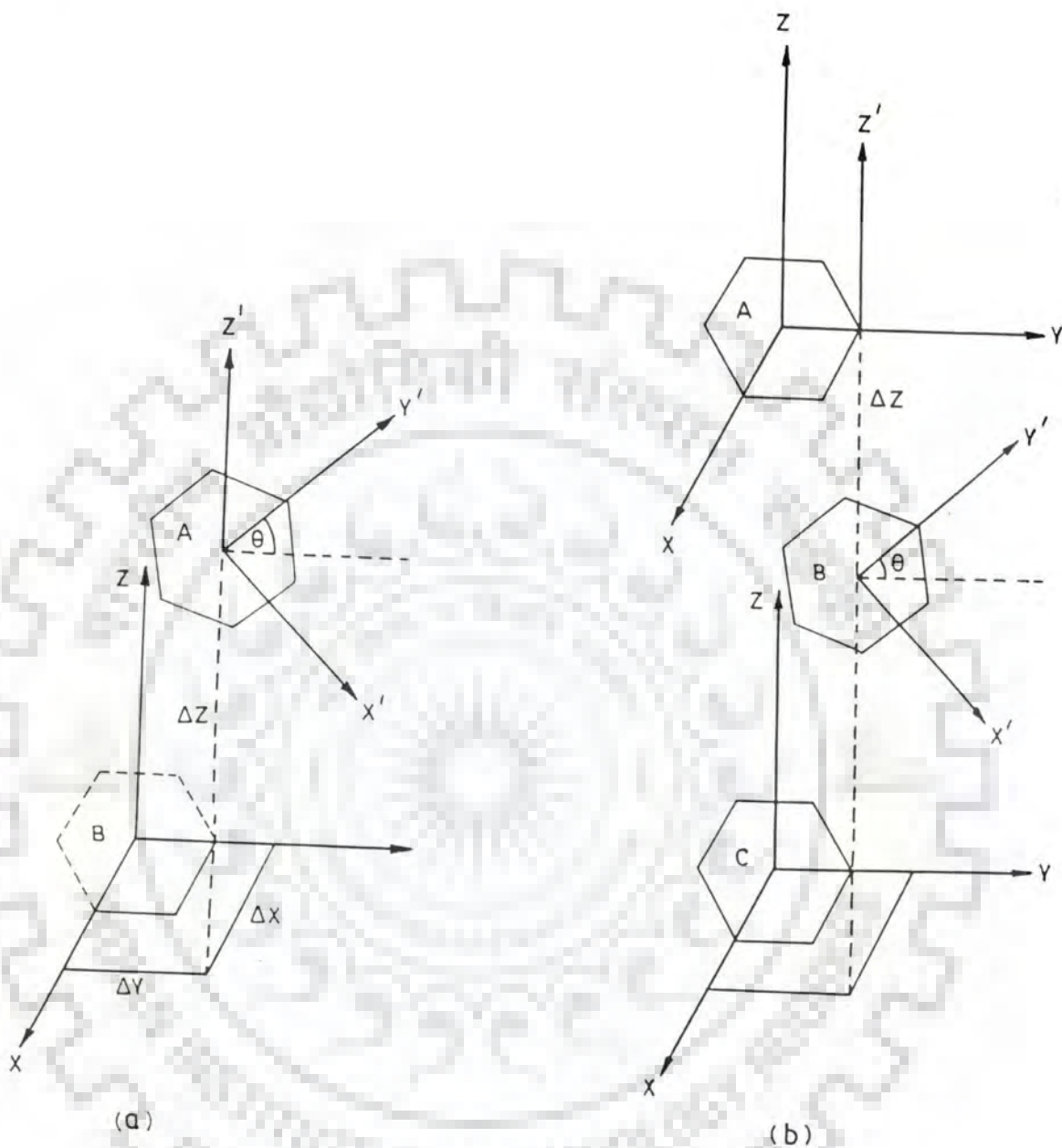


Figure 7.1: Schematic representation showing relative orientation of (a) base B with respect to drug chromophore A and (b) two base pairs with drug chromophore intercalated between them

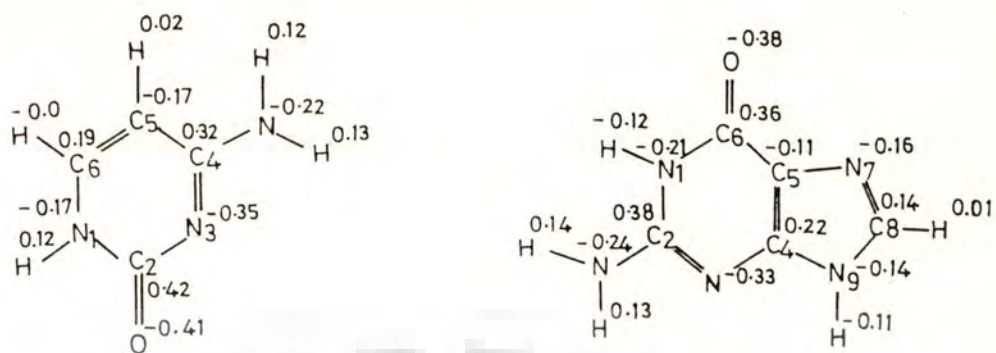
calculated.

ENERGY CALCULATIONS

The distribution of charge at the atomic centres of nucleic acid bases, base pairs and drug chromophores is shown in Figure 7.2. For simplicity, only the planar part of drugs has been considered. It was observed that the difference between the charge distribution in drug chromophore part obtained by calculating the same for entire molecule and only planar part is minor.

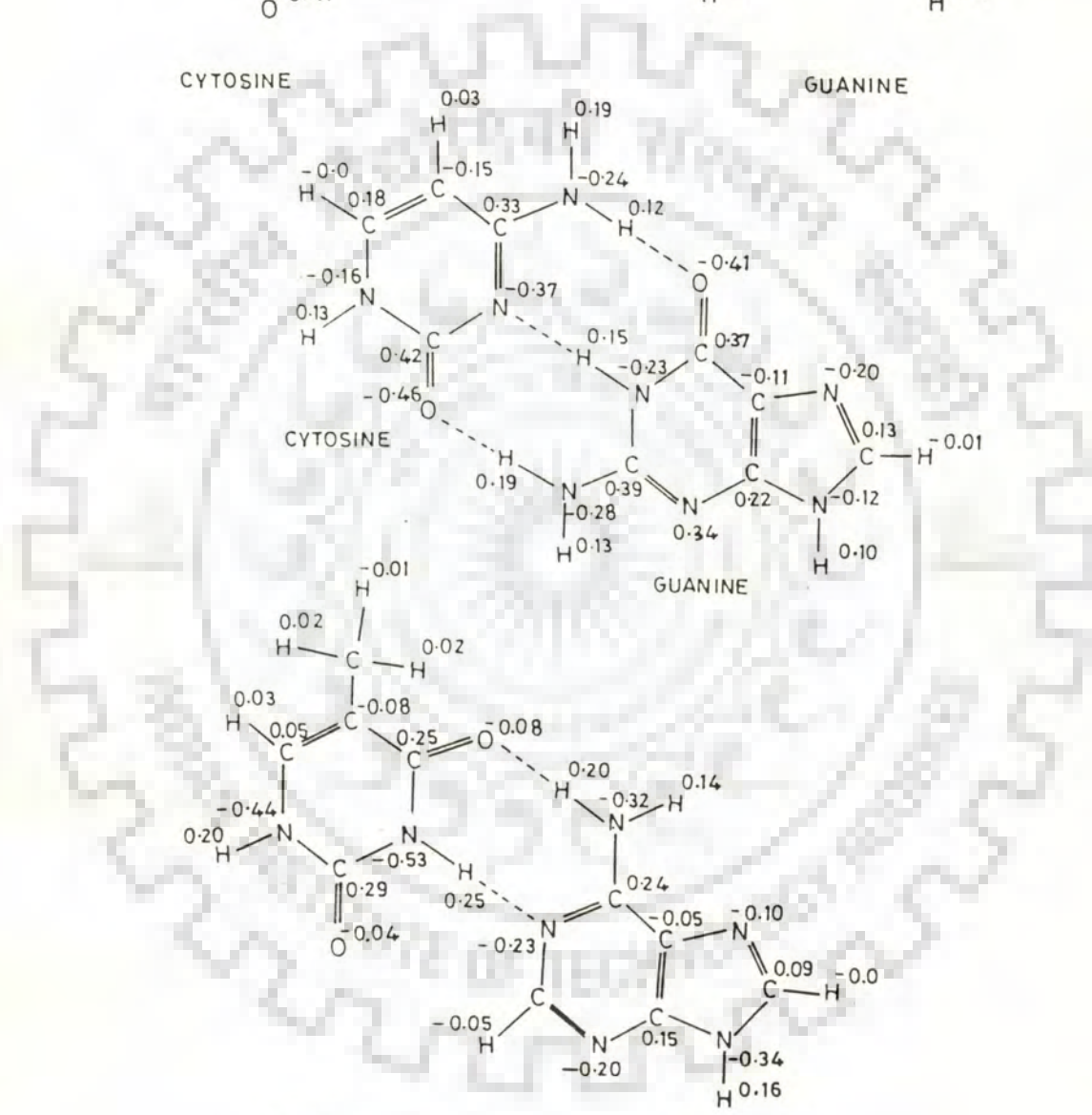
Interactions with bases

Tables 7.1 (a & b) show the stacking energy values and their partitioning for complexes of four nucleic acid bases A,T,G and C with daunomycin and actinomycin D chromophores. Maximum contribution seems to come from dispersion term of energy which arises due to stacking. Daunomycin - cytosine appear to be with least energy involvement and maximum stacking and for actinomycin, guanine seems to be most favourable. Distances between drug and bases are optimised and being shown in Tables 7.1a & b. Daunomycin shows base preference as $C > G > T > A$ while for actinomycin it comes out to be $G > C > T > A$. Overlap geometries for these complexes are being shown in Figures 7.4 and 7.5. Comparison of these stacking energies of the complexes of drug chromophores with the bases reveals that among the purines, the interaction energy is most favourable for guanine complexes. Further, among the



CYTOSINE

GUANINE



THYMINE

ADENINE

Figure 7.2: Distribution of charge at the atomic centres of nucleic acid bases, base pairs and drug chromophores

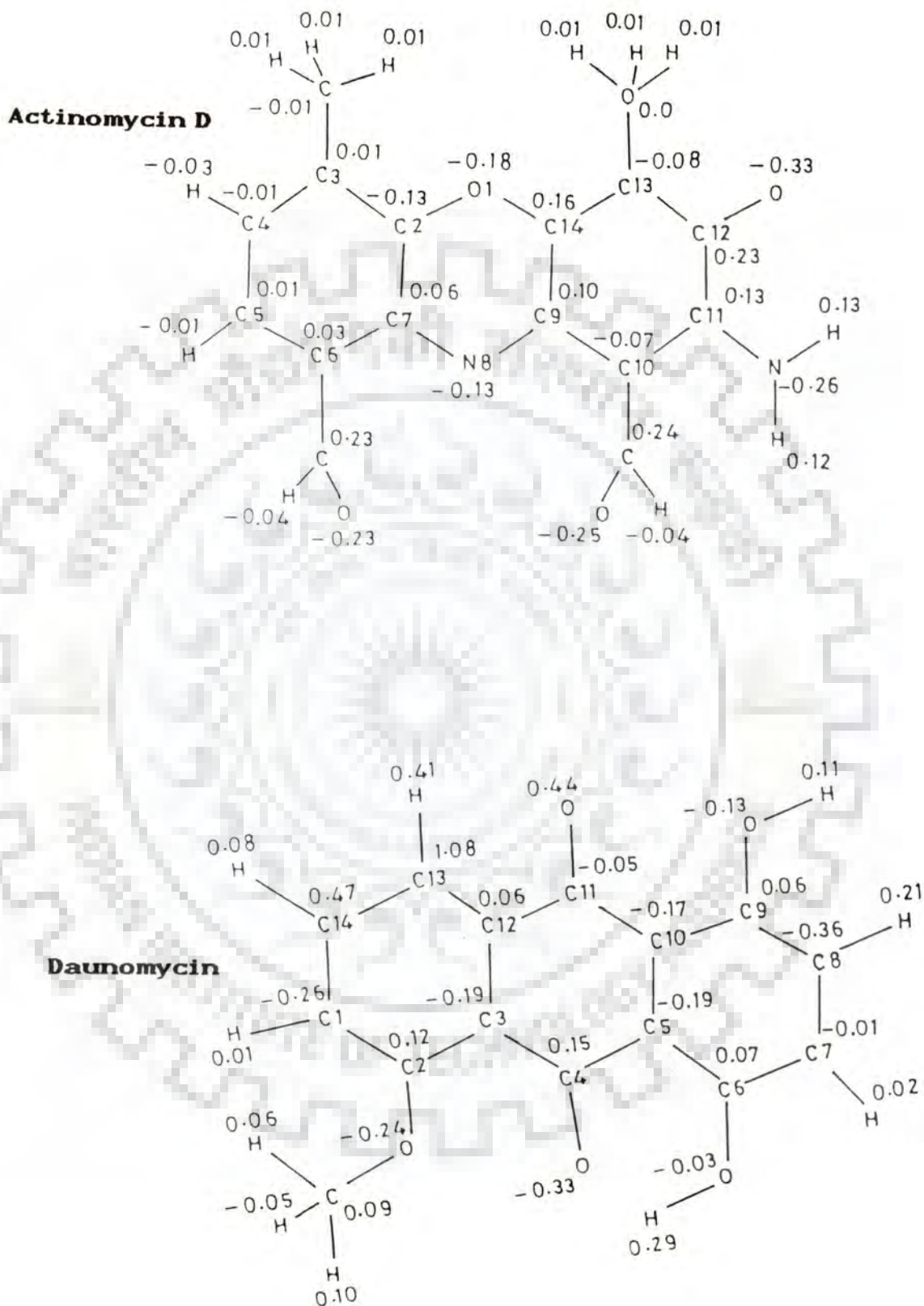


Figure 7.2: ...Continued..

Table 7.1:(a) Partitioning of Stacking Energy values. (in K Cal/mole) of the stacked complexes of Daunomycin drug chromophore with nucleic acid bases .

Base	Distance (Å)	E _{tot}	E _{el}	E _{pol}	E _{disp}	E _{rep}
C	3.2	-16.27	-7.22	-2.20	-15.58	8.73
G	3.1	-15.49	-6.28	-2.79	-20.92	14.49
T	3.3	-12.05	-3.41	-0.72	-14.69	6.77
A	3.3	-12.67	-3.46	-1.61	-13.53	5.93

Table 7.1:(b) Partitioning of stacking energy values (in KCal/mole) of the stacked complexes of Actinomycin drug chromophore with nucleic acid bases

Base	Distance (Å)	E _{tot}	E _{el}	E _{pol}	E _{disp}	E _{rep}
C	3.2	-14.41	-3.72	-2.55	-16.27	8.13
G	3.1	-19.78	-7.93	-3.55	-23.91	15.60
T	3.2	-13.58	-3.10	-1.25	-18.75	9.52
A	3.2	-16.64	-5.88	-2.64	-17.55	9.42

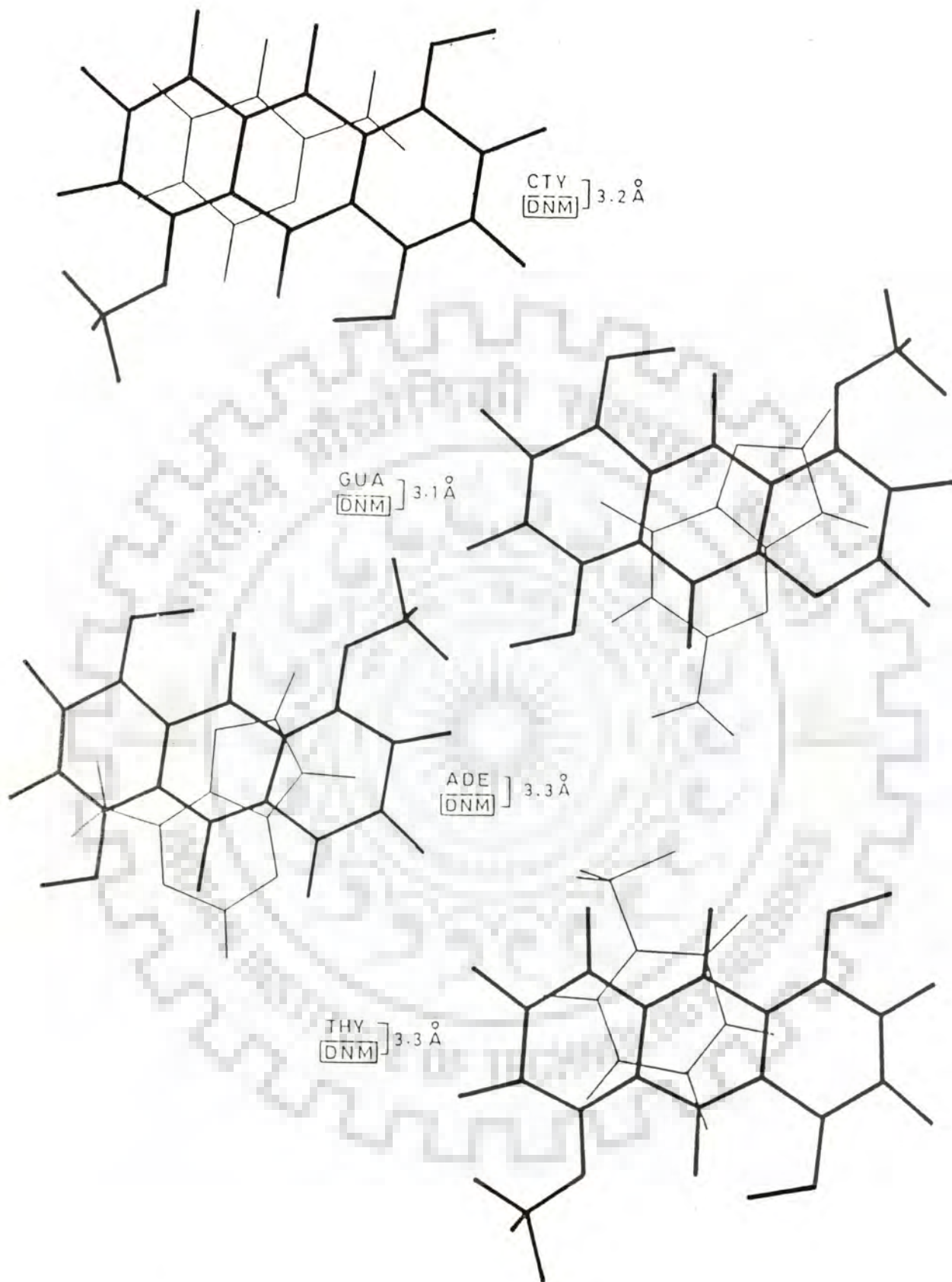


Figure 7.3: Overlap geometries of the complexes of nucleic acid bases with daunomycin

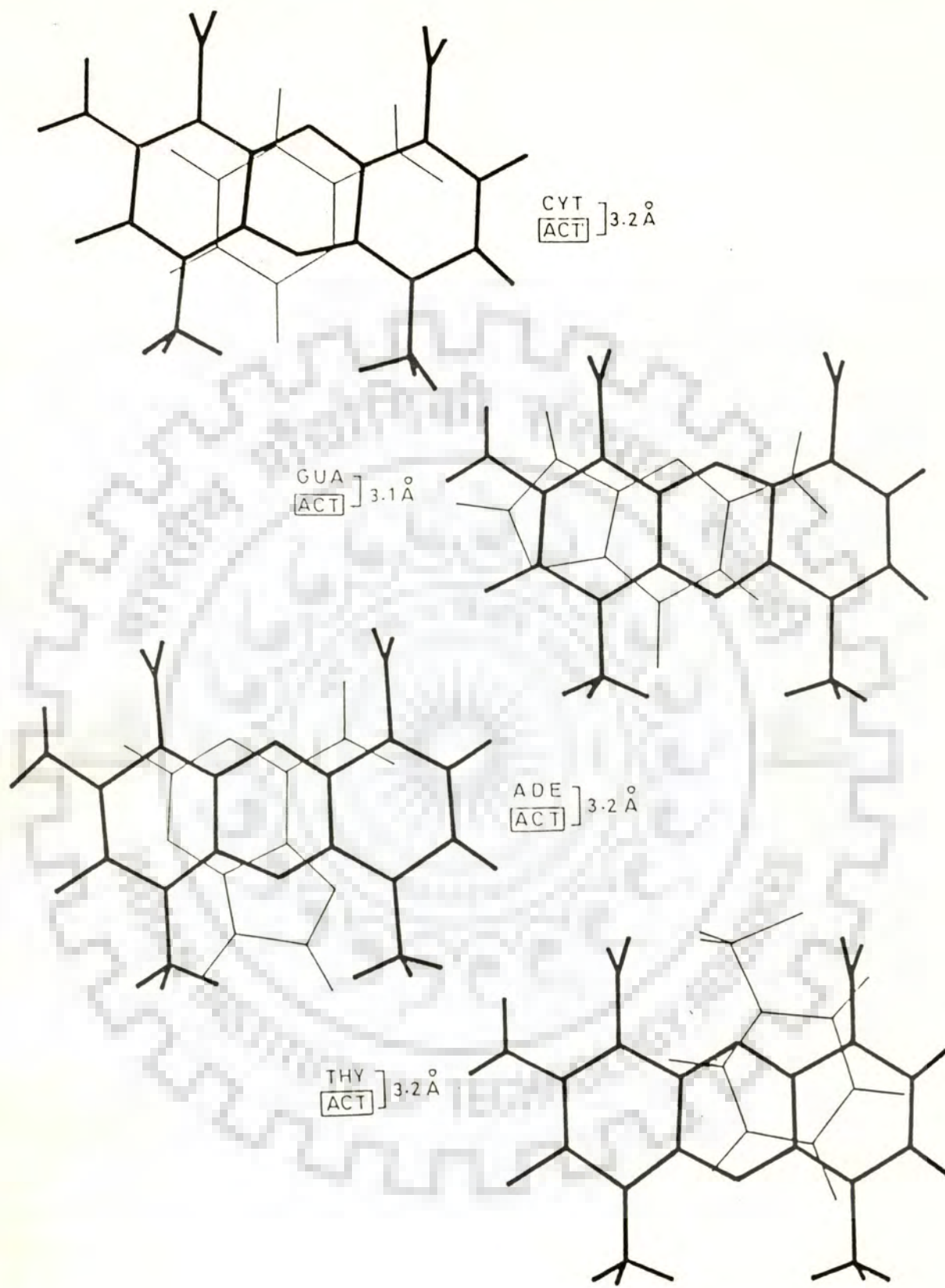


Figure 7.4: Overlap geometries of the complexes of nucleic acid bases with actinomycin D

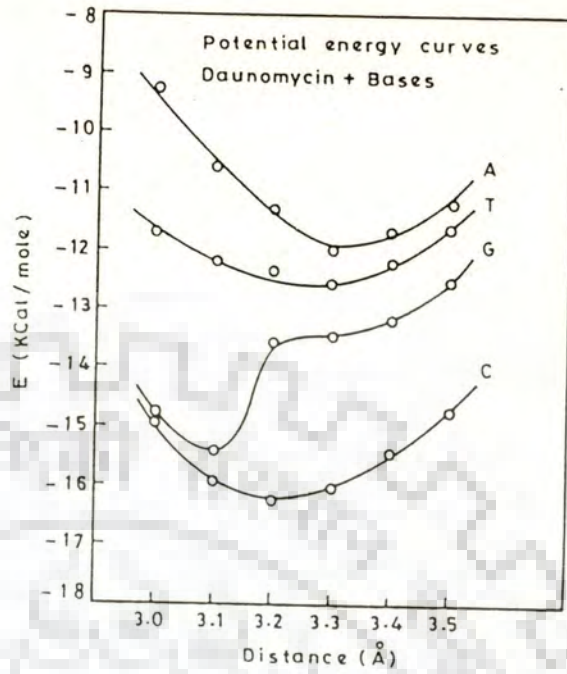
pyrimidine-drug stacks, cytosine complexes are associated with the highest stability.

The complexes of daunomycin chromophore with A and T have energy of almost same order as 12.05 and 12.67 KCal/mole, respectively. It is noted that in cytosine-daunomycin complex, E_{el} term is maximum (7.22 K Cal/mole) among all the four complexes. Same order value of E_{el} has been observed for actinomycin-guanine complex. In all these complexes, although the electrostatic contribution is significant, but major effective contribution seem to be of dispersion term. Potential energy values for complexes of drug chromophores with bases, have been plotted as a function of distance between drug chromophore and base along Z axis in Figure 7.5. Distance was varied from 3.0\AA to 3.5\AA in step of 0.1\AA . In case of daunomycin complexes with A, T and C bases, minimum energy conformation was found to be at a distance of 3.3\AA , while this distance for daunomycin - guanine complex was optimised at 3.1\AA . For actinomycin-base complexes optimum distance has been found to be 3.2\AA .

Interactions with base-pairs

The interaction energies summarised in Tables 7.2 a & b show that the stacked complexes of CG base pair with daunomycin and actinomycin chromophores are associated with lowest energies. For actinomycin, energies of AT, AU complexes are differed only by 0.3 kCal/mole, while for daunomycin, this difference is 3.5 KCal/mole. It is interesting to note that complexes

a.



b.

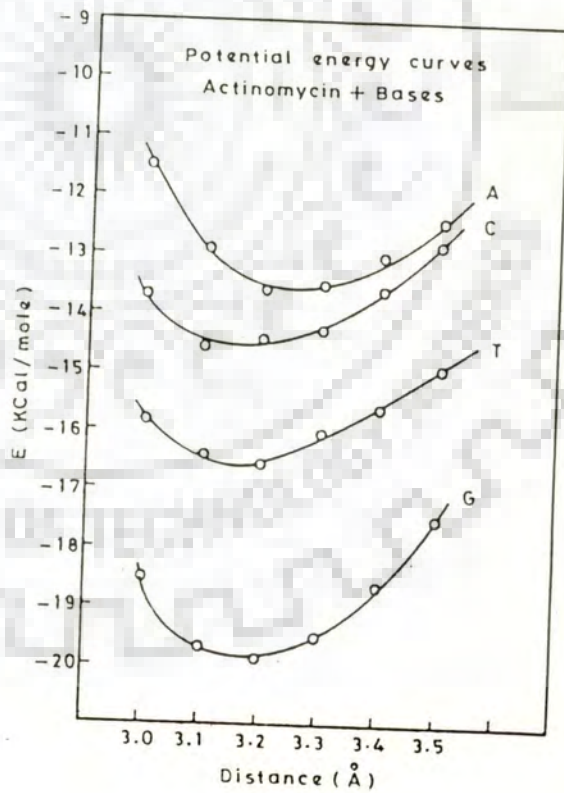


Figure 7.5: Potential energy as a function of distance between base and drug chromophore (a) daunomycin (b) actinomycin D.

Table 7.2 (a): Partitioning of stacking energy values (in KCal/mole) of the stacked complex of daunomycin drug chromophore with nucleic acid base pairs

Base Pair	Distance* (Å)	E _{tot}	E _{el}	E _{pol}	E _{disp}	E _{rep}
CG	3.2	-19.51	-5.27	-2.05	-25.71	13.53
AT	3.3	-16.56	-2.73	-1.04	-23.93	11.14
AU	3.3	-19.05	-5.02	-1.63	-22.87	10.47

Table 7.2 (b): Partitioning of stacking energy values (in KCal/mole) of the stacked complex of actinomycin drug chromophore with nucleic acid base pairs

Base Pair	Distance* (Å)	E _{tot}	E _{el}	E _{pol}	E _{disp}	E _{rep}
CG	3.3	-24.67	-6.89	-2.60	-26.79	11.61
AT	3.2	-18.31	-4.53	-1.52	-23.78	11.42
AU	3.3	-18.63	-4.53	-1.62	-21.63	9.16

* Optimised distance between base pair and drug chromophore

with base pairs are associated with higher energies than the corresponding complexes with the component bases. However, the interaction energies with different base pairs follow same order : CG > AU > AT for both chromophoric systems of drugs. Optimization of distance along Z axis in these complexes shows (Figure 7.6) that for AU and AT base pair complexes with daunomycin, distance value 3.3\AA is favourable and for CG base pair complex it stands as 3.2\AA . In case of actinomycin complexes with AU and CG base pairs minimum energy is at 3.3\AA , while for AT base pair complex it comes out to be at 3.4\AA . Overlap geometries for base pair-drug complexes are drawn in Figure 7.7 for daunomycin and in Figure 7.8 for actinomycin chromophore. Maximum overlap for both drugs is observed for CG base pair which explains the high dispersion energy value in these complexes.

Interactions with dinucleotide model systems

A series of dinucleotide model systems with all possible complementary and mismatched sequences has been studied for energy calculations of complexes with daunomycin and actinomycin chromophores. The distance between base pairs in each case was increased from 3.4 to 6.8\AA to generate intercalation site. Optimisation of this distance was also made by changing it from 6.0 to 7.2\AA in steps of 2\AA . Potential energy curves with respect to distance have been shown in Figure 7.9 (a) for daunomycin complex with dinucleotide model system $\begin{bmatrix} \text{CG} \\ \text{GC} \end{bmatrix}$ and (b) for actinomycin complex with the same model system. Energy minima in first case has

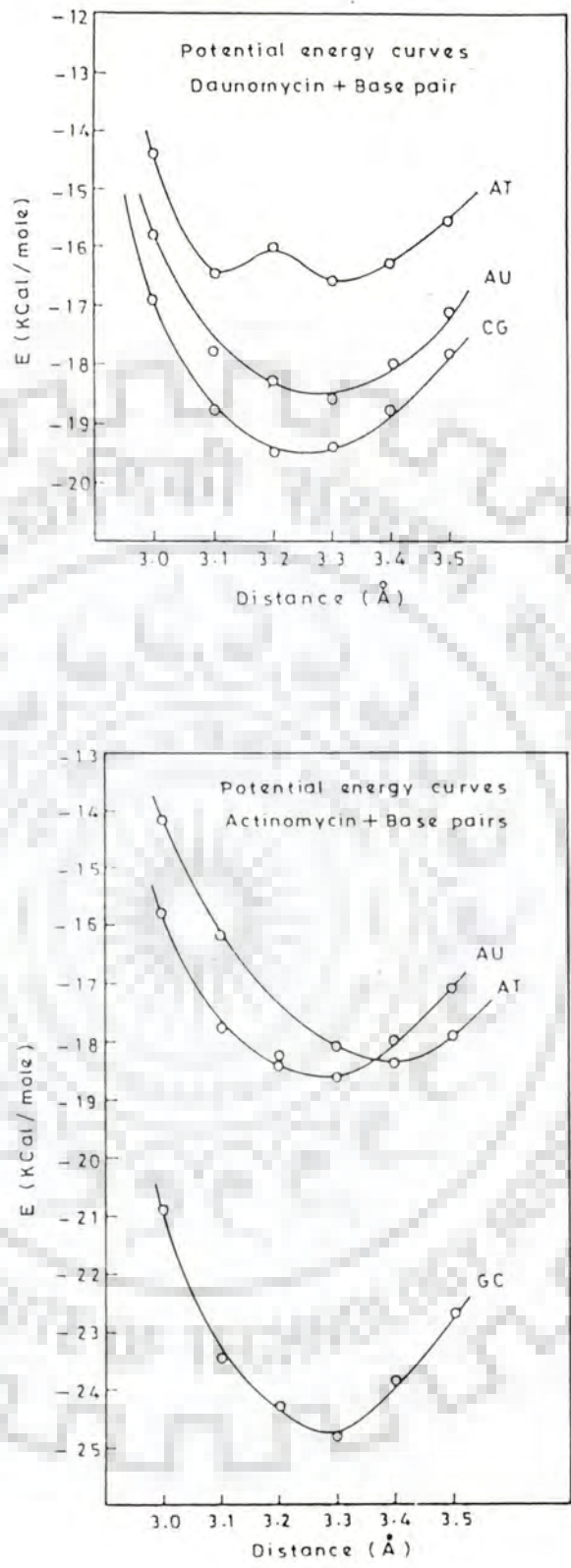


Figure 7.6: Potential energy as a function of distance between base pair and drug chromophore (a) daunomycin (b) actinomycin D

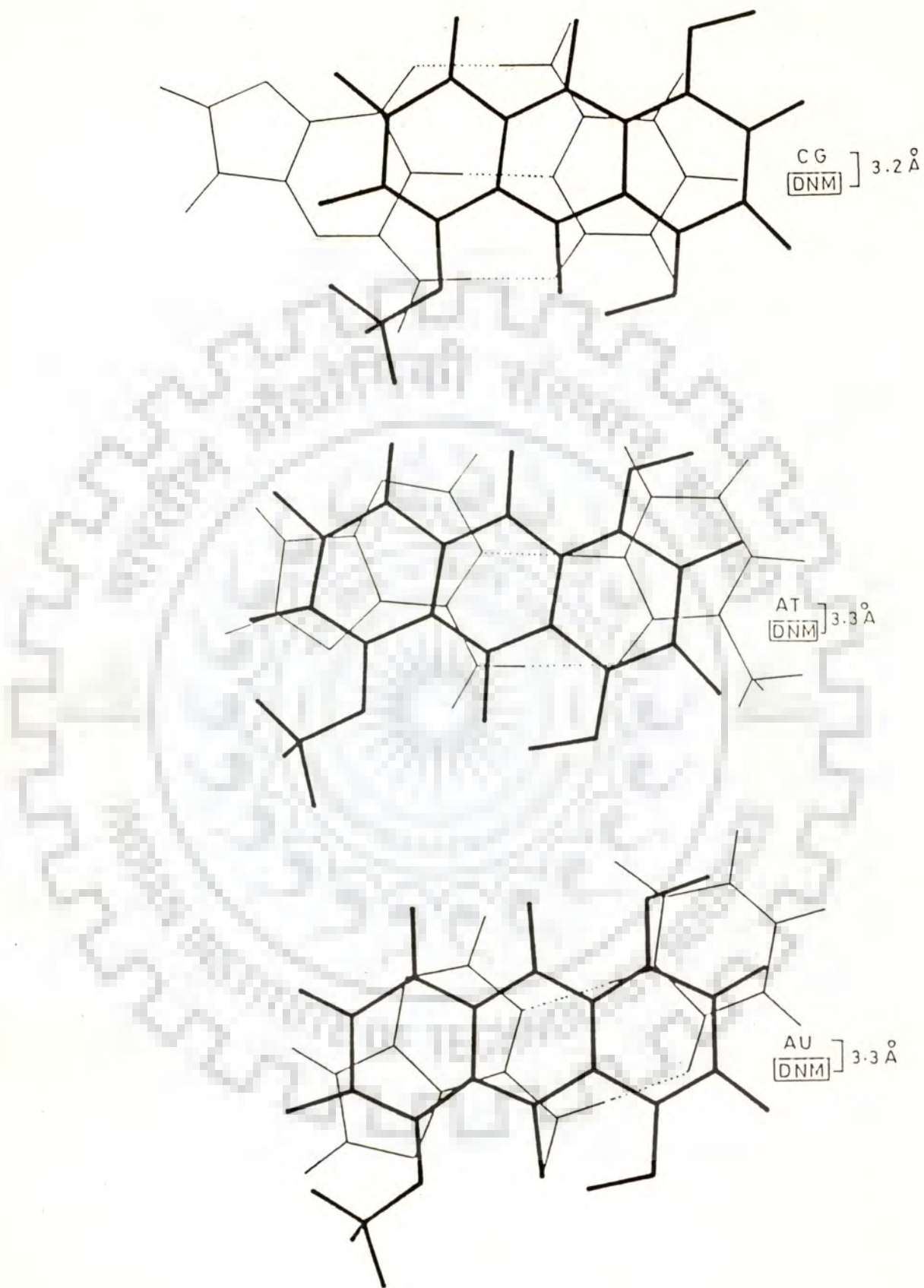


Figure 7.7: Overlap geometries of the complexes of nucleic acid base pairs with daunomycin

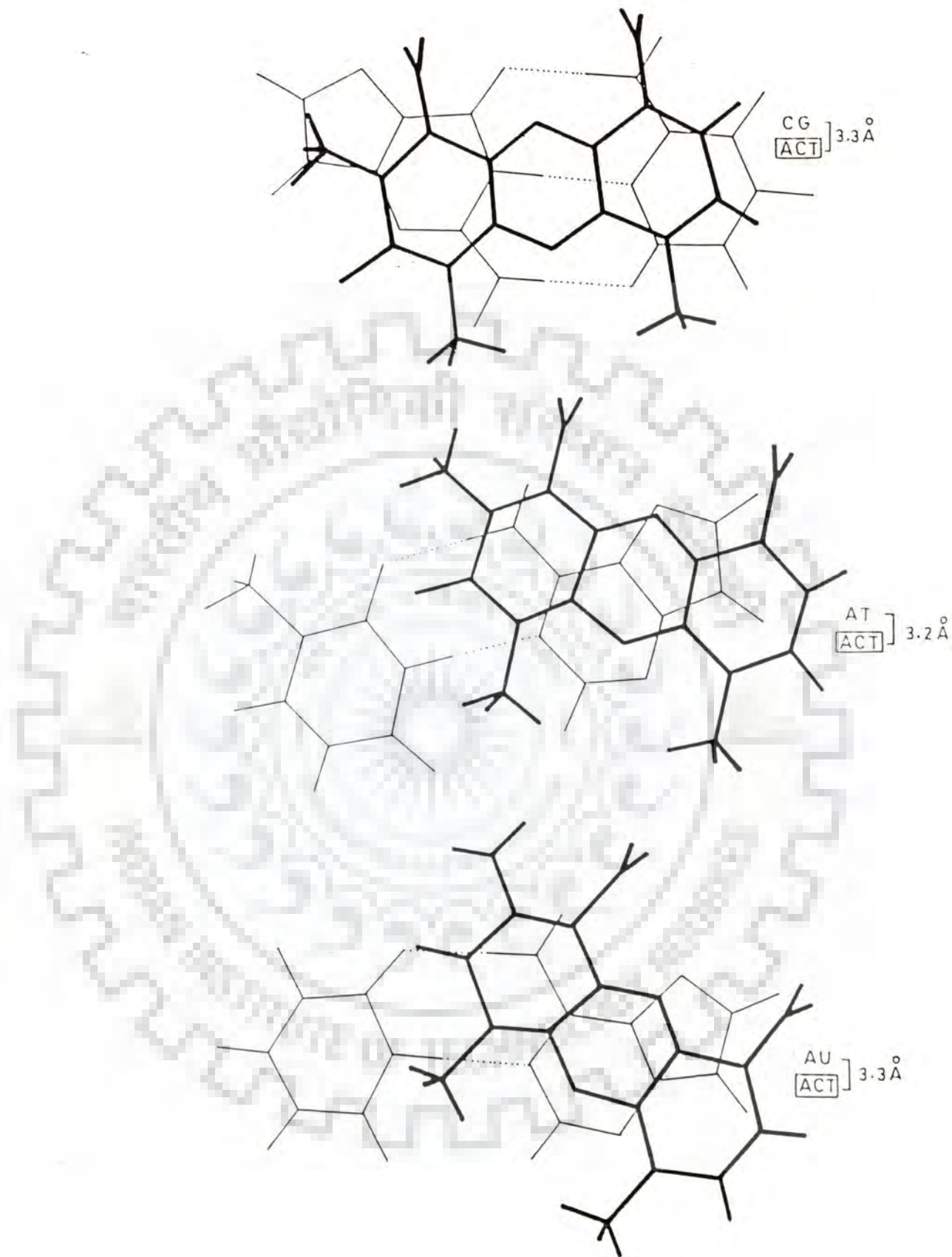


Figure 7.8: Overlap geometries of the complexes of nucleic acid base pairs with actinomycin D

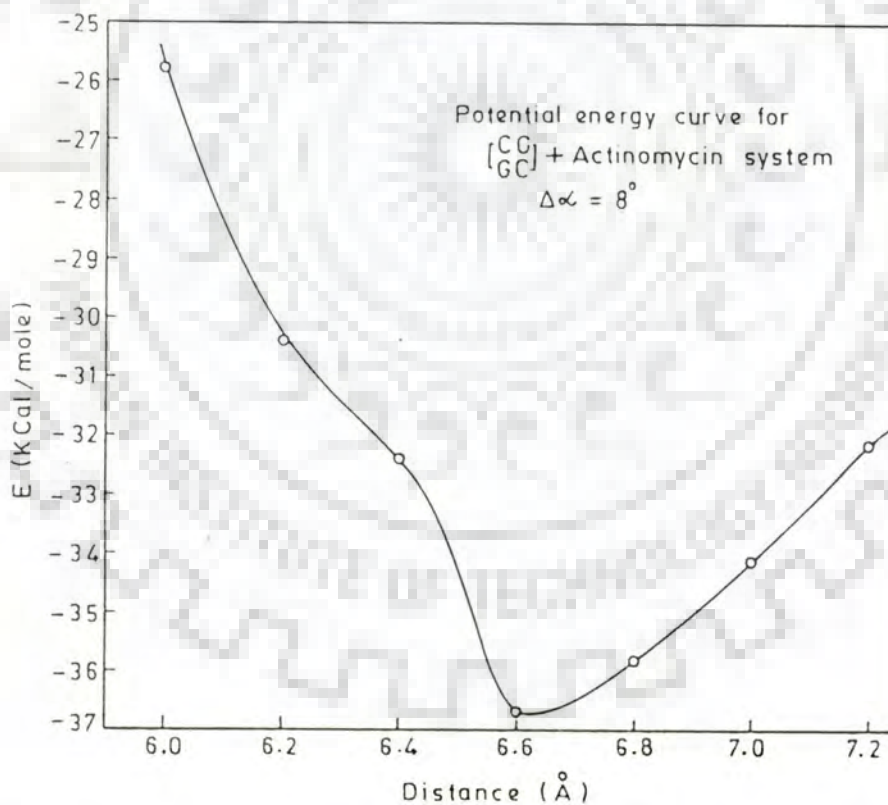
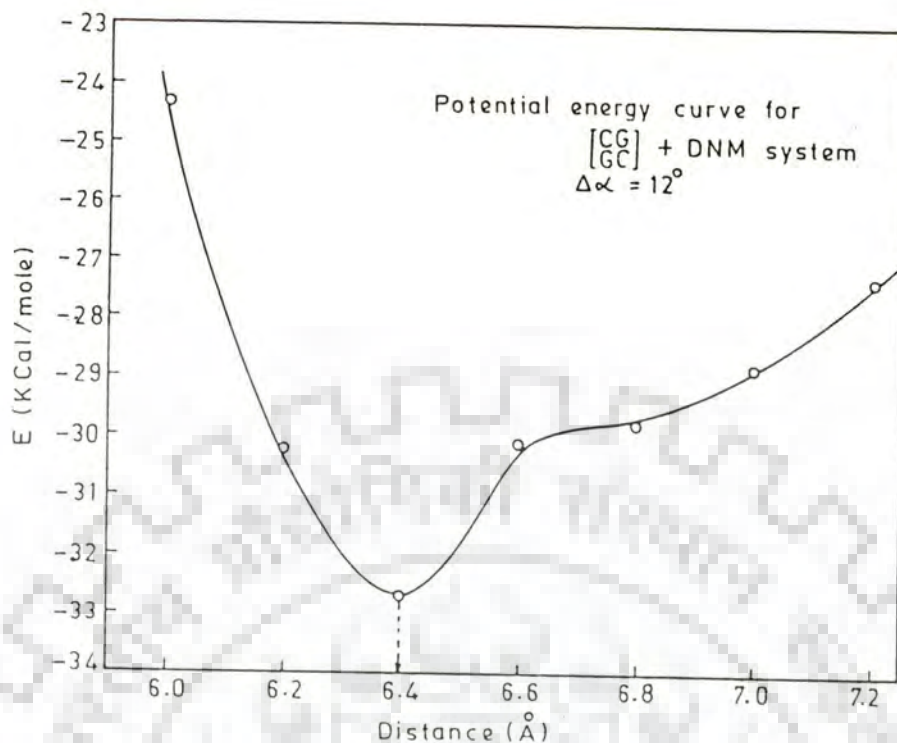


Figure 7.9: (a) Potential energy curve for $\begin{bmatrix} \text{CG} \\ \text{GC} \end{bmatrix}$ - daunomycin complex
(b) Potential energy curve for $\begin{bmatrix} \text{CG} \\ \text{GC} \end{bmatrix}$ - Actinomycin complex

been observed at 6.4\AA and at 6.6\AA in second case. To facilitate the search in conformational space of possible site, it was assumed that each base pair is planar and adjacent base pairs are parallel. Potential energy values for other complexes of daunomycin and actinomycin D with different model dinucleotides are being plotted as a function of distance between base pairs in Figures 7.10a & b, respectively.

One of the features associated with intercalation in a DNA double helix is the fact that it gradually unwinds the helix. Studies on ethidium intercalation into supercoiled DNA has made possible a calculation of unwinding angle ($\Delta\alpha$) in DNA associated with each molecule of ethidium [133]. The studies indicate that insertion of ethidium between the base pairs decreases the twist angle (α) between the base pairs by $26^\circ \pm 2^\circ$. This value is very close to 23° observed by Wang et al [132].

This concept of unwinding angle was quantitatively studied in present work in terms of stacking energy and overlap geometries. The optimised orientation of two base pairs in model dinucleotide systems in presence of intercalated chromophores of drugs has been deduced. Global search for unwinding angle gave three energy minima in a range of angle value $+180^\circ$ to -180° (see Figures :7.11a & b and Tables : 7.3 a and b). Two minima in both cases were discarded as they were sterically forbidden in presence of phosphate back bone. It was confirmed through Dreiding model building for complex.

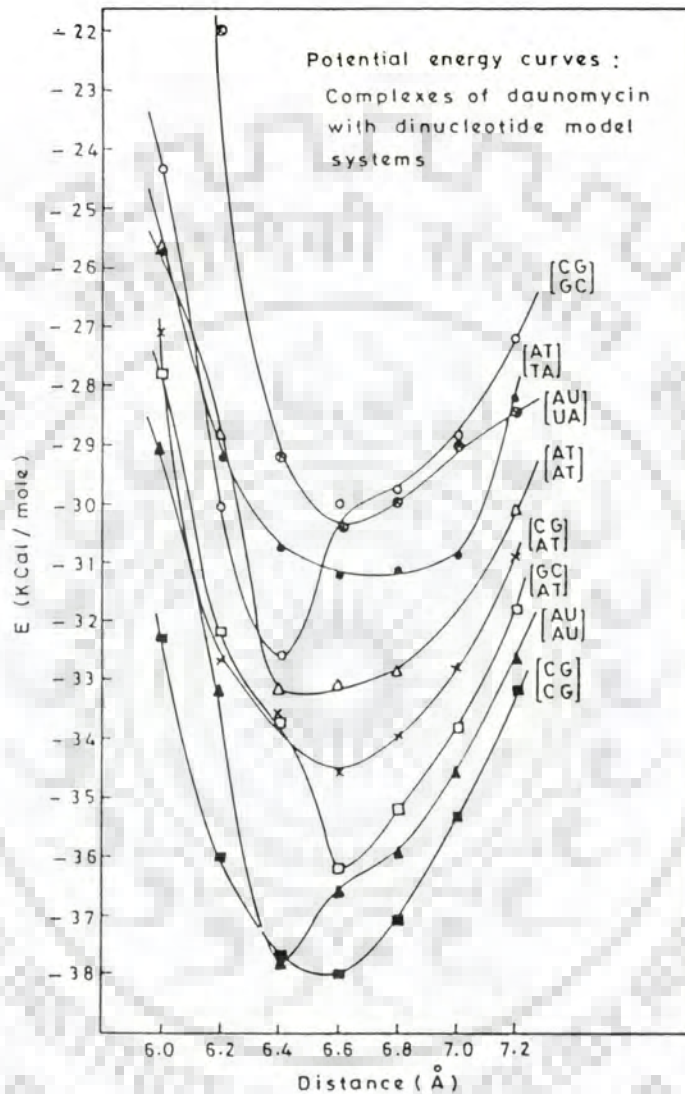


Figure 7.10: (a) Potential energy curves of the complexes of dinucleotide model systems with daunomycin

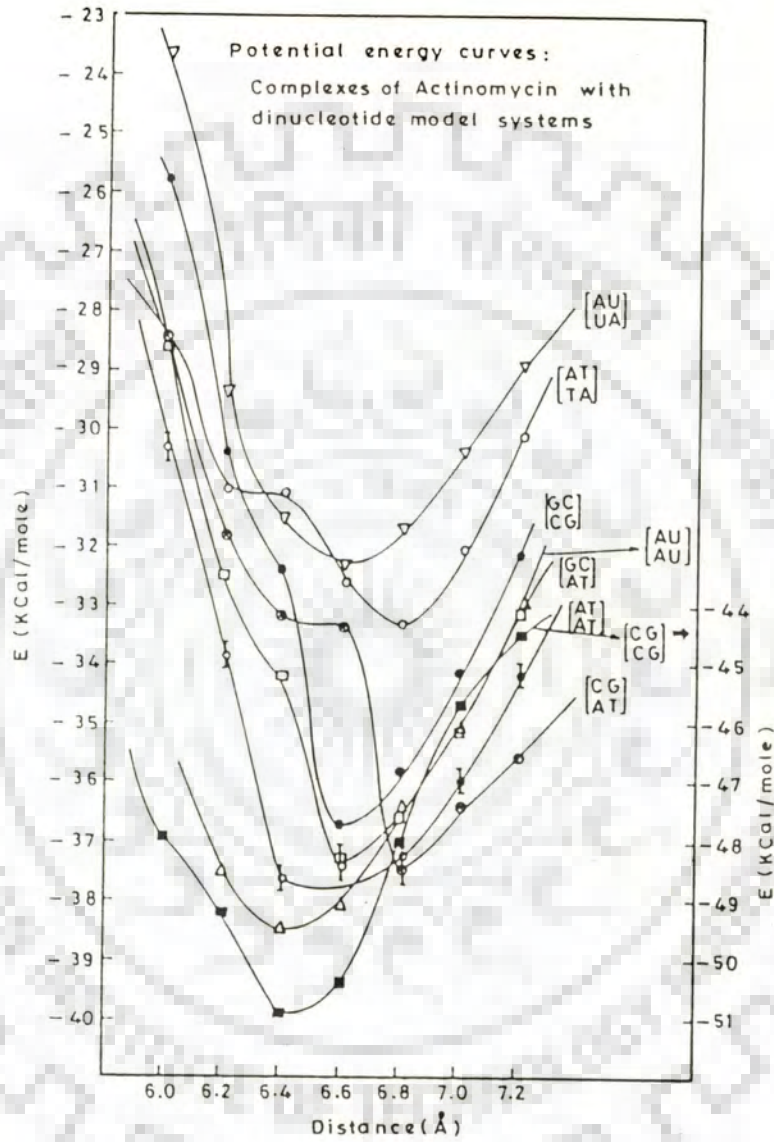


Figure 7.10: (b) Potential energy curves of the complexes of dinucleotide model systems with actinomycin D

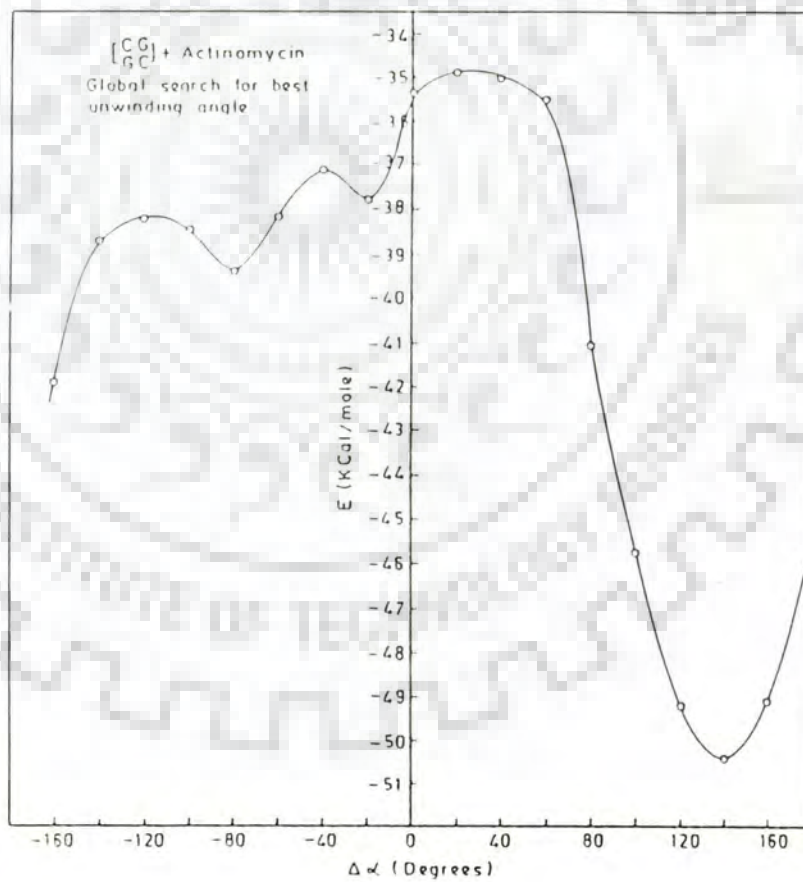
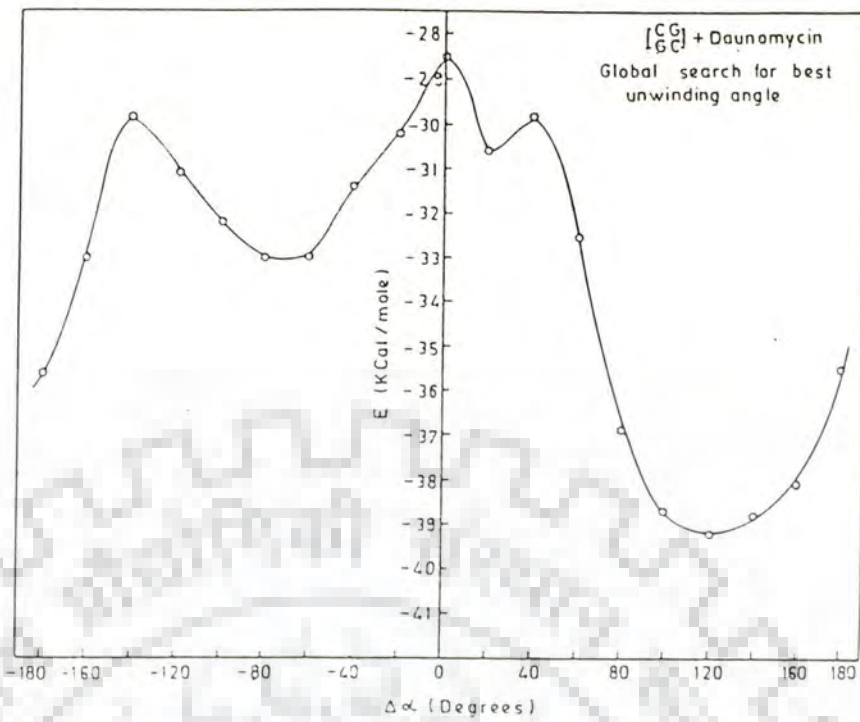


Figure 7.11: Global search of unwinding angle - (a) daunomycin complex (b) actinomycin complex

Table 7.3 (a) : Global search for best unwinding angle ($\Delta\alpha$) value for Daunomycin complexes.
Standard System - $_{GC}^{CG}$

	$\Delta\alpha$ (in degrees)						
CG							
DNM	-180	-160	-140	-120	-100	-80	-60
GC	-35.59	-33.04	-29.84	-31.16	-32.17	-33.09	-32.99

	$\Delta\alpha$ (in degrees)						
CG							
DNM	-40	-20	0	20	40	60	80
GC	-31.46	-30.25	-28.59	-30.61	-29.84	-32.59	-36.90

	$\Delta\alpha$ (in degrees)				
CG					
DNM	100	120	140	160	180
GC	-38.72	-39.22	-38.88	-38.17	-35.52

Table 7.3 (b) : Global search for best unwinding angle ($\Delta\alpha$) value for Actinomycin complexes.
Standard System $\begin{bmatrix} CG \\ GC \end{bmatrix}$

	$\Delta\alpha$ (in degrees)						
CG							
ACT	-180	-160	-140	-120	-100	-80	-60
GC	-42.12	-41.93	-38.78	-38.24	-38.53	-39.41	-38.26

	$\Delta\alpha$ (in degrees)						
CG							
ACT	-40	-20	0	20	40	60	80
GC	-37.12	-37.82	-35.41	-34.98	-35.02	-35.55	-41.16

	$\Delta\alpha$ (in degrees)				
CG					
ACT	100	120	140	160	180
GC	-45.85	-49.24	-50.46	-49.12	-45.79

Further, local refinements of unwinding angle value for both drugs were also made (Figure 7.12a and b) and stacking energies were calculated for the complexes at an interval of 1° - 2° value of $\Delta\alpha$. Observed optimised values of $\Delta\alpha$, 10° for daunomycin and 28° for actinomycin in dCpG model system, agrees well with that of reported by Miller [129] and Waring [130]. Waring has reported unwinding angle value $11.3 \pm 3.0^{\circ}$ for intercalation of daunomycin and $24.7 \pm 6.5^{\circ}$ for actinomycin. From present potential energy calculations, minimum energy conformation for above systems have been found at $\Delta\alpha$ as 10° for daunomycin and 28° for actinomycin. However, a little variation in these unwinding angle values has been observed with a change in base sequence at intercalation site. This variation of $\pm 2^{\circ}$ suggests the sequence dependence of degree of helix opening on complex formation. Optimisation curves for unwinding angle at optimised distance between base pairs of stacked complexes of daunomycin and actinomycin D with different dinucleotide model systems have been shown in Figure 7.13 a & b:

Tables 7.4a and b summarise the partitioning of stacking energy at optimised distance for daunomycin and actinomycin complexes with dinucleotide model system, respectively. Tables 7.5 (a to h) list the optimisation of unwinding angle at the optimised distance between base pairs of model dinucleotides for daunomycin. Parallel studies with actinomycin are tabulated in Table 7.6 (a to h). It is noted that value of $\Delta\alpha$ differs for different sequences in both sets. Overlap

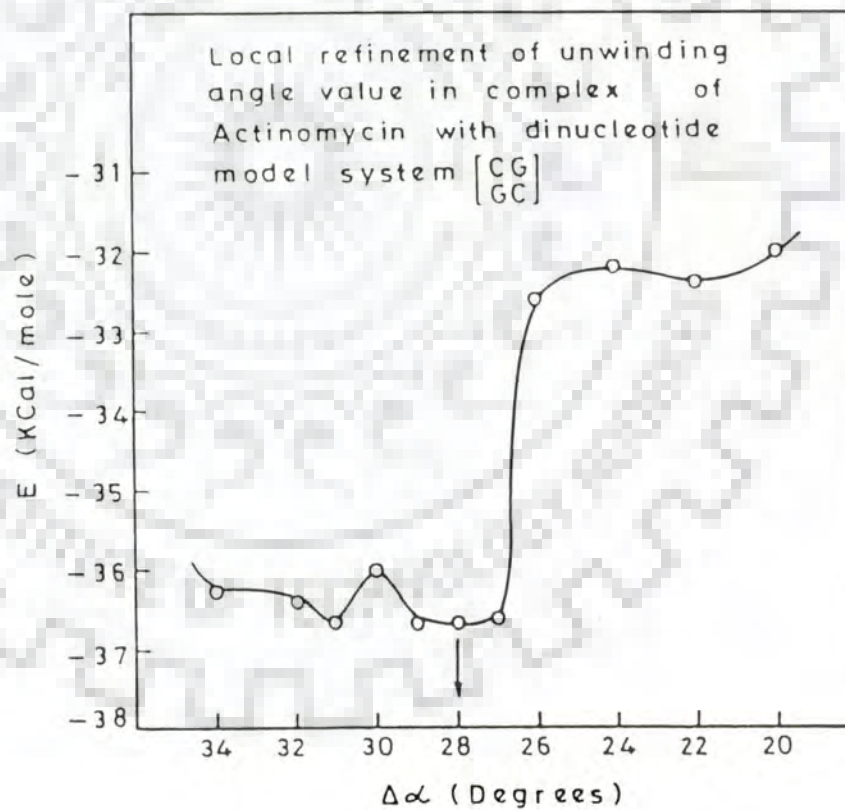
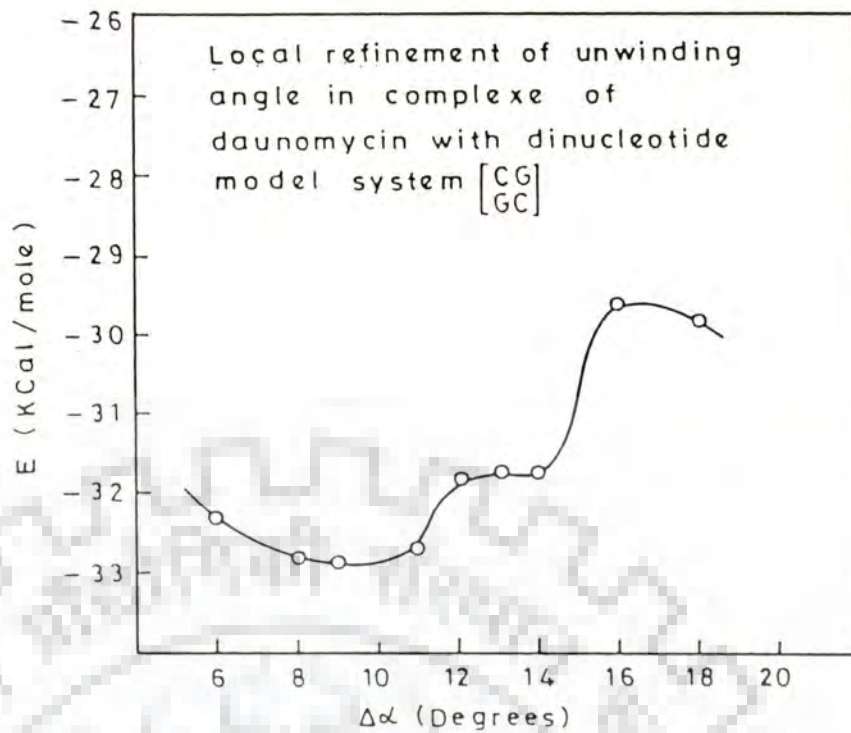


Figure 7.12: Local refinement of unwinding angle - (a) daunomycin complex (b) actinomycin complex

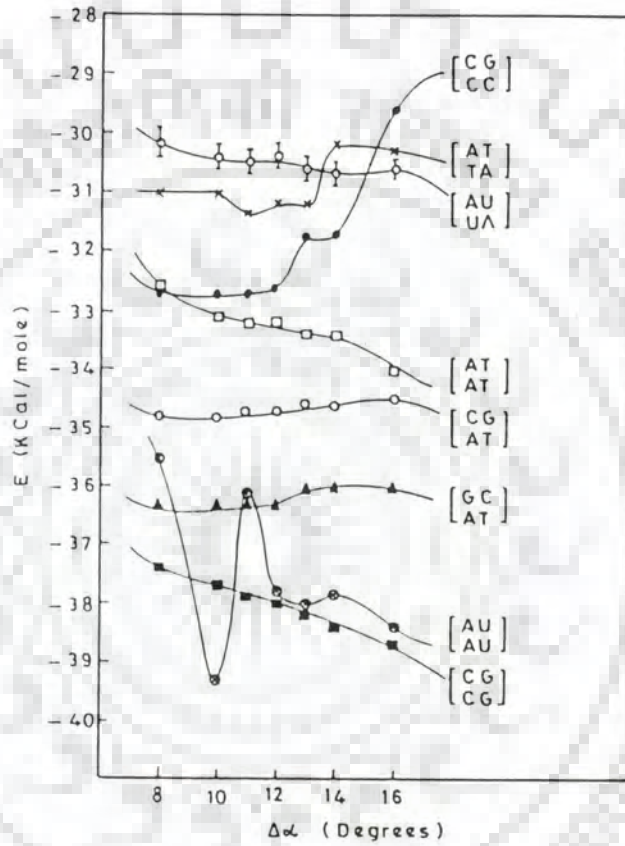


Figure 7.13: (a) Optimisation curves for unwinding angle at optimised distance between base pairs of stacked complexes of daunomycin with different dinucleotide systems

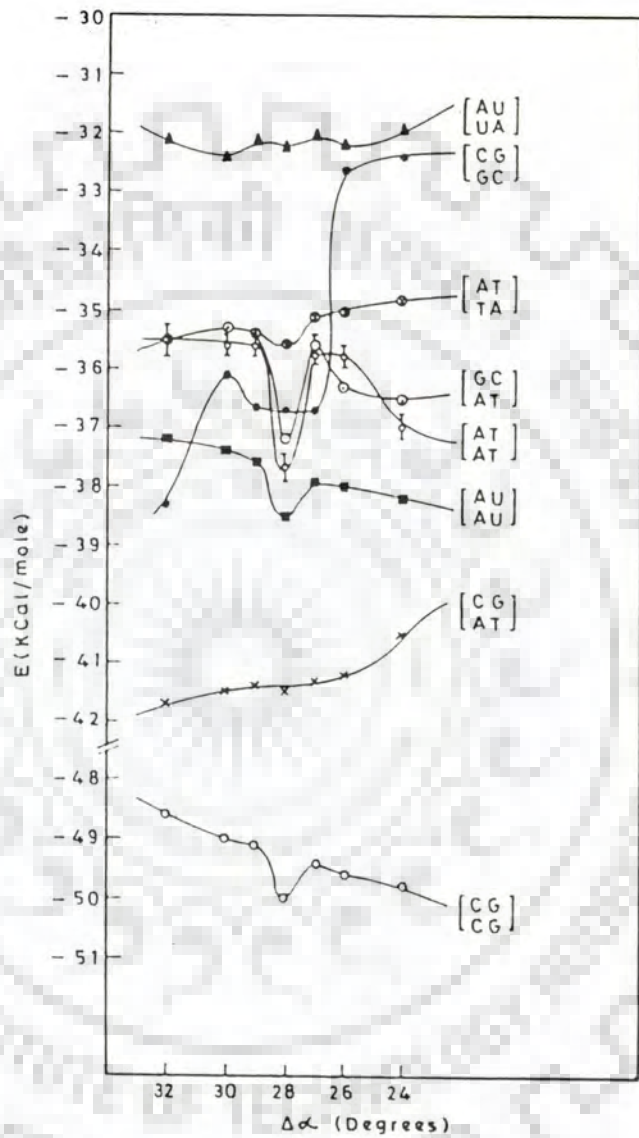


Figure 7.13: (b) Optimisation curves for unwinding angle at optimised distance between base pairs of stacked complexes of actinomycin D with different dinucleotide systems

Table 7.4: (a) Partitioning of stacking energy values (in KCal/mole) of the stacked complex of Daunomycin drug chromophore with dinucleotide model systems

SYSTEM	DISTANCE* (Å)	E _{tot}	E _{el}	E _{pol}	E _{disp}	E _{rep}
[^{CG} _{GC}]	6.4	-32.68	-4.77	-2.67	-53.50	28.25
[^{CG} _{CG}]	6.6	-38.05	-6.63	-4.75	-48.94	22.26
[^{CG} _{AT}]	6.6	-34.68	-6.84	-2.76	-46.48	21.40
[^{AT} _{AT}]	6.6	-36.30	-6.67	-2.77	-48.59	21.73
[^{AT} _{TA}]	6.4	-33.27	-7.41	-3.30	-55.26	32.44
[^{GC} _{AT}]	6.6	-31.20	-5.48	-2.85	-36.90	14.02
[^{AU} _{AU}]	6.4	-37.94	-11.39	-4.76	-50.49	28.71
[^{AU} _{UA}]	6.6	-30.45	-3.79	-2.67	-44.93	20.95

* Optimised distance between two base pairs. Drug chromophore is held exactly in the middle.

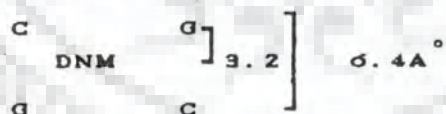


Table 7.4: (b) Partitioning of stacking energy values (in KCal/mole) of the stacked complex of Actinomycin drug chromophore with dinucleotide model systems

SYSTEM	DISTANCE* (Å)	E _{tot}	E _{el}	E _{pol}	E _{disp}	E _{rep}
[^{CG} _{GC}]	6.6	-36.70	-2.37	-3.86	-52.42	21.95
[^{CG} _{CG}]	6.4	-50.01	-13.39	-6.73	-60.89	31.00
[^{CG} _{AT}]	6.8	-37.50	-5.29	-2.99	-45.84	16.58
[^{AT} _{AT}]	6.4	-37.68	-8.40	-4.37	-48.20	23.29
[^{AT} _{TA}]	6.8	-38.61	-5.68	-2.74	-40.89	13.88
[^{GC} _{AT}]	6.6	-37.25	-4.53	-3.85	-52.31	23.44
[^{AU} _{AU}]	6.4	-38.55	-10.38	-4.70	-48.06	24.59
[^{AU} _{UA}]	6.6	-32.30	-4.65	-2.55	-43.06	17.96

* Optimised distance between two base pairs.
Drug chromophore is held exactly in the middle.

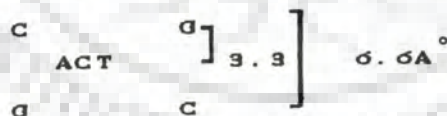


Table 7.5: Optimisation of unwinding angle at optimised distance between base pairs for the stacked complex of daunomycin with different dinucleotide model systems

* α and $\Delta\alpha$ are given in degrees

(a) SYSTEM $\begin{matrix} c\alpha \\ [ac] \end{matrix}$; distance = 6.4 Å

α^*	$\Delta\alpha^*$	E_{tot}	E_{el}	E_{pol}	E_{disp}	E_{rep}
28	8	-32.75	-4.88	-2.69	-53.45	28.27
26	10	-32.76	-4.83	-2.68	-53.47	28.22
25	11	-32.72	-4.80	-2.66	-53.48	28.23
24	12	-32.68	-4.77	-2.68	-53.50	28.25
23	13	-31.74	-4.28	-2.59	-52.47	27.61
22	14	-31.73	-4.27	-2.59	-52.50	27.63
20	16	-29.66	-4.36	-3.06	-50.14	27.90

(b) SYSTEM $\begin{matrix} c\alpha \\ [ca] \end{matrix}$; distance = 6.6 Å

α^*	$\Delta\alpha^*$	E_{tot}	E_{el}	E_{pol}	E_{disp}	E_{rep}
28	8	-37.46	-5.14	-4.67	-49.00	22.16
26	10	-37.72	-6.16	-4.69	-48.99	22.11
25	11	-37.88	-6.27	-4.72	-48.97	22.08
24	12	-38.05	-6.63	-4.75	-48.93	22.26
23	13	-38.21	-6.77	-4.76	-48.91	22.22
22	14	-38.41	-6.77	-4.81	-48.89	22.06
20	16	-38.70	-6.91	-4.84	-48.85	21.90

(c) SYSTEM $\begin{matrix} \text{GC} \\ \text{AT} \end{matrix}$; distance = 6.6 A°

α^*	$\Delta\alpha^*$	E _{tot}	E _{el}	E _{pol}	E _{disp}	E _{rep}
28	8	-36.28	-6.60	-2.80	-48.91	22.04
26	10	-36.30	-6.64	-2.78	-48.75	21.87
25	11	-36.30	-6.65	-2.77	-48.67	21.80
24	12	-36.30	-6.67	-2.77	-48.59	21.73
23	13	-36.02	-6.07	-2.85	-48.95	21.84
22	14	-36.03	-6.11	-2.82	-48.88	21.77
20	16	-36.04	-6.15	-2.78	-48.71	21.64

(d) SYSTEM $\begin{matrix} \text{CG} \\ \text{AT} \end{matrix}$; distance = 6.8 A°

α^*	$\Delta\alpha^*$	E _{tot}	E _{el}	E _{pol}	E _{disp}	E _{rep}
28	8	-34.87	-7.07	-2.70	-45.89	20.78
26	10	-34.79	-7.07	-2.68	-45.78	20.75
25	11	-34.73	-7.06	-2.68	-45.73	20.75
24	12	-34.68	-6.84	-2.76	-46.48	21.40
23	13	-34.64	-6.81	-2.76	-46.46	21.39
22	14	-34.60	-6.79	-2.75	-46.36	21.31
20	16	-34.85	-6.02	-2.85	-46.89	21.00

(e) SYSTEM $\begin{bmatrix} AT \\ AT \end{bmatrix}$; distance = 6.4 Å°

α^*	$\Delta\alpha^*$	E _{tot}	E _{el}	E _{pol}	E _{disp}	E _{rep}
28	8	-32.68	-6.77	-3.20	-56.26	33.56
26	10	-33.22	-7.22	-3.20	-55.56	32.76
25	11	-33.34	-7.33	-3.21	-55.38	32.58
24	12	-33.28	-7.42	-3.04	-55.26	32.44
23	13	-33.43	-7.49	-3.22	-55.22	32.50
22	14	-33.39	-7.56	-3.23	-55.24	32.64
20	16	-33.99	-7.61	-3.28	-56.88	33.78

(f) SYSTEM $\begin{bmatrix} AT \\ TA \end{bmatrix}$; distance = 6.6 Å°

α^*	$\Delta\alpha^*$	E _{tot}	E _{el}	E _{pol}	E _{disp}	E _{rep}
28	8	-30.97	-5.86	-3.32	-35.98	14.18
26	10	-31.02	-5.97	-3.26	-35.92	14.14
25	11	-31.43	-5.76	-3.34	-36.11	13.78
24	12	-31.21	-5.48	-2.85	-36.90	14.02
23	13	-31.28	-5.56	-2.85	-36.84	13.99
22	14	-30.23	-4.12	-3.29	-37.39	14.58
20	16	-30.32	-4.29	-3.25	-37.29	14.51

(g) SYSTEM $\begin{bmatrix} \text{AU} \\ \text{AU} \end{bmatrix}$; distance = 6.4 A°

α^*	$\Delta\alpha^*$	E _{tot}	E _{el}	E _{pol}	E _{disp}	E _{rep}
28	8	-35.53	-9.82	-3.91	-48.22	26.48
26	10	-39.31	-12.71	-4.66	-48.27	26.33
25	11	-36.12	-9.72	-4.88	-51.38	29.56
24	12	-37.94	-11.39	-4.76	-50.49	28.71
23	13	-38.12	-11.50	-4.81	-50.52	28.72
22	14	-37.79	-1.897	-5.05	-51.13	29.28
20	16	-38.43	-11.34	-5.06	-50.90	23.87

(h) SYSTEM $\begin{bmatrix} \text{AU} \\ \text{UA} \end{bmatrix}$; distance = 6.6 A°

α^*	$\Delta\alpha^*$	E _{tot}	E _{el}	E _{pol}	E _{disp}	E _{rep}
28	8	-30.22	-4.17	-2.58	-43.83	20.37
26	10	-30.46	-4.24	-2.59	-43.72	20.09
25	11	-30.53	-4.27	-2.60	-43.68	20.01
24	12	-30.44	-3.79	-2.67	-44.93	20.95
23	13	-30.59	-3.84	-2.66	-44.88	20.79
22	14	-30.70	-3.88	-2.66	-44.84	20.68
20	16	-30.58	-4.38	-2.58	-43.43	19.81

Table 7.6: Optimisation of unwinding angle at optimised distance between base pairs for the stacked complex of actinomycin with different dinucleotide model systems

* α and $\Delta\alpha$ are given in degrees

(a) SYSTEM ${}_{CG}^{CG}$; distance = 6.6 Å°

α^*	$\Delta\alpha^*$	E_{tot}	E_{el}	E_{pol}	E_{disp}	E_{rep}
32	4	-38.38	-2.23	-3.79	-52.30	21.93
30	6	-36.11	-2.38	-3.31	-52.00	21.58
29	7	-36.72	-2.40	-3.87	-52.39	21.94
28	8	-36.70	-2.37	-3.86	-52.42	21.94
27	9	-36.70	-2.19	-3.51	-52.72	21.72
26	10	-32.63	-2.30	-3.72	-53.61	25.00
24	12	-32.44	-2.44	-3.65	-53.59	27.04

(b) SYSTEM ${}_{CG}^{CG}$; distance = 6.4 Å°

α^*	$\Delta\alpha^*$	E_{tot}	E_{el}	E_{pol}	E_{disp}	E_{rep}
32	4	-48.65	-13.48	-6.49	-60.55	31.88
30	6	-49.01	-13.59	-6.59	-60.71	32.02
29	7	-49.19	-13.80	-6.65	-60.80	32.06
28	8	-50.01	-13.39	-6.73	-60.89	31.00
27	9	-49.45	-13.34	-7.12	-61.17	32.17
26	10	-49.64	-13.44	-7.19	-61.23	32.21
24	12	-49.88	-13.69	-7.17	-61.76	32.73

(c) SYSTEM $\begin{bmatrix} CG \\ AT \end{bmatrix}$; distance = 6.8 A°

α^*	$\Delta\alpha^*$	E _{tot}	E _{el}	E _{pol}	E _{disp}	E _{rep}
32	4	-41.77	-9.33	-3.34	-44.78	15.66
30	6	-41.46	-9.04	-3.30	-44.67	15.58
29	7	-41.42	-9.00	-3.33	-44.70	15.61
28	8	-41.54	-9.29	-3.99	-44.84	16.58
27	9	-41.30	-8.92	-3.30	-44.75	15.67
26	10	-41.24	-8.87	-3.29	-44.78	15.70
24	12	-40.49	-8.02	-3.11	-45.51	16.15

(d) SYSTEM $\begin{bmatrix} GC \\ AT \end{bmatrix}$; distance = 6.6 A°

α^*	$\Delta\alpha^*$	E _{tot}	E _{el}	E _{pol}	E _{disp}	E _{rep}
32	4	-35.53	-4.76	-3.59	-44.62	17.45
30	6	-35.34	-4.87	-3.62	-44.27	17.42
29	7	-35.39	-4.90	-3.60	-44.30	17.44
28	8	-37.25	-4.53	-3.85	-52.31	23.44
27	9	-35.66	-4.86	-3.54	-44.93	17.59
26	10	-36.30	-4.25	-4.02	-45.69	17.69
24	12	-36.37	-4.29	-3.99	-45.77	17.68

(e) SYSTEM $\begin{bmatrix} AT \\ AT \end{bmatrix}$; distance = 6.4 A°

α^*	$\Delta\alpha^*$	E _{tot}	E _{el}	E _{pol}	E _{disp}	E _{rep}
32	4	-35.54	-7.92	-3.48	-49.19	25.06
30	6	-35.65	-7.98	-3.53	-49.18	25.04
29	7	-35.68	-8.00	-3.55	-49.11	24.98
28	8	-37.68	-8.40	-4.37	-48.20	23.29
27	9	-35.75	-8.06	-3.52	-49.34	25.17
26	10	-35.78	-8.09	-3.52	-49.40	25.23
24	12	-37.08	-8.97	-3.95	-45.86	21.71

(f) SYSTEM $\begin{bmatrix} AT \\ TA \end{bmatrix}$; distance = 6.8 A°

α^*	$\Delta\alpha^*$	E _{tot}	E _{el}	E _{pol}	E _{disp}	E _{rep}
32	4	-35.52	-5.68	-2.84	-40.14	14.14
30	6	-35.37	-5.78	-2.80	-40.73	13.94
29	7	-35.50	-5.71	-2.78	-40.70	13.89
28	8	-35.61	-5.86	-2.74	-40.89	13.88
27	9	-35.18	-5.56	-2.78	-40.65	13.81
26	10	-35.03	-5.39	-2.71	-40.23	13.30
24	12	-34.86	-5.60	-2.67	-40.24	13.86

(g) SYSTEM $\begin{bmatrix} \text{AU} \\ \text{AU} \end{bmatrix}$; distance = 6.4 A°

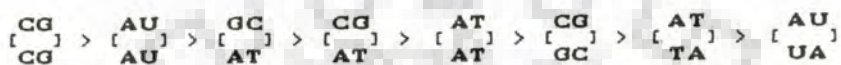
α^*	$\Delta\alpha^*$	E_{tot}	E_{el}	E_{pol}	E_{disp}	E_{rep}
32	4	-37.21	-9.49	-4.16	-46.01	22.45
30	6	-37.48	-9.65	-4.25	-45.99	22.42
29	7	-37.62	-9.71	-4.14	-46.20	22.44
28	8	-38.55	-10.38	-4.70	-48.06	24.59
27	9	-37.92	-9.89	-4.31	-46.14	22.42
26	10	-38.00	-9.96	-4.30	-46.18	22.43
24	12	-38.24	-10.07	-4.35	-46.26	22.45

(h) SYSTEM $\begin{bmatrix} \text{AU} \\ \text{UA} \end{bmatrix}$; distance = 6.4 A°

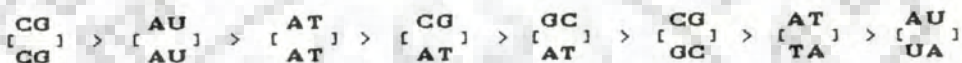
α^*	$\Delta\alpha^*$	E_{tot}	E_{el}	E_{pol}	E_{disp}	E_{rep}
32	4	-32.18	-4.34	-2.67	-43.79	18.62
30	6	-32.40	-4.74	-2.54	-43.14	18.00
29	7	-32.21	-3.73	-2.83	-44.56	18.92
28	8	-32.30	-4.65	-2.55	-43.06	17.96
27	9	-32.12	-3.77	-2.81	-44.76	19.23
26	10	-32.23	-4.56	-2.58	-42.98	17.91
24	12	-31.93	-3.68	-2.95	-45.79	20.50

geometries for all complexes are shown in Figure 7.14 (for daunomycin complexes) and Figure 7.15 (for actinomycin complexes).

Although it is not clear whether theoretical and experimental binding sites are identical, it appears that daunomycin shows a preferential order in binding sites as :



While this order for actinomycin has been found as :



It is clear that the selection of a particular site, depends on the binding energy of intercalant in which electrostatic and repulsion forces play a major role. It is expected that daunomycin molecule including daunosamine sugar moiety which is positively charged, may show a changed behaviour when energy value for intercalated complexes is observed taken backbone also into consideration. It is well known that the most of the electrostatic interactions would occur due to phosphate backbone interactions. This may also affect the total stacking energy values which have been observed in present work. Actinomycin because of the steric constraints Proposed by the peptide ring may interplay between steric and electrostatic effects which determine the selection of a particular site.

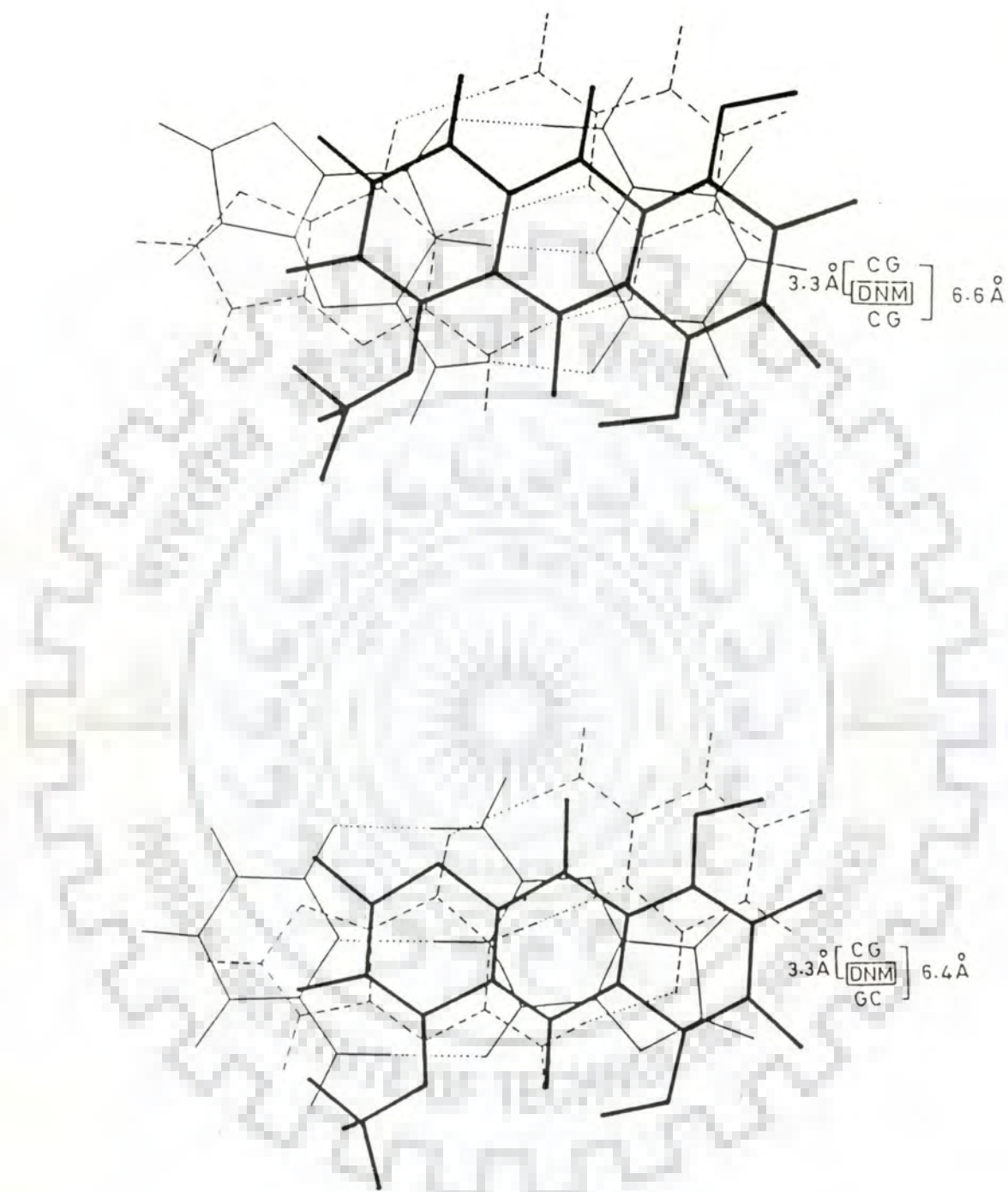


Figure 7.14: Overlap geometries of the complexes of dinucleotide model systems with daunomycin of

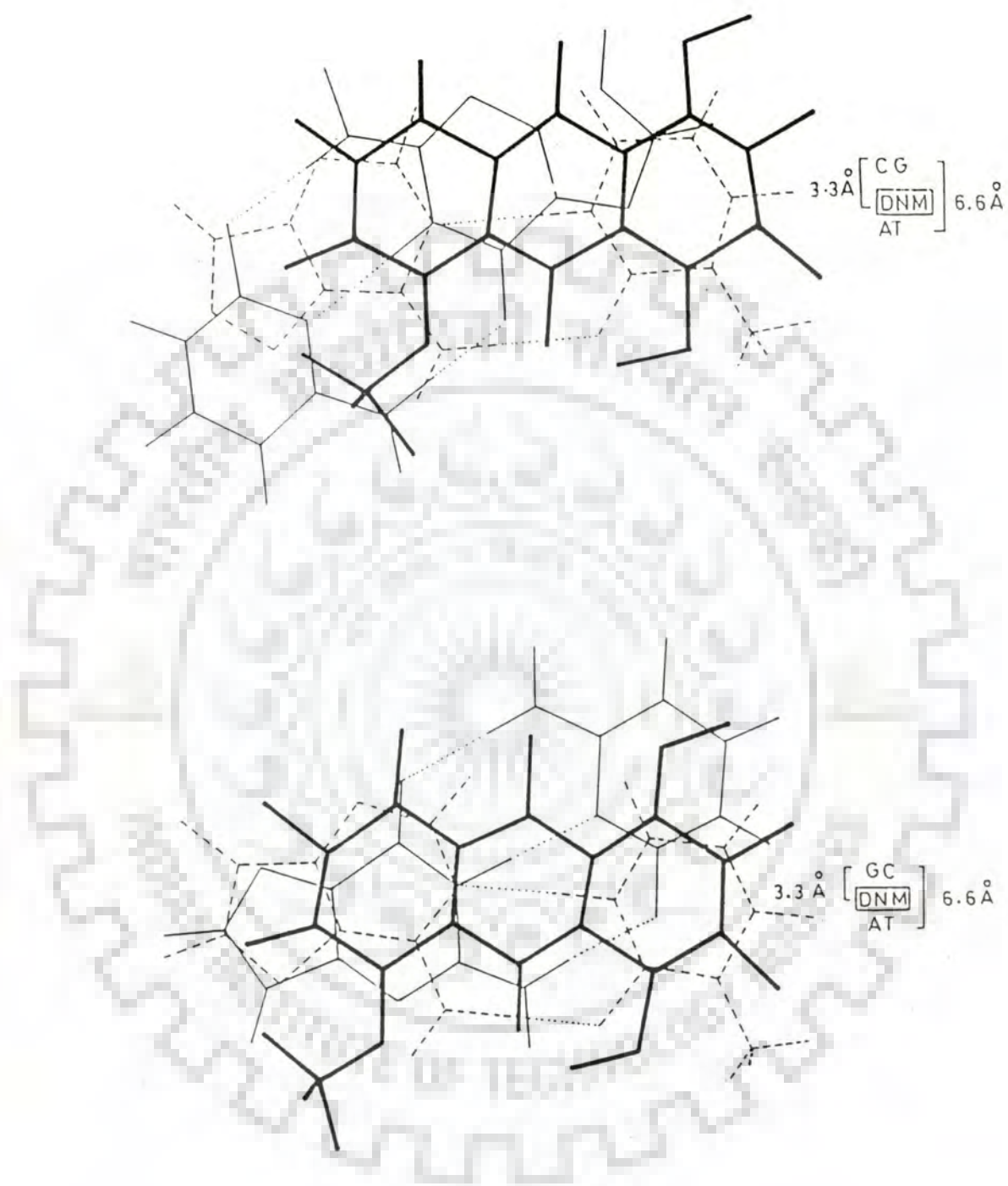


Figure 7.14: ...Continued...

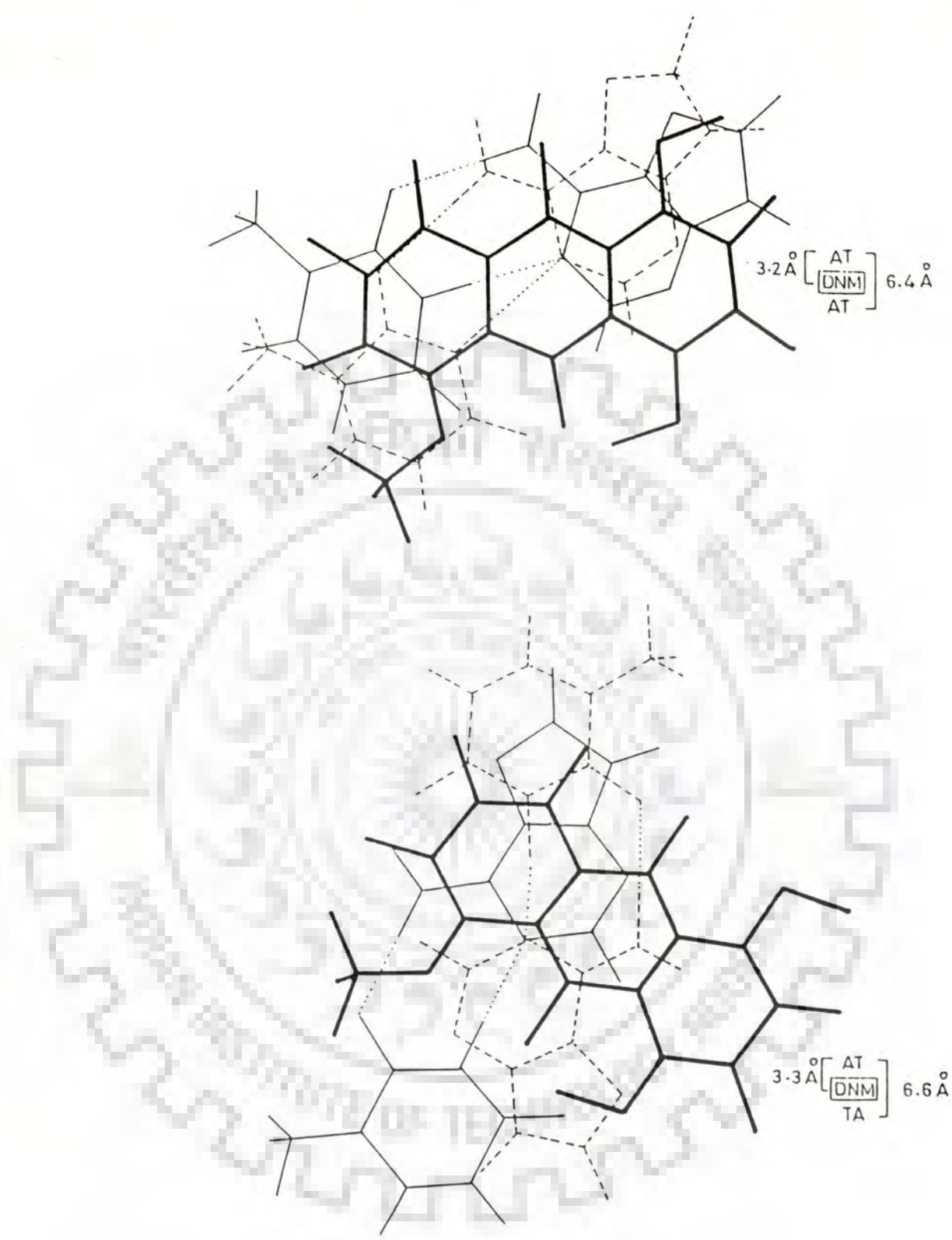


Figure 7.14: ...Continued...

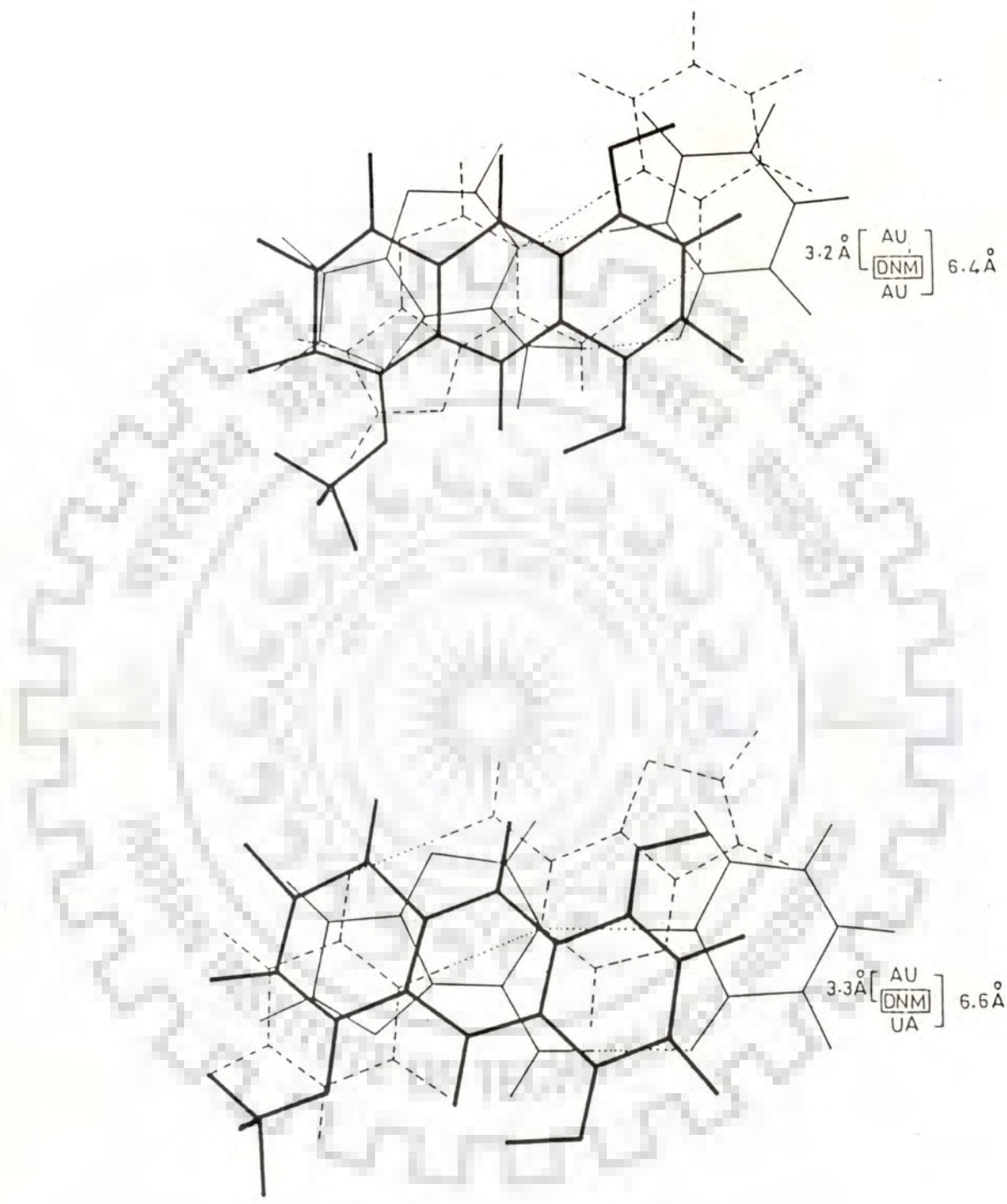


Figure 7.14: ...Continued...

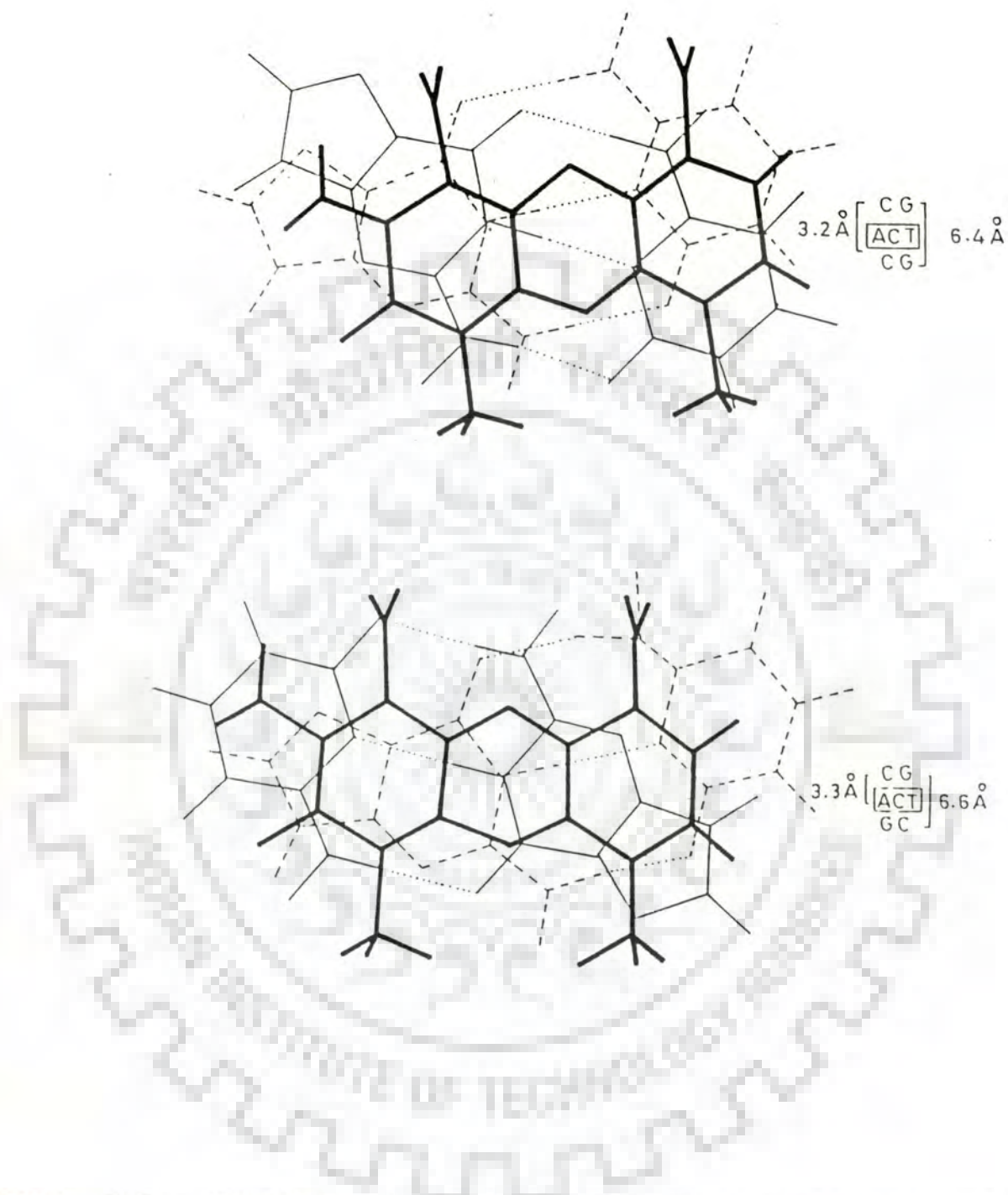


Figure 7.15: Overlap geometries of the complexes of dinucleotide model systems with actinomycin D

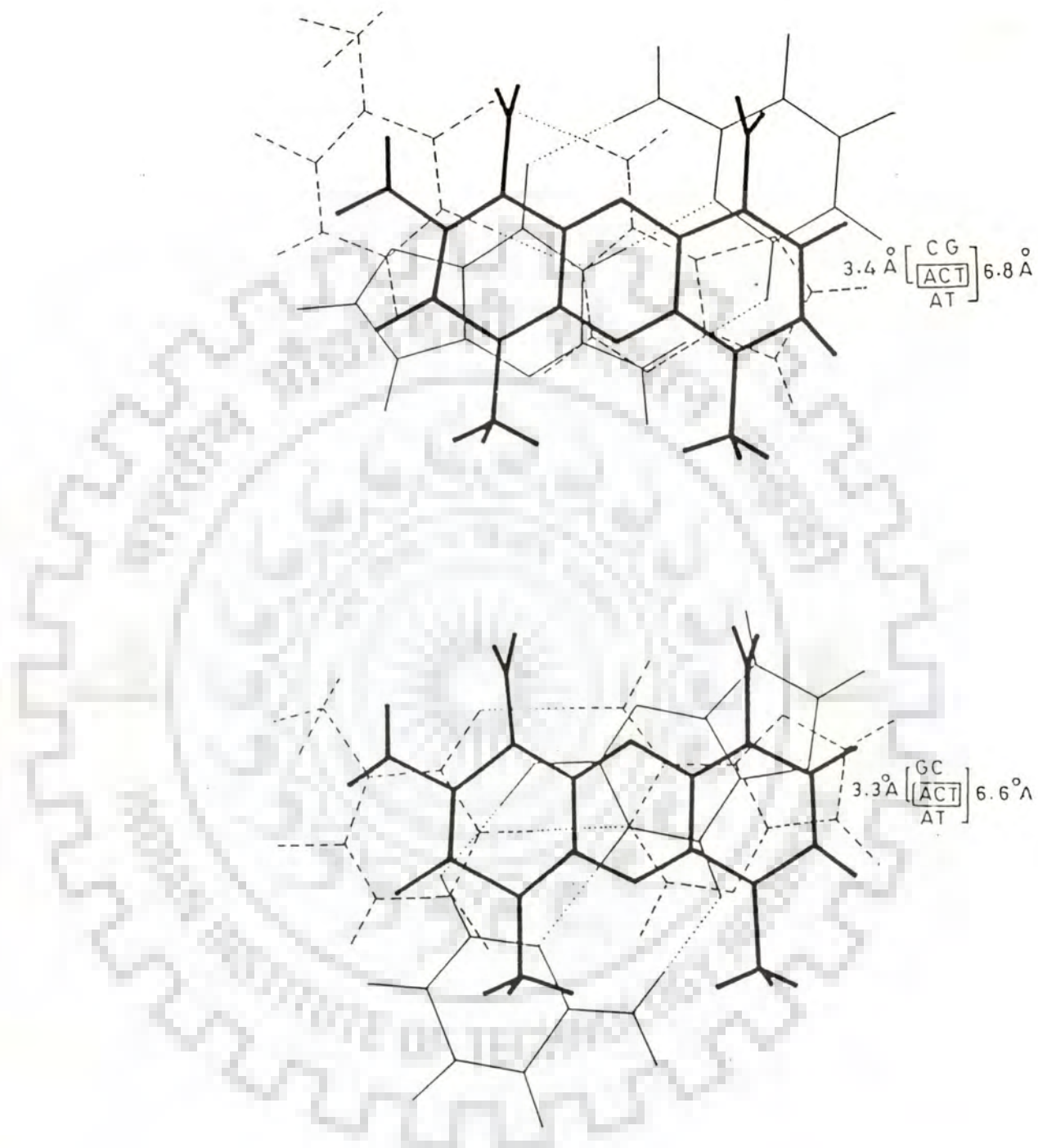


Figure 7.15: ...Continued...

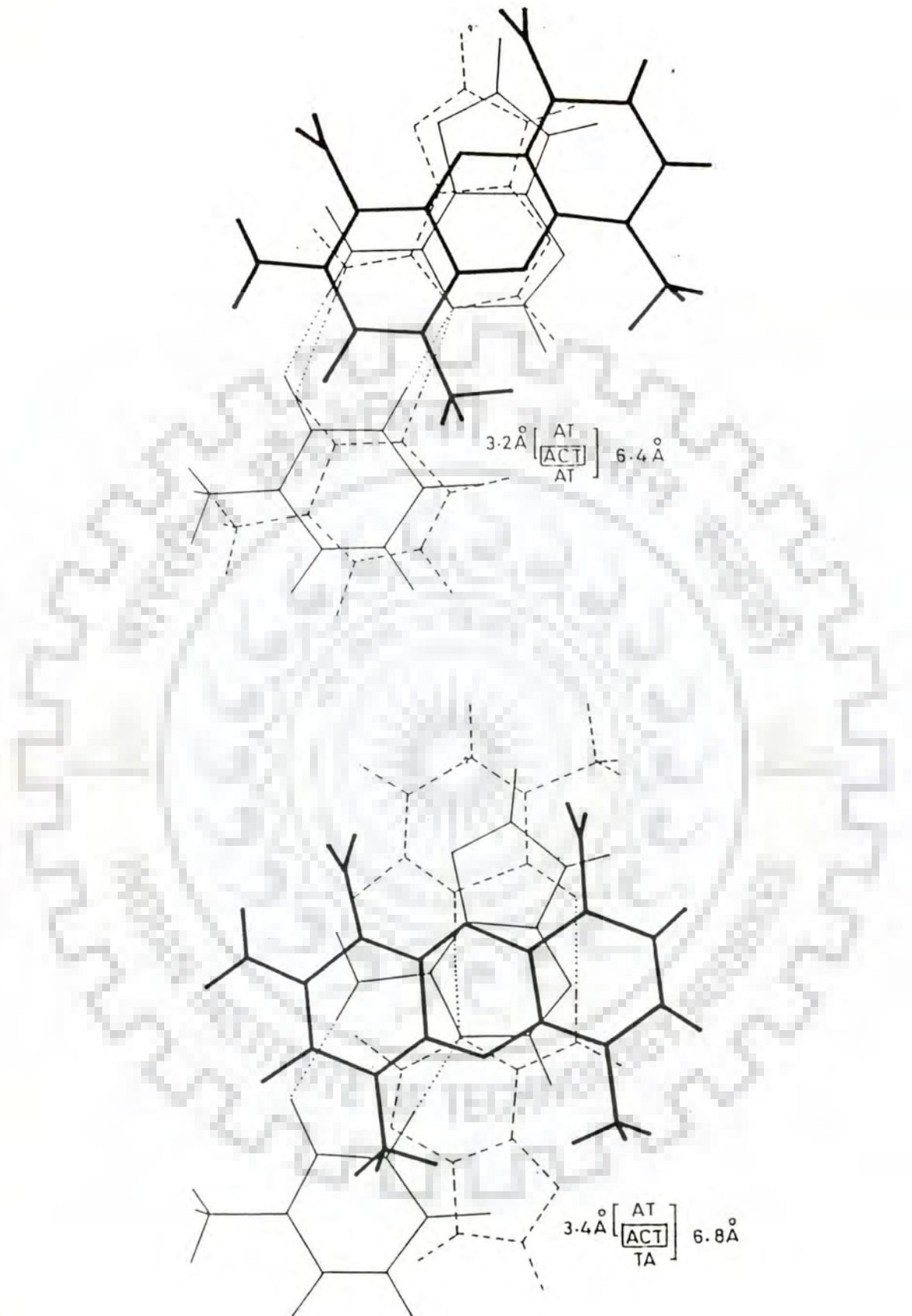


Figure 7.15: ...Continued...

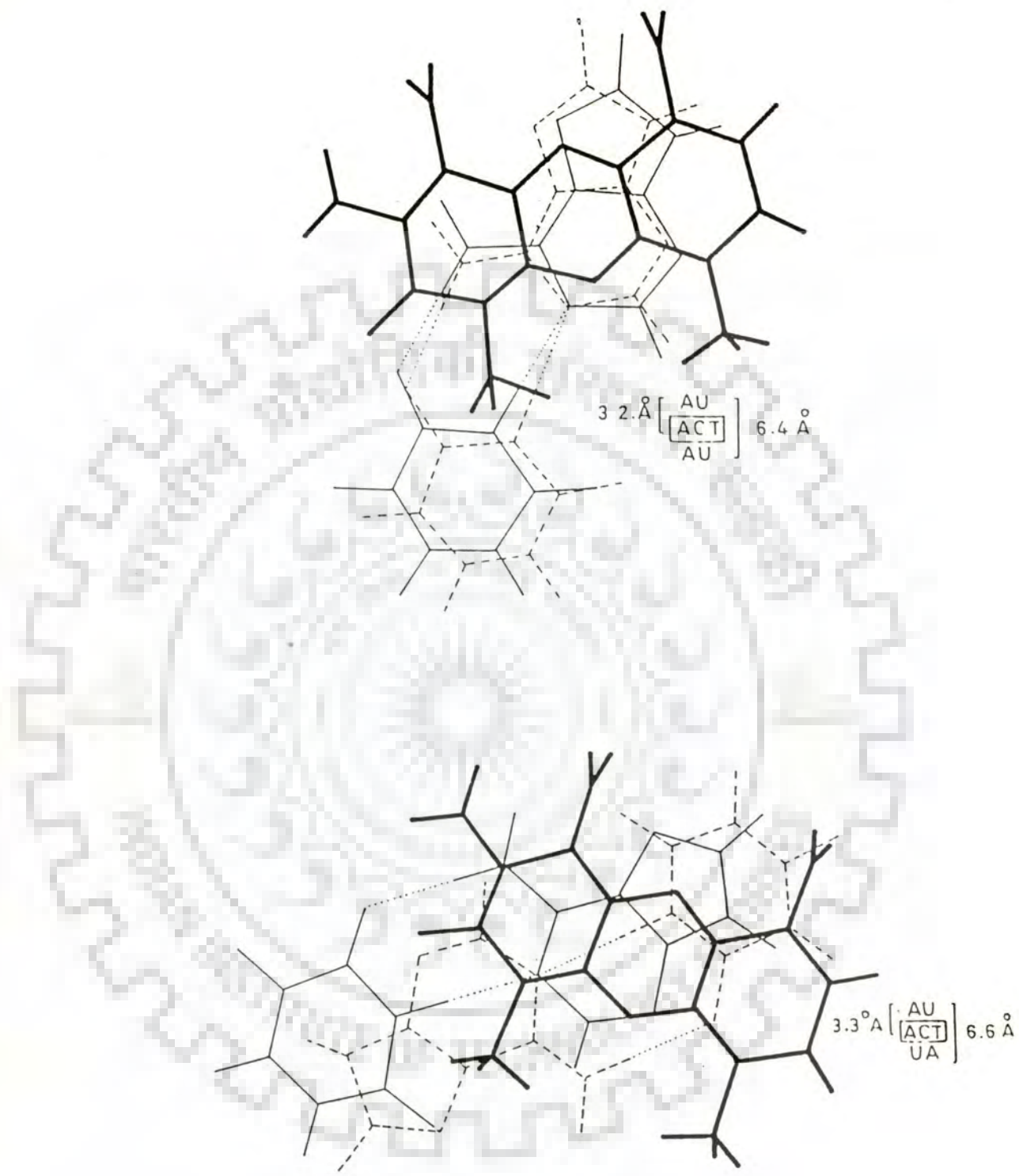


Figure 7.15: ...Continued...

Theoretical interpretation of unwinding provides an insight of optimum binding orientations of molecule. Competition for more than one intercalation site will lead to a statistical averaging of unwinding over several sites; therefore, they should also be taken care of for calculating unwinding angle for intercalation in longer nucleotides. In present work, local refinement of $\Delta\alpha$ value gave a much narrow range for it, which agrees well with results from X-ray studies by Pigram et al.[133] for daunomycin, in which a value of 12A° is reported. Sobell [52] calculated a value of 28° for $\Delta\alpha$ by X-ray methods for actinomycin - DNA crystal complex. This is perfectly in accordance with our results. A theoretical exploration of conformational aspects of ethidium bromide intercalation into dCpG minihelix has been made by Pullman et al.[108]. The energy value for EthBr-DNA complex reported therein has been found in same range as calculated by us. Both can not be directly compared because of different intercalators, but accordance in range is remarkable. Empirical energy calculation carried out and reported by Nuss et al. [92] for different acridine cations and GpC/CpG nucleotide complexes is a component analysis of interaction energy. Drug-base energy values reported therein are very low (-79.09 K Cal/mole) as compare to present results. But again the consideration of backbone interactions does not allow us to compare these two reports, straight. However, as we get, energy value for CpG and GpC site almost same in all cases, it is clear that in comparing the interaction energies of two different intercalation sites CpG and GpC, the different binding energies result mainly from

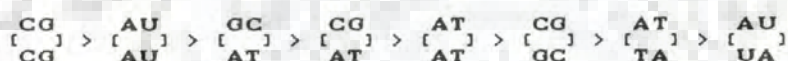
the interaction of the drug with sugar phosphate backbone. With present type of analysis, one would also not expect there to be a significant difference in the binding energy, without back bone and drug's side chain in actinomycin or amino sugar of daunomycin.



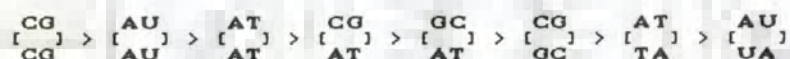
CONCLUSIONS

NMR studies on daunomycin in D₂O have revealed that phenomenon of self adduction of daunomycin molecules causes observed upfield shifts in NMR signals of chromophoric protons. Presence of two nOe's; 4COCH₃...2H and 4COCH₃...5'H in NOESY spectrum, makes it more clear that more than one conformers of daunomycin molecule are present in solution; which could even be a dimer. J splitting for H-7 proton signal has not been observed; which makes the occurrence of half chair conformation in ring A, less probable. SYN position of 5'H to 3'H is expected on the basis of observed nOe. Measured distance between these two protons has been found as 3.6Å. Binding of daunomycin with d-CpG results a change in helix sense and glycosidic bond rotation. A change in χ , the glycosidic bond rotation, from ANTI/high ANTI to SYN can not be ruled out. It is in accordance with X-ray results reported earlier that d-CpG adopts a left handed structure in complexed form. However, no change in sugar conformations after complex formation has been observed and it remains O1'endo, as NMR data show. Interesting results of NMR studies on actinomycin D solution conformation reveal that an inverted dimer structure of drug is supposedly present in solution. No effect of temperature was observed on peptide chain protons. However, most of the nonexchangeable protons on these two identical peptide chains could be successfully assigned. Intra molecular nOe's observed in NOESY spectrum of actinomycin suggest a relative conformation of peptide chains.

Theoretical potential energy calculations have provided insight for interaction of daunomycin and actinomycin D complexes with bases, base pairs and dinucleotide model sequences. A sequential preference for binding with bases is as $G > G > T > A$ for daunomycin with minimum energy value as -16.27 Kcal/moles for Cytosine complex while for actinomycin D preference of binding comes out to be as $G > C > T > A$. This confirms the earlier reports of necessity of presence of G at actinomycin binding site. For base pairs the preference of binding has been found as $CG > AU > AT$ in both cases and energy values for CG and GC base pairs are found to be almost equal. In model dinucleotide systems the order of preference goes as:



and



for actinomycin D. Dispersion energy shows maximum involvement in the total interaction energy value. It also indicates that stacking interactions between aromatic rings of drug chromophores & nucleic acid bases are forces which regulate these interactions. It can also be suggested that a change in electrostatic term of energy is well expected when back bone interactions are also taken into consideration. Helix unwinding tendency is well versed in each case and the global search and optimisation calculations for this angle ($\Delta\alpha$) led us to a value of 10° for daunomycin and 28° for actinomycin D. This suggests that binding/intercalation of actinomycin D causes helix opening to a higher degree than daunomycin.

REFERENCES

1. Kreishman, G.P., Chan, S.I. and Bauer, W. (1971) Proton magnetic resonance study of the interaction of ethidium bromide with several uracil residues, uridylyl (3'-5') Uridine and polyuridylic acid. *Biochemistry*. 61, 45 - 58.
2. Patel, D.J. and Canuel, L.L. (1976) Ethidium bromide. (dC-dG-dC-dG)₂ complex in solution : Intercalation and sequence specificity of drug binding at the tetranucleotide duplex level. *Proc. Natl. Acad. Sci. USA*. 73(10), 3343 - 3347.
3. Patel, D.J. and Canuel, L.L. (1977) Sequence specificity of mutagen-base pair overlap geometries for proflavin binding to dC-dC-dG-dG and dG-dG-dC-dC self-complementary duplexes. *Proc. Natl. Acad. Sci. USA*. 74(7), 2624 - 2628.
4. Patel, D.J. (1977) Mutagen - nucleic acid complexes at the polynucleotide duplex level in solution : Intercalation of proflavin into Poly (dA-dT) and the melting transition of the complex. *Biopolymers*. 16, 2739 - 2754.
5. Reuben, J.B., Baer, B.M. and Kallenbach, N.R. (1978) Structure of mutagen nucleic acid complex in solution. Proton chemical shifts in 9-Aminoacridine complexes with dG-dC, dC-dG and dA-dT-dG-dC-dA-dT. *Biochemistry*. 17 (14), 2915 - 2919.
6. Patel, D.J. and Shen, S. (1978) Sugar pucker geometries at the intercalation site of propidium diiodide into miniature RNA and DNA duplexes in solution, *PROC. Natl. Acad. Sci. USA*. 75(6), 2553 - 2557.

7. Sakore, T.D., Reddy, B.S. and Sobell, H.M. (1979) Visualization of drug-nucleic acid interactions at atomic resolution. IV. Structure of an aminoacridine - dinucleoside monophosphate crystalline complex, 9-aminoacridine-5-iodocytidylyl (3'5') guanosine. J. Mol. Biol. 135, 763 - 785.
8. Reddy, B.S., Seshadri, T.P., Sakore, T.D. and Sobell, H.M. (1979) Visualization of drug-nucleic acid interactions at atomic resolution. V. Structure of two amino-acridine-dinucleoside monophosphate crystalline complexes, proflavin-5-iodocytidylyl (3'-5') guanosine, J. Mol. Biol. 135, 787 - 812.
9. Miller, K.J., Lauer, M. and Archer, S. (1980) Interactions of molecules with nucleic acids. V. Intercalation of thioxanthenes into DNA, Intl. J. Quant. Chem. 7, 11 - 34.
10. Crawford, J.L., Koplak, F.J., Wang, A.H.J., Quigley, G.J., Boom J.H.V., Marel, G.V.D. and Rich, A. (1980) The tetramer d(CpGpCpG) crystallises as a left handed double helix. Proc. Natl. Acad. Sci. USA. 77(7), 4016 - 4020.
11. Neidle, S., Achai, A., Taylor, G.L., Berman, H.M., Carell, H.L., Glusker, J.P. and Stallings, W.E. (1977) Structure of a dinucleotide phosphate - drug complex as model for nucleic acid-drug interaction. Nature. 269, 304 - 307.
12. Aggarwal, A.K. and Neidle, S. (1985) Nucleic acid binding drugs. XIII. Molecular motion in a drug-nucleic acid model system : thermal motion analysis of a proflavin - dinucleoside crystal structure. Nucl. Acid Res. 13(15), 5671 - 5684.

13. Lancelot, G. and Thuong, N.T. (1986) Nuclear magnetic resonance studies of complex formation between the oligonucleotide d(TATC) covalently linked to an acridine derivative and its complementary sequence d(GATA). *Biochemistry*. 25, 5357 - 5363.
14. Dasgupta, D., Rajagopalan, M. and Sasisekharan, V. (1986) DNA binding characteristics of a synthetic analogue of distamycin. *Biochem. Biophys. Res. Comm.* 140(2), 626 - 631.
15. Dhingra, M.M. and Narula, S.S. (1986) Interaction of Puromycin and Puromycin aminonucleoside with Poly (A) - A proton magnetic resonance investigation. *Ind. J. Biochem. Biophys.* 23, 316 - 321.
16. Alvi, N.K., Rizvi, R.Y. and Hadi, S.M. (1986) Interaction of Quercetin with DNA. *Bioscience Report.* 16(10), 861 - 868.
17. Jones, M.B., Hollstein, U. and Allen, F. (1987) Site specificity of binding of antitumor antibiotics to DNA. *Biopolymers.* 26, 121 - 135.
18. Mendel, D. and Dervan, P.B. (1987) Hoogsteen base pair proximal and distal to echinomycin binding sites on DNA. *Proc. Natl. Acad. Sci. USA.* 84, 910 - 914.
19. Reid, D.G. and Gajjar, K. (1987) A proton and carbon 13 nuclear magnetic resonance study of neomycin B and its interactions with phosphatidylinositol 4,5- bisphosphate. *J. Biol. Chem.* 262(17), 7967 - 7972.
20. Veselkova, A.N., Karawajew, L. and Dijament, L.N. (1987) Proton magnetic resonance study of complex formation between proflavin and ribonucleotide monophosphate in aqueous solution. *Studia biophysica.* 120(1), 87 - 97.

21. Delepierre, M., Delbarre, A., D'estaintot, B.L., Igolene, J. and Roques, B.P. (1987) ^1H NMR studies of a monointercalating drug into a $d(\text{CpGpCpG})_2$ minihelix. *Biopolymers*. 26, 981 - 1000.
22. Nagayamma, K., Wuthrich, K., Bachmann, P. and Ernst, R.R. (1977) Two dimensional J- resolved ^1H NMR spectroscopy for studies of biological macromolecules. *Biochem. Biophys. Res. Comm.* 78, 99 - 105.
23. Canada, R.G., Swamy, W. and Thompson, H. (1988) Interaction of adriamycin with a calcium binding site. *Biochem. Biophys. Res. Comm.* 151(2), 679 - 685.
24. Slobodynasky, E., Stellwagen, J. and Stellwagen, N.C. (1988) CD of ethidium bromide complexes with normal and electrophoretically anomalous DNA restriction fragments. *Biopolymers*. 27, 1107 - 1126.
25. Searle, M.S., Hall, J.G., Denny, W.A. and Wakelin, L.P.G. (1988) NMR studies of the interaction of the antibiotic Nogalamycin with hexadeoxyribo nucleotide duplex $d(5'-\text{GCATGC})_2$. *Biochemistry*. 27, 4340 - 4349.
26. Iwamoto, R.H., Lin, P. and Bhacca, N.S. (1968) The structure of daunomycin. *Tet.Lett.* 36, 3891 - 3894.
27. Neidle, S. and Taylor, G. (1977) Nucleic acid binding drugs : Part IV. The crystal structure of the anti cancer agent daunomycin. *Biochim. et Biophys. Acta* 479, 450 - 459.
28. Bohner, R. and Hagon, U. (1977) Action of intercalating agents on the activity of DNA polymerase I. *Biochem. Biophys. Acta*. 479, 300 - 310.

29. Patel, D.J. and Canual, L.L.(1978) Anthracycline antitumour antibiotic nucleic acid interactions : structural aspects of the daunomycin . poly (dA - dT) complexes in solution. *Eur.J. Biochem.* 90, 247 - 254.
30. Quigley, G.J., Wang, A.H.J., Ughetto, G., Marcel, G.V.D., Boom, J.H.V. and Rich, A. (1980) Molecular Structure of an anticancer drug - DNA complex : Daunomycin plus d(CpGpTpApCpG), *Proc. Natl. Acad. Sci. USA* 77(12), 7204 - 7208.
31. Philips, D.R. and Roberts, G.C.K. (1980) Proton Nuclear Magnetic Resonance study of the self complementary hexanucleotide d(pTpA)₃ and its interaction with daunomycin. *Biochemistry.* 19, 4795 - 4801.
32. Patel, D.J., Koslowski, S.A. and Rice, A. (1981) Hydrogen bonding, overlap geometry and sequence specificity in anthracycline antitumour antibiotic . DNA complexes in solution. *Proc. Natl. Acad. Sci. USA.* 78(6), 3333 - 3347.
33. Patcher, J.A., Huang, C.H., Virgil, H.D., Prestayko, A.W. and Crooke, S.T. (1982) Viscometric and flourometric studies of deoxyribonucleic acid interactions of several new anthracyclines. *Biochemistry.* 21, 1541 - 1547.
34. Chaires, J.B., Dattagupta, N. and Crothers, D.M., (1982) Self association of daunomycin, *Biochemistry*, 21, 3927 - 3932.
35. Chaires, J.B., Dattagupta, N. and Crothers, D.M. (1982) Studies on interaction of anthracycline antibiotics and deoxyribonucleic acid : Equilibrium binding studies on interaction of daunomycin with deoxyribonucleic acid. *Biochemistry.* 21, 3933 - 3940.

36. Chaires, J.B., Dattagupta, N. and Crothers, D.M. (1983) Binding of daunomycin to calf thymus nucleosomes. *Biochemistry*. 22, 284 - 292.
37. Chaires, J.B. (1983) Daunomycin inhibits the B-Z transition in poly d(G-C). *Nucl. Ac. Res.* 11(23), 8485 - 8495.
38. Aue, W.P., Bertholdi, E. and Ernst, R.R. (1976a) Two dimensional spectroscopy. Application to nuclear magnetic resonance. *J. Chem. Phys.* 64, 2229 - 2246.
39. Chaires, J.B. (1985) Thermodynamics of the daunomycin DNA interaction : ionic strength dependence of the enthalpy and entropy. *Biopolymers*. 24, 403 - 419.
40. Sen, D. and Crothers, D.M. (1986) Influence of DNA binding drugs on chromatin condensation. *Biochemistry*. 25, 1503 - 1509.
41. Mondelli, R., Ragg, E., Fronza, G. and Arnone, A. (1987) Nuclear magnetic resonance conformational study of daunomycin and related antitumor antibiotics in solution. The structure of ring A. *Perkin Trans.* 11, 15 -26.
42. Mondelli, R., Ragg, E. and Fraonza, G. (1987) Conformational analysis of N-acetyldaunomycin in solution. A transient ¹H nuclear overhauser effect study of the glycosidic linkage geometry. *J. Chem. Soc. Perkin Trans.* 11, 27 - 32.
43. Kreibardis, T., Meng, D. and Aktipis, S. (1987) Inhibition of the RNA polymerase-catalysed synthesis of RNA by daunomycin : Effect of the inhibitor on the late steps of RNA chain inhibition. *J. Biol. Chem.* 262(26), 12632 - 12640.

44. Xodo, L.E., Manzini, G., Ruggiero J. and Quadrifoglio, F. (1988) On the interaction of daunomycin with synthetic alternating DNAs : Sequence specificity and poly electrolyte effect on the intercalation equilibrium. *Biopolymers*. 27, 1839 - 1857.
45. Muller, W. and Crothers, D.M. (1968) Studies of the binding of actinomycin and related compounds to DNA. *J. Mol. Biol.* 35, 251 - 290.
46. Arison, B.H. and Hoogsteen, K. (1970) Nuclear magnetic resonance spectral studies on Actinomycin D. Preliminary observations on the effect of complex formation with 5'-deoxyguanylic acid. *Biochemistry*. 9(20), 3976 - 3983.
47. Angerman, N.S., Victor, T.A., Bell, C.A. and Danyluk, S.S. (1972) A proton magnetic resonance study of the aggregation of actinomycin in D₂O. *Biochemistry*. 11(13), 2402 - 2411.
48. Sobell, H.M. (1974) How actinomycin binds to DNA. *Sci. Am.* 231(2), 82 - 91.
49. Patel, D.J. (1974) Peptide antibiotic - oligopeptide interaction. Nuclear magnetic resonance investigations of complex formation between actinomycin D and d- A_pT_pG_pC_pA_pT in aqueous solution. *Biochemistry*. 13(11), 2396 - 2402.
50. Patel, D.J. (1976) Proton and phosphorus NMR studies of d-C_pG (pC_pG)_n duplexes in solution. Helix coil transition and complex formation with actinomycin D. *Biopolymers*. 15, 533 - 558.
51. Tsurugi, K. and Ogata, K. (1977) Preferential degradation of newly synthesized ribosomal proteins in rat liver treated with a low dose of actinomycin D. *Biochim. Biophys. Res. Comm.* 75(2), 525 - 531.

52. Sobell, H.M., Tsai, C.C., Jain, S.C. and Gilbert, S.G. (1977) Visualization of drug - nucleic acid interaction at atomic resolution. III. *J. Mol. Bio.* 114, 333 - 345.
53. Krugh, T.R., Mooberry, E.S. and Chen, Y.C. (1977) Proton magnetic resonance studies of actinomycin D complexes with mixtures of nucleotides as models for the binding of the drug to DNA. *Biochemistry.* 16(4), 740 - 746.
54. Chen, Y.C. and Krugh, T.R. (1977) Actinomycin D complexes with oligonucleotides as models for the binding of drug to DNA. Paramagnetic induced relaxation experiments on drug - nucleic acid complexes. *Biochemistry.* 16(4), 747 - 755.
55. Reinhardt, C.G. and Krugh, T.R. (1977) Phosphorus-31 nuclear magnetic resonance studies of actinomycin D, ethidium and 9- aminoacridine complexes with dinucleotides. *Biochemistry.* 16 (13), 2890 - 2895.
56. Jones, G.H. (1978) Sensitivity of transcription by purified *Streptomyces antibioticus* RNA polymerase to actinomycin. *Biochem. Biophys. Res. Comm.* 84(4), 962 - 968.
57. D'orazi, D., Fracacimi, S.D. and Bagni, N. (1979) Polyamine effects on the stability of DNA - actinomycin D complex. *Biochem. Biophys. Res. Comm.* 90(1), 362 - 367.
58. Chen chiao, C.Y., Rao, G.K., Hook, J.W., Krugh, T.R. and Sengupta, S.K. (1979) 7- amino actinomycin D complexes with deoxynucleotides as models for the binding of the drug to DNA. *Biopolymers.* 18, 1749 - 1762.
59. Winkle, S.A. and Krugh, T.R. (1981) Equilibrium binding of carcogens and antitumour antibiotics to DNA : site selectivity, cooperativity, allostherism. *Nucl. Ac. Res.* 9, 3175 - 3186.

60. Willkins, R.J. (1982) Selective binding of actinomycin D and distamycin A to DNA. Nucl. Ac. Res. 10(2), 7273 - 7282.
61. Takusagawa, F., Dabrow, M., Neidle, S. and Bermann, H.M. (1982) The structure of a pseudo intercalated complex between actinomycin and the DNA binding sequence d(GpC). Nature. 296, 466 - 469.
62. Van Dyke, M.W., Hertzberg, R.P. and Dervan, P.B. (1982) Map of distamycin, netropsin and actinomycin binding site in heterogenous DNA : DNA cleavage inhibition patterns with methidiumpropyle - EDTA . Fe(II). Proc. Natl. Acad. Sci. USA. 79, 5470 - 5474.
63. Wilson, W.D. and Jones, R.L. (1982) Interaction of actinomycin D, ethidium, quinacrine daunorubicin and tetralysine with DNA : ³¹P NMR chemical shift and relaxation investigation. Nucl. Ac. Res. 10(4), 1399 - 1410.
64. Mirau, P.A. and Shafer, R.H. (1982) High resolution nuclear magnetic analysis of conformational properties of biosynthetic actinomycin analogues. Biochemistry. 21, 2622 - 2626.
65. Mirau, P.A. and Shafer, R.H. (1982) Role of actinomycin pentapeptides in actinomycin - deoxyribonucleic acid binding and kinetics. Biochemistry. 21, 2626 - 2631.
66. Reid, D.G., Doddrell, D.M., Fox, R.K., Salisbury, S.A. and Dudley, H.W. (1983) Application of proton NMR spectral editing techniques for selective observation of N-H protons in an actinomycin D complex with a tetranucleotide duplex. J. Am. Chem. Soc. 105, 5945 - 5946.

67. Reid, D.G., Salisbury, S.A. and Williams, D.H. (1983) Proton Nuclear Overhauser effect study of the structure of an Actinomycin D complex with a self complementary tetranucleotide triphosphate. *Biochemistry*. 22, 1377 - 1385.
68. Pardi, A., Morden, K.M., Patel, D.J. and Tinoco, I. (1983) Kinetics for exchange of the imino protons of the d(CGCGAATTCGCG) double helix in complexes with the antibiotics netropsin and/or actinomycin. *Biochemistry*. 22, 1107 - 1113.
69. Gupta, G., Dhingra, M.M. and Sarma, R.H. (1983) Left handed intercalated DNA double helix : Rendezvous of ethidium and actinomycin D in Z-helical conformation space. *J. Biomol. Str. Dyn.* 1, 97 - 113.
70. Lane, M.J., Dabrowiak, J.C. and Vournakis, J.N. (1983) Sequence specificity of actinomycin D and Netropsin binding to pBR322 DNA analyzed by protection from DNase I. *Proc. Natl. Acad. Sci. USA*. 80, 3260 - 3264.
71. Takusagawa, F., Goldstein, B.M., Youngster, S., Jones R.A., and Berman, H.M., (1984) Crystallization and preliminary X-Ray study of a complex between d(ATGCAT) and actinomycin D. *J. Biol. Chem.* 259(8), 4714 - 4715.
72. Juretschke, H.P. and Lapidot, A. (1984) Actinomycin D, ¹H NMR studies on intramolecular interaction and on the planarity of the chromophore. *Eur. J. Biochem.* 145, 651 - 658.
73. Brown, S.G., Mullis, K., Levenson, C. and Shafer, R.H. (1984) Aqueous solution structure of an intercalated Actinomycin D - dATGCAT complex by two dimensional and one dimensional proton NMR. *Biochemistry*. 23, 403 - 408.

74. Gorenstein, D.G., Kofen, L. and Shah, D.O. (1984) $^{31}\text{P}/^1\text{H}$ correlated NMR spectra of duplex $d(\text{A}_p[\text{Cp}^{17}\text{O}]\text{G}_p[\text{Cp}^{18}\text{O}]\text{C}_p[\text{Cp}^{16}\text{O}]\text{T})_2$ and assignment of ^{31}P signals in $d(\text{A}_p\text{G}_p\text{C}_p\text{T})_2$ - Actinomycin D complex. *Biochemistry*. 23, 6717 - 6723.
75. Flamee, P.A. (1985) The action of actinomycin D on the transcription of T7 coliphage DNA by *Escherichia coli* RNA polymerase. *Biochem. J.* 230, 557 - 560.
76. Sobell, H.M. (1985) Actinomycin and transcription. *Proc. Natl. Acad. Sci. USA.* 82, 5328 - 5331.
77. Kostura, M. and Craig, N. (1986) Treatment of chinese hamster ovary cells with transcriptional inhibitor actinomycin D inhibits of messenger RNA to ribosomes. *Biochemistry*. 25, 6384 - 6391.
78. Fu-Ming, C. (1988) Kinetics and equilibrium binding studies of Actinomycin D with some $d(\text{TGCA})$ containing dodecamers. *Biochemistry*. 27, 1843 - 1848.
79. Ginell, S., Lessinger, L. and Berman, H.M. (1988) The crystal and molecular structure of the anticancer drug actinomycin D : Some explanations for its unusual properties. *Biopolymers*. 27, 843 - 864.
80. Scott, E.V., Zon, G., Marzilli, L.G. and Wilson, W.D. (1988) NMR investigations of the binding of anticancer drug actinomycin D to duplexed $d\text{ATGCGCAT}$: Conformational features of the unique 2:1 adduct. *Biochemistry*. 27, 7940 - 7951.
81. Tsai, C.C., Jain, S.C. and Sobell, H.M. (1977) Visualization of drug-nucleic acid interaction at atomic resolution. I. Structure of an ethidium/dinucleoside monophosphate crystalline complex, ethidium : 5 - iodouridylyl (3'-5') adenosine. *J. Mol. Biol.* 114, 301 - 315.

82. Jain, S.C., Tsai, C.G. and Sobell, H.M. (1977) Visualization of drug nucleic acid interaction at atomic resolution. II. Structure of an ethidium/dinucleoside monophosphate crystalline complex, ethidium : 5 - iodocytidylyl(3'-5')guanosine. *J. Mol. Bio.* 114, 317 - 331.
83. Berman, H.M., Neidle, S. and Stodola, R.K. (1978) Drug nucleic acid interactions : Conformational flexibility at the intercalation site. *Proc. Natl. Acad. Sci. USA.* 75(2), 828 - 832.
84. Pack, G.A. and Loew, G. (1978) Origin of the specificity in the intercalation of ethidium into nucleic acids. A theoretical analysis. *Biochim. Biophys. Acta.* 519, 163 - 172.
85. Miller, K.J. (1979) Interaction of molecules with nucleic acids. I. An algorithm to generate nucleic acid structures with an application to the B-DNA structure and a counterclock wise helix. *Biopolymers.* 18, 959 - 980.
86. Miller, K.J. and Pycior, J.F. (1979) Interaction of molecules with nucleic acids. II. Two pairs of families of intercalation sites, unwinding angles and the neighbour exclusion principle. *Biopolymers.* 18, 2683 - 2719.
87. Miller, K.J., Marcea, J. and Pycior, J.F. (1980) Interaction of molecules with nucleic acids. III. Steric and electrostatic energy counters for the principle intercalation sites, prerequisites for binding and the exclusion of essential metabolites from intercalation. *Biopolymers.* 19, 2067 - 2089.
88. Miller, K.J., Brodzinsky, R. and Hall, S. (1980) Interactions of molecules with nucleic acids. IV. Binding energies and conformations of acridine and phenanthridine compounds in the two principal and in several unconstrained dimer duplex intercalation sites. *Biopolymers.* 19, 2091-2122.

89. Miller, K.J., Laur, M. and Archer, S. (1980) Interactions of molecules with nucleic acids. V. Intercalation of thioxanthenes into DNA. Intl. J. Quant. Chem.: Quant. Biol.Symp. 7, 11 - 34.
90. Miller, K.J. and Newlin, D.D. (1982) Interaction molecules with nucleic acids. VI. Computer design of chromophoric intercalating agents. Biopolymers. 21, 633 - 652.
91. Ornstein, R.L. and Rein, R. (1979) Energetics and structural aspects of ethidium cation intercalation into DNA minihelices. Biopolymers. 18, 2821 - 2847.
92. Nuss, M.E., Marsh, F.J. and Kollman, P.A. (1979) Theoretical studies of drug dinucleotide interactions. Emperical energy function calculations on the interaction of ethidium, 9-aminoacridine and proflavin cations with the base paired dinucleotides GpC and CpG. J. Am. Chem. Soc. 101(4), 825 - 833.
93. Sanyal, N.K., Roychoudhry, M. and Ojha, R.P. (1981) Biological activity of the nucleoside analogs : A theoretical study. Intl. J. Quant. Chem. 20, 159 - 166.
94. Sanyal, N.K., Roychoudhry, M. and Ojha, R.P. (1984) Molecular basis of drug action of some antibiotics. J. Theor. Biol. 110, 505 - 521.
95. Sanyal, N.K., Roychoudhry, M. and Tiwari, S.N. (1985) Quantum mechanical studies on the activity of anticacerous drug - ellepticine. Intl. Symp. Biomol. Struct.8(3,4), 713 - 720.
96. Sanyal, N.K., Ojha, R.P. and Roychoudhry, M. (1987) Interaction energy studies of pyrazolo-pyrimidine antibiotics during transcripyion. Formycin B. Intl. J. Biol. Macromol. 9, 20 - 26.

97. Ojha, R.P., Roychoudhry, M. and Sanyal, N.K. (1988) Interaction energy studies on 6-azapyrimidine antimetabolites during transcription process. *Ind. J. Biochem. & Biophys.* 25 237 - 243.
98. Sanyal, N.K., Roychoudhry, M. and Ojha, R.P. (1987) Molecular basis of the biological processes. (Private Communication).
99. Broyde, S., Hingerty, B. and Stellman, S. (1982) Deformation of DNA by carcinogenic agents. *Proc. SUNYA conversation in the discipline : Biomolecular stereo-dynamics.* 11, 455 - 467.
100. Taylor, E.R. and Olson, W.K. (1983) Theoretical studies of nucleic acid interactions. I. Estimations of conformational mobility in intercalated chains. *Biopolymers.* 22, 2667 - 2702.
101. Jain, S.C. and Sobell, H.M. (1984) Visualization of drug nucleic acid interactions at atomic resolutions. VII. Structure of an ethidium/ dinucleoside monophosphate crystalline complex, Ethidium : Uridyl (3'-5') adenosine. *J. Biomol. Str. Dyn.* 1(V), 1161 - 1177.
102. Jain, S.C. and Sobell, H.M. (1984) Visualization of drug nucleic acid interactions at atomic resolution. VIII. Structures of two ethidium/dinucleoside monophosphate crystalline complexes containing ethidium : cytidyl (3'-5') guanosine. *J. Biomol. Str. Dyn.* 1(V), 1179 - 1194.
103. Bhandary, K.K., Sakore, T.D. and Sobell, H.M., King, D. and Gabby, E.J. (1984) Visualization of drug nucleic acid interactions at atomic resolutions. IX. Structure of two N, N- dimethylproflavin : 5-iodocytidyl (3'-5') guanosine crystalline complexes. *J. Biomol. & Str. Dyn.* 1(V), 1195 - 1217.

104. Sakore, T.D., Bhandary, K.K. and Sobell, H.M. (1984) Visualization of drug nucleic acid interactions at atomic resolution. X. Structure of a N, N-dimethylproflavin : deoxycytidylyl (3'-5') deoxyguanosine crystalline complex. *J. Biomol. Str. Dyn.* 1(V), 1219 - 1227.
105. Kumar, N.V. and Govil, G. (1984) Theoretical studies on protein - nucleic acid interactions. I. Interaction of positively charged amino acids with nucleic acid fragments. *Biopolymers.* 23, 1979 - 1993.
106. Kumar, N.V. and Govil, G. (1984) Theoretical studies on protein - nucleic acid interactions. II. Hydrogen bonding of amino acid chains with bases and base pairs of nucleic acids. *Biopolymers.* 23, 1995 - 2008.
107. Kumar, N.V. and Govil, G. (1984) Theoretical studies on protein - nucleic acid interactions. III. Stacking of aromatic amino acids with bases and base pairs of nucleic acids. *Biopolymers.* 23, 2009 - 2024.
108. Chen, K.X., Gresh, N. and Pullman, B. (1985) A theoretical investigation on the sequence selective binding of daunomycin to double stranded polynucleotides. *J. Biomol. Str. & Dyn.* 3(3), 445 - 466.
109. Chen, K.X., Gresh, N. and Pullman, B. (1986) A theoretical study of anthracene and phenanthrene intercalators. *Nucl. Ac. Res.* 14(22), 9103 - 9115.
110. Chen, K.X., Gresh, N. and Pullman, B. (1986) A theoretical investigation on the sequence selective binding of adriamycin to double stranded polynucleotides. *Nucl.Ac. Res.* 14(5), 2251 - 2267.
111. Hingerty, B.E. (1985) Carcinogen - base stacking and base - base stacking in dCpdG modified by (+) and (-) anti - BPDE. *Biopolymers.* 24, 2279 - 2299.

112. Shapiro, R., Underwood, G.R., Zwadzka, H., Broyde, S. and Hingerty, E.B. (1986) Conformation of d(CpG) modified by the carcinogen 4- aminobiphenyl : A combined experimental and theoretical analysis. *Biochemistry*. 25, 2198 - 2205.
113. Rao, N.S., Singh, U.C. and Kollman, P.A. (1986) Molecular mechanism simulations on covalent complexes between anthramycin and B DNA. *J. Med. Chem.* 29, 2484 - 2492.
114. Rao, N.S. and Kollman, P.A. (1987) Molecular mechanical simulations on double intercalation of 9- aminoacridine into d (CGCGCGC).d(GCGCGCG) : Analysis of physical basis for the neighbour exclusion principle. *Proc. Natl. Acad. Sci. USA.* 84, 5735 - 5739.
115. Broyde, S. and Hingerty, B.E. (1987) Visualization of an AAF induced frameshift mutation : Molecular view of base displacement energy calculations. *Nucl. Ac. Res.* 15(6), 6539 -6551.
116. Parbhakaran, M. and Harvey, S.C. (1988) Molecular dynamics of structural transition and intercalations in DNA. *Biopolymers.* 27, 1239 - 1248.
117. Voet, D. and Rich, A. (1970) Structure of nucleic acid bases and base pairs adapted from the crystal structures of Purines, Pyrimidines and their intermolecular complexes. *Prog. Nucl. Res. Mol. Biol.* 10, 183 - 265.
118. Pople, J.A. and Segal, G.A. (1965) Approximate self - consistent molecular orbital theory. I. Invariant procedures. *J. Chem. Phys.* 43, S129 - S135.
119. Pople, J.A. and Segal, G.A. (1965) Approximate self - consistent molecular orbital theory. II. *J. chem. Phys.* 43, S136 - S151.

120. Courseille, C., Busetta, B., Geoffre, S. and Hospital, M. (1979) Complex daunomycin - butanol. *Acta. Cryst.* B35, 764 - 767.
121. Neidle, S. (1977) The molecular basis for the action of some DNA - binding drugs. *Prog. Med. Chem.* 16, 152 - 221.
122. Aue, W.P., Bartholdi, E. and Ernst, R.R. (1976) Two dimensional spectroscopy. Application to nuclear magnetic resonance. *J. Chem. Phys.* 64, 2229 - 2246.
123. Hosur, R.V., Kumar, M.R., Roy, K.B., ZuKun, T., Miles, H.T. and Govil, G. (1984) in *Magnetic Resonance in Biology and Medicine*, Tata McGraw Hill, India.
124. Frechet, D., Cheng, D.M., Kan, S.M. and Ts'o, P.O.P. (1983) Nuclear Overhauser effect as a tool for the complete assignment of non - exchangeable proton resonances in short deoxyribonucleic acid helices. *Biochemistry.* 22, 5194 - 5200.
125. Scheek, R.M., Boelens, R., Russo, N., Van Boom, J.H. and Kaptein, R. (1984) Sequential resonance assignment in ¹H NMR spectra of oligonucleotides by 2D NMR. *Biochemistry.* 23, 1371 - 1376.
126. Aue, W.P., Karthan, J. and Ernst, R.R. (1976b) Homonuclear broad band decoupling and two dimensional J-resolved NMR spectroscopy. *J. Chem. Phys.* 64, 4226 - 4227.
127. Saenger, W. (1984) in 'Principles of nucleic acid structures', Springer Verlag, New York.
128. Altona, C. and Sundralingam, M. (1973) Conformational analysis of the sugar ring in nucleosides and nucleotides. Improved methods of interpretation of proton magnetic resonance coupling constants. *J. Am. Chem. Soc.* 95, 2333 - 3244.

129. Miller, K.J. (0000) Three families of intercalation sites for parallel base pairs : A theoretical model. Proceedings of the second SUNYA conversation in the discipline Biomolecular stereodynamics. 2, 469 - 486.
130. Waring, M. (1970) Variation of the supercoils in closed circular DNA by binding of antibiotics and drugs : Evidence for molecular models involving intercalation. *J. Mol. Bio.* 54, 247 - 279.
131. Wang, A.H.J., Nathans, J., Marel, G.V.D., Van boom, J.H. and Rich, A. (1978) Molecular structure of a double helical DNA fragment intercalator complex between deoxy dCpG and a terpyridine platinum compound. *Nature.* 276, 471 - 474.
132. Wang, J.C. (1974) The degree of unwinding of the DNA helix by ethidium. I. Titration of twisted PM2 DNA molecules in alkaline Cesium chloride density gradients. *J. Mol. Bio.* 89, 783 - 801.
133. Pigram, W.J., Fuller, W. and Hamilton, L.D. (1972) Stereochemistry of intercalation : Interaction of Daunomycin with DNA. *Nature.* 235, 17 - 19.
134. Patel, D. (1980) in *Nucleic Acid geometry and dynamics* (Sarma, R.H., Ed.) Pergamon Press, New York, 224.
135. Chary, K.V.R., Modi, S., Hosur, R.V. and Govil, G. (1989) Quantification of DNA structure from NMR data : Conformation of d-ACATCGATGT. *Biochemistry.* 28, 1012 - 1019.

136. Ramakrishnan, B. and Wiswamitra, M.A. (1988) Crystal and molecular structure of ammonium salt of dinucleoside monophosphate d(CpG). *J. Biomol. Str. & Dyn.* 6(3), 511 - 523. *Biochemistry.* 21, 3933 - 3940.
137. Ramachandran, G.N. and Sasisekharan, V. (1968) Conformation of polypeptides and proteins. *Adv. Proc. Chem.* 23, 283 - 437.
138. Scheraga, H.A. (1968) Calculations of conformation of polypeptides. *Adv. Phys. Org. Chem.* 6, 103 - 183.
139. Lakshminarayana, A.V. and Sasisekharan, V. (1969) Stereochemistry of nucleic acids and polynucleotides. IV. Conformational energy of base - sugar units. *Biopolymers.* 8, 475 - 488.
140. Olson, W.K. and Flory, P.J. (1972) Spatial configurations of polynucleotide chains. II. Conformational energies and average dimensions of polyribonucleotides. *Biopolymers.* 11, 25 - 56.
141. Govil, G. (1976) Conformational structure of polynucleotides around the O-P bonds: Refined parameters for CPF calculations. *Biopolymers.* 15, 2303 - 2307.
142. Chen, K.I., Gresh, N. and Pullman, B. (1987) A theoretical exploration of conformational aspects of Ethidium bromide intercalation into a d(CpG)₂ minihelix. *Biopolymers.* 26, 831 - 848.
143. Slater, J.C. and Kirkwood, J.G. (1931) The Vander Waal's forces in gases. *Phys. Rev.* 37, 682 - 697.

144. Claverie, P. (1978) Elaboration of approximate formulas for the interactions between large molecules. Applications in organic chemistry. In 'Intermolecular interactions : from Diatomics to Biopolymers'. (Pullman, B., ed.) pp. 69 - 305, John Wiley, New York.
145. Kumar, N.V. and Govil, G. (1981) Role of stacking in protein - nucleic acid interactions. In 'Conformation in Biology', (Srinivasan, R. and Sarma, R.H., eds.) pp. 313 - 321, Adenine Press, New York.
146. Caillet, J. and Claverie, P.(1975) Theoretical evaluation of the intermolecular interaction energy of a crystal : Application to the analysis of crystal geometry. Acta Cryst. A31, 448 - 461.

